

2.15.3 Seal Region Stress Results

The contact stresses that represent the maximum nodal stresses on the sealing surfaces are summarized in Table 2.15.4-2. The resulting membrane plus bending stresses are compared to the yield stress of the material at the maximum NCT temperature for each HAC case.

For the lid gasket grooves, the linearized stress is calculated for each peak stress location as described in Section 2.15.1 and multiplied by the stress concentration factor calculated in Section 2.15.2. Table 2.15.4-3 provides a summary of the resulting factored stress values. As the table shows the minimum factor of safety is 1.2. in accordance with Regulatory Guide 7.6 [Ref.4], the RT-100 seal region experiences no inelastic deformation during all HAC events.

2.15.4 Displacement Results

To determine whether the seal remains tight during HAC, the relative displacement of each sealing surface is determined. Table 2.15.4-4 calculates the relative displacement for each sealing surface and Figure 2.15.4-4 through Figure 2.15.4-9 provide graphical representations of the displacement for each case. From the containment evaluation, the permanent plastic deformation for the EPDM O-ring is approximately 25%. Therefore, based on the seal dimensions, the maximum permissible gap is 1.61mm. Reviewing the relative displacements from Table 2.15.4-4, the maximum separation that occurs is 0.07706mm. Since this maximum separation is less than the permissible gap, the seals are predicted to remain tight during all HAC events.

Table 2.15.4-1 Stress Concentration Factors

D/d	r/d							
	0.01	0.02	0.04	0.06	0.1	0.15	0.2	0.3
1.01	1.76	1.53	1.37	1.32	1.28	1.25	1.22	1.19
1.02	2.05	1.74	1.52	1.42	1.35	1.28	1.25	1.22
1.05	2.58	2.11	1.77	1.62	1.47	1.40	1.34	1.29
1.10	3.09	2.45	2.00	1.80	1.59	1.49	1.40	1.31
1.20	3.62	2.81	2.23	1.97	1.70	1.55	1.44	1.34
1.50	3.80	2.98	2.38	2.15	1.83	1.63	1.52	1.38
2.00		3.14	2.59	2.23	1.88	1.66	1.54	1.40
3.00		3.30	2.68	2.34	1.93	1.67	1.53	1.38













Table 2.15.4-2 Sealing Surface Stress Summary

Accident Condition	Yield Strength at Max. NCT Seal Temp (MPa)	Primary Sealing Surface Contact		Primary Seal Linearized Stress Intensity		Secondary Sealing Surface Contact Stress		Secondary Seal Linearized Stress Intensity	
		Stress (MPa)	FS	P_m+P_b (MPa)	FS	(MPa)	FS	P_m+P_b (MPa)	FS
Side Drop	184.2	40.1	4.6	15.6	11.8	5.7	32.3	33.7	5.5
End Drop	184.2	22.8	8.1	14.3	12.9	0.0	N/A	62.7	2.9
Puncture	184.2	93.2	2.0	77.0	2.4	83.4	2.2	89.7	2.1

Table 2.15.4-3 Lid Seal Groove Region Stresses

Accident Condition	Yield Strength at Max NCT Seal Temp (MPa)	Stress Concentration	Linearized Stress in Primary Lid Primary Seal		FS	Stress Concentration	Linearized Stress in Secondary Lid Primary Seal		FS
			Maximum Stress (MPa)	FS			Maximum Stress (MPa)	FS	
Side Drop	184.2	2.6	15.0	38.9	4.7	2.2	66.1	145.3	1.3
End Drop	184.2	2.6	45.1	115.9	1.6	2.2	47.7	102.6	1.8
Puncture	184.2	2.6	59.1	153.6	1.2	2.2	71.8	158.0	1.2

Table 2.15.4-4 HAC Seal Region Displacement

Location	Minimum Displacement (mm)	Maximum Displacement (mm)
HAC Side Drop		
Primary Lid Sealing Surface	-0.047281	-0.33065
Primary Seal Flange Surface	-0.043598	-0.40771
Relative Displacement	 -0.003683	 0.07706
Secondary Lid Sealing Surface	-0.12481	-0.31864
Secondary Lid Sealing Surface on Primary Lid	-0.12238	-0.34072
Relative Displacement	 -0.00243	 0.02208
HAC End Drop		
Primary Lid Sealing Surface	-0.27689	-0.43679
Primary Seal Flange Surface	-0.27867	-0.43227
Relative Displacement	 0.00178	 -0.00452
Secondary Lid Sealing Surface	-0.93881	-1.08
Secondary Lid Sealing Surface on Primary Lid	-0.93328	-1.1009
Relative Displacement	 -0.00553	 0.0209
Puncture		
Primary Lid Sealing Surface	0.044821	-0.12329
Primary Seal Flange Surface	0.046104	-0.1212
Relative Displacement	 -0.001283	 -0.00209
Secondary Lid Sealing Surface	-0.85594	-1.1537
Secondary Lid Sealing Surface on Primary Lid	-0.84898	-1.1475
Relative Displacement	 -0.00696	 -0.0062

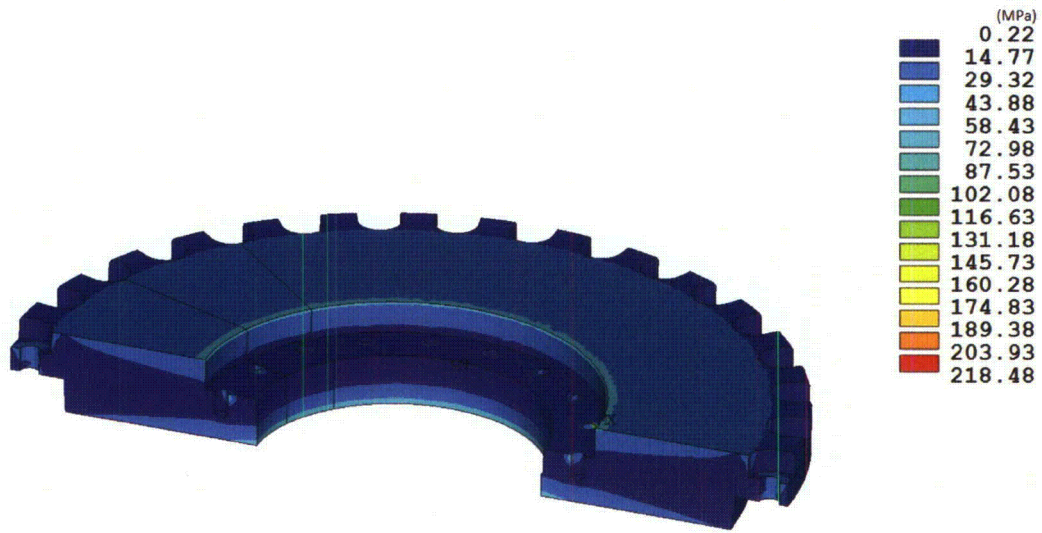


Figure 2.15.4-1 Stress Intensity Contour Plot of Primary Lid Following End Drop.

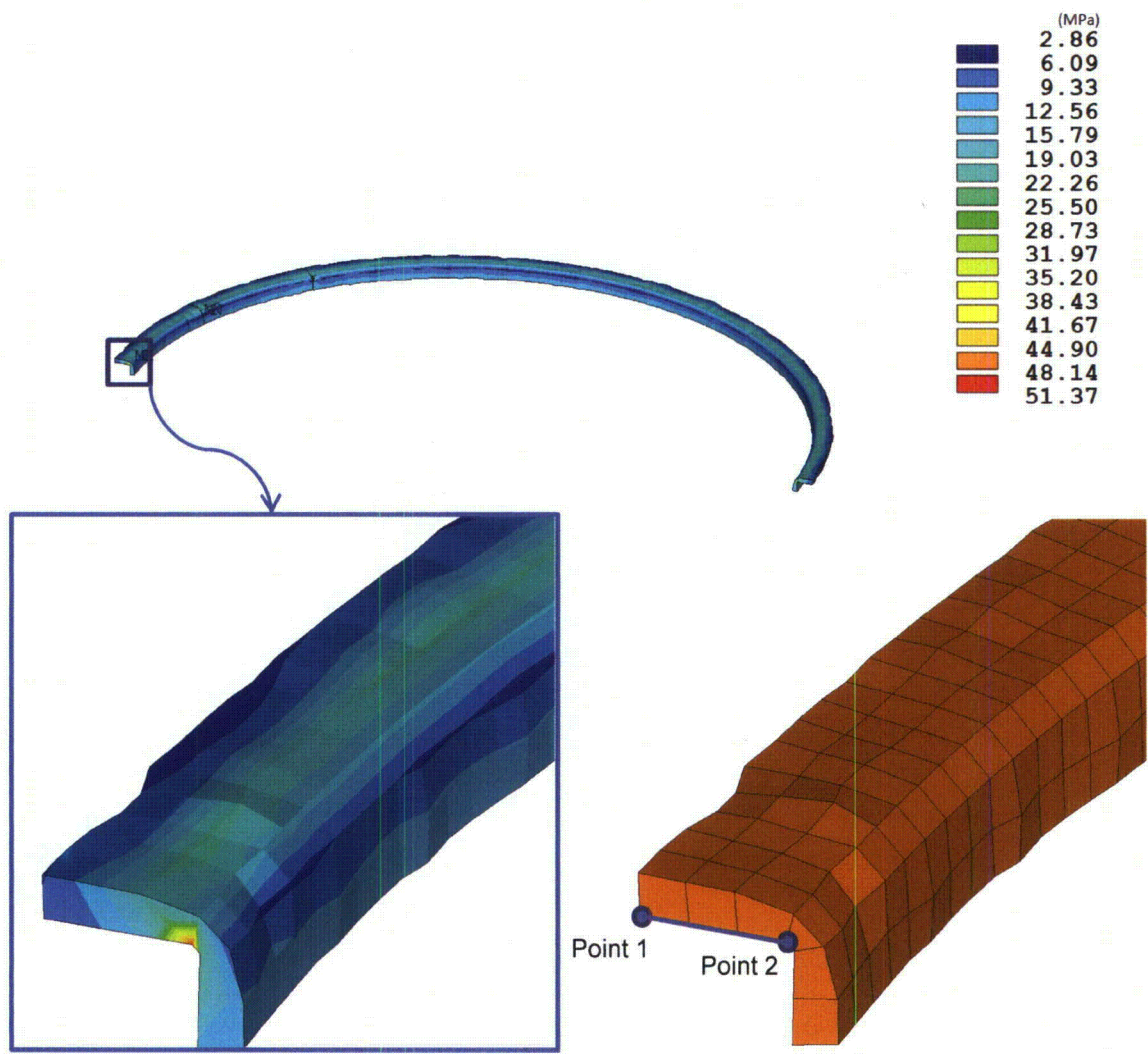


Figure 2.15.4-2 Stress Intensity Contour Plot of the Primary Seal Region

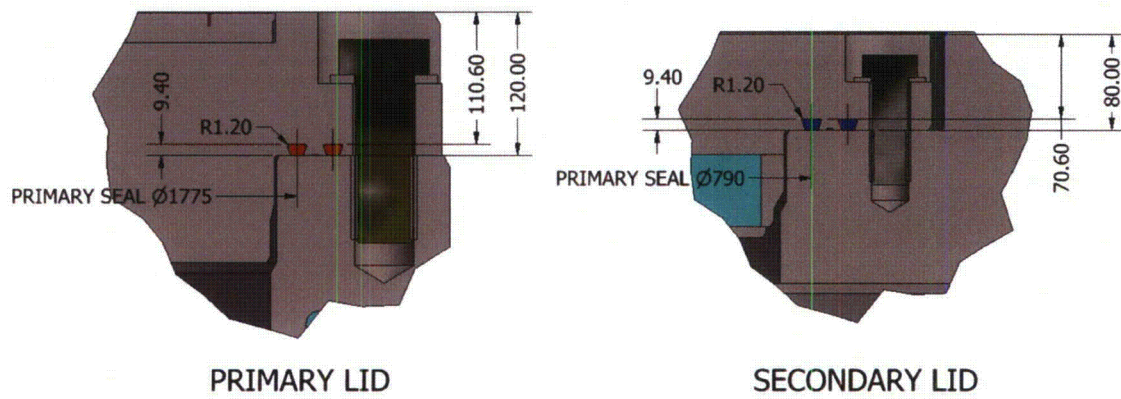
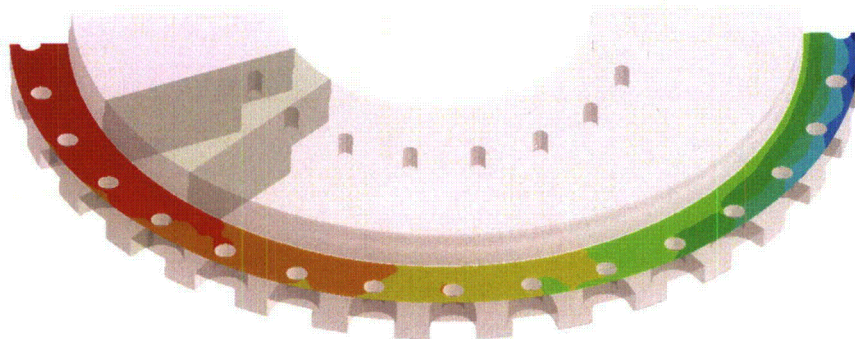


Figure 2.15.4-3 Lid Seal Geometry

O: HAC Side Drop V2
Directional Deformation 4
Type: Directional Deformation(Y Axis)
Unit: mm
Global Coordinate System
Time: 6
7/1/2013 7:44 AM

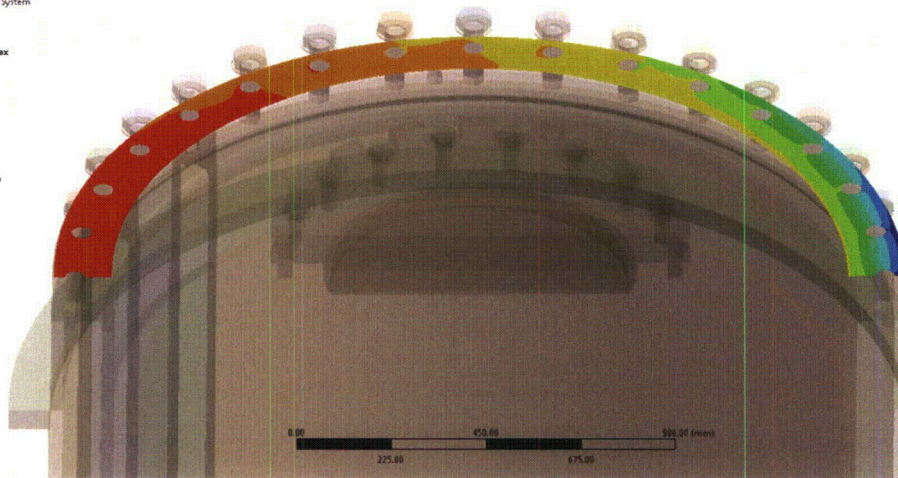
-0.047281 Max
-0.078766
-0.11025
-0.14174
-0.17322
-0.20471
-0.23619
-0.26768
-0.29917
-0.33065 Min



0.00 225.00 450.00 675.00 900.00 (mm)

O: HAC Side Drop V2
Directional Deformation
Type: Directional Deformation(Y Axis)
Unit: mm
Global Coordinate System
Time: 6
7/1/2013 7:40 AM

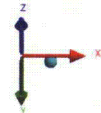
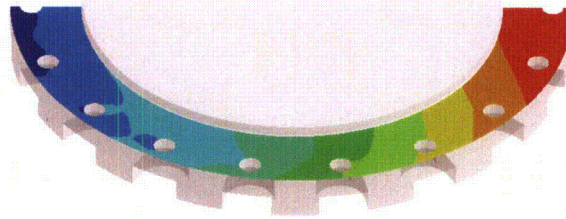
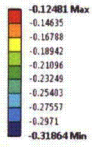
-0.042590 Max
-0.084055
-0.12451
-0.16497
-0.20543
-0.24588
-0.28634
-0.3268
-0.36725
-0.40771 Min



0.00 225.00 450.00 675.00 900.00 (mm)

Figure 2.15.4-4 Primary Lid Sealing Surface Displacement during Side drop

O: HAC Side Drop V2
Directional Deformation 6
Type: Directional Deformation(Y Axis)
Unit: mm
Global Coordinate System
Time: 6
7/1/2013 7:47 AM



O: HAC Side Drop V2
Directional Deformation 5
Type: Directional Deformation(Y Axis)
Unit: mm
Global Coordinate System
Time: 6
7/1/2013 7:45 AM

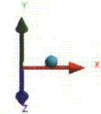
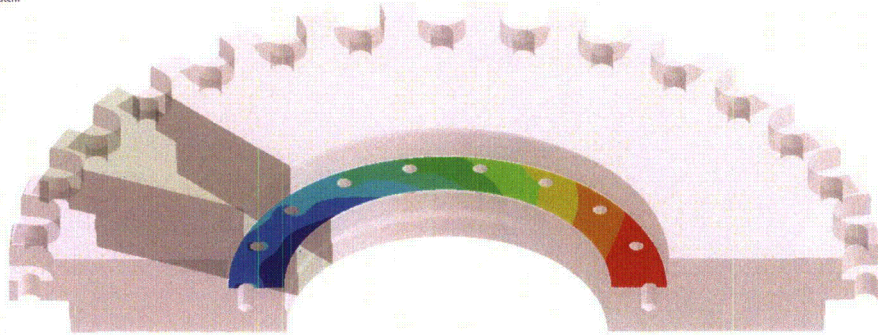
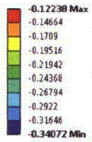
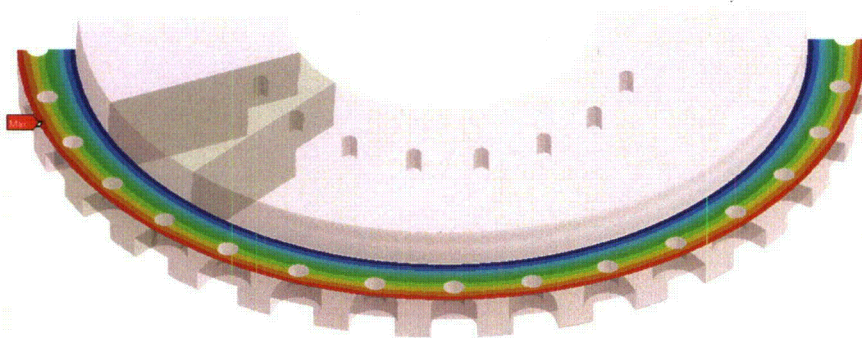
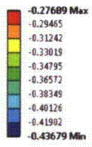


Figure 2.15.4-5 Secondary Lid Sealing Surface Displacement during Side drop

N: HAC Bottom Drop V2
Directional Deformation
Type: Directional Deformation(Y Axis)
Unit: mm
Global Coordinate System
Time: 6
6/28/2013 5:13 PM



N: HAC Bottom Drop V2
Directional Deformation
Type: Directional Deformation(Y Axis)
Unit: mm
Global Coordinate System
Time: 6
6/28/2013 5:10 PM

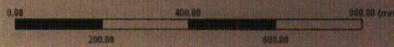
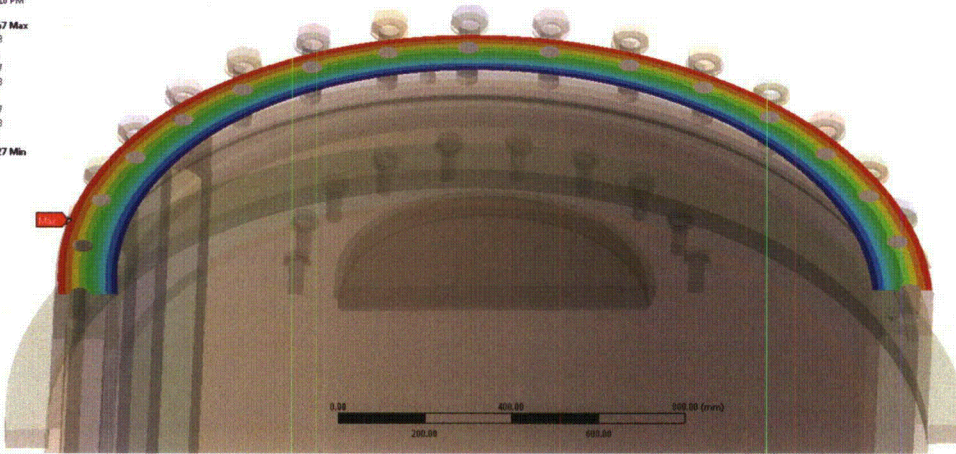
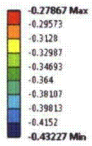
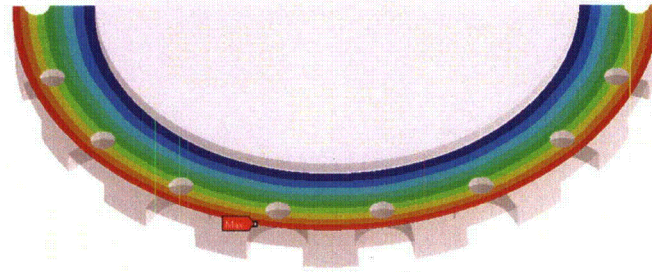


Figure 2.15.4-6 Primary Lid Sealing Surface Displacement during End drop

N: HAC Bottom Drop V2
Directional Deformation 4
Type: Directional Deformation(Y Axis)
Unit: mm
Global Coordinate System
Time: 6
6/28/2013 5:15 PM

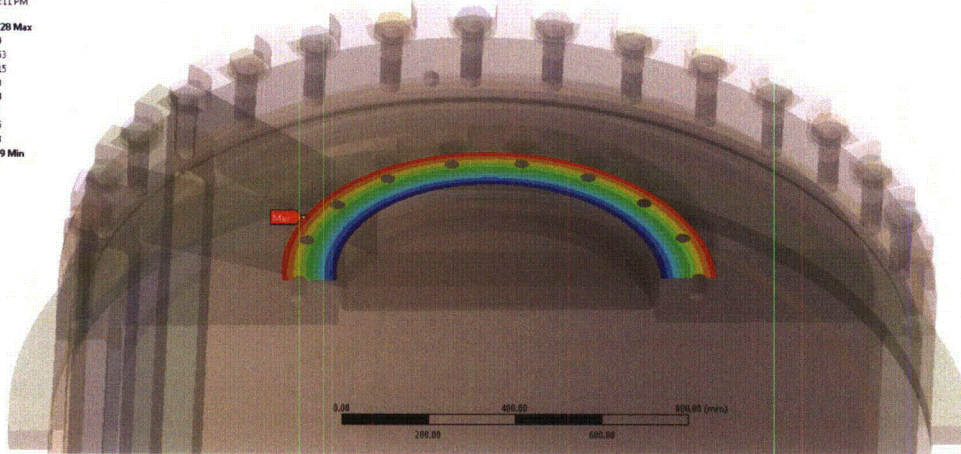
-0.93881 Max
-0.9545
-0.97018
-0.98587
-1.0016
-1.0172
-1.0329
-1.0486
-1.0643
-1.08 Min



0.00 125.00 250.00 375.00 500.00 (mm)

N: HAC Bottom Drop V2
Directional Deformation 2
Type: Directional Deformation(Y Axis)
Unit: mm
Global Coordinate System
Time: 6
6/28/2013 5:11 PM

-0.93328 Max
-0.9519
-0.97053
-0.98915
-1.0078
-1.0264
-1.045
-1.0636
-1.0823
-1.1009 Min

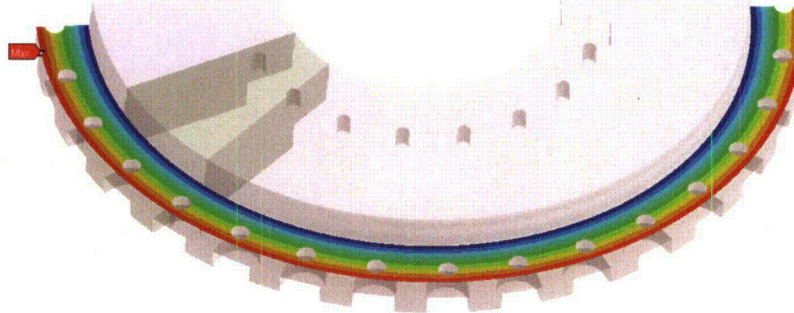


0.00 200.00 400.00 600.00 (mm)

Figure 2.15.4-7 Secondary Lid Sealing Surface Displacement during End drop

E: Pin Puncture
Directional Deformation
Type: Directional Deformation(Y Axis)
Unit: mm
Global Coordinate System
Time: 1
7/1/2013 8:34 AM

0.044821 Max
0.026142
0.0074631
-0.011216
-0.029895
-0.048574
-0.067252
-0.085931
-0.10461
-0.12329 Min



E: Pin Puncture
Directional Deformation.3
Type: Directional Deformation(Y Axis)
Unit: mm
Global Coordinate System
Time: 1
7/1/2013 8:47 AM

0.046104 Max
0.027515
0.0089257
-0.0096633
-0.028252
-0.046941
-0.06543
-0.084019
-0.10261
-0.1212 Min

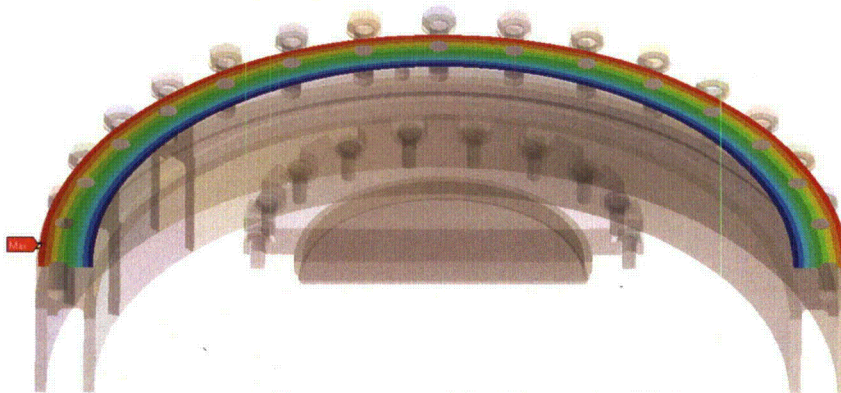
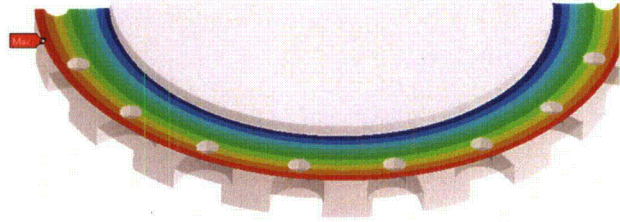
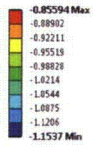


Figure 2.15.4-8 Primary Lid Sealing Surface Displacement during Puncture

E: Pin Puncture
Directional Deformation: 4
Type: Directional Deformation(Y Axis)
Unit: mm
Global Coordinate System
Time: 1
7/1/2013 8:56 AM



E: Pin Puncture
Directional Deformation: 2
Type: Directional Deformation(Y Axis)
Unit: mm
Global Coordinate System
Time: 1
7/1/2013 8:39 AM

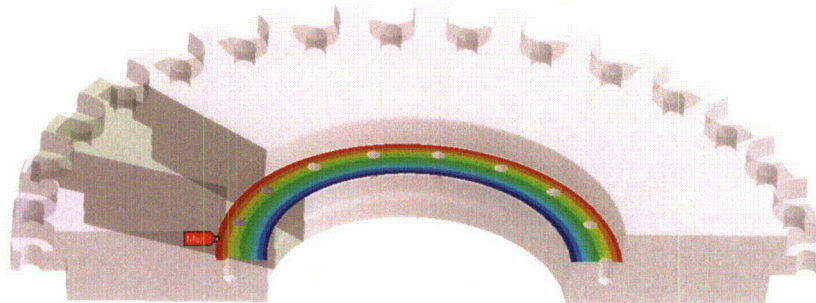
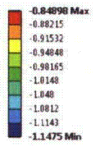


Figure 2.15.4-9 Secondary Lid Sealing Surface Displacement during Puncture

2.16 References

1. Robatel Technologies, LLC, Quality Assurance Program for Packaging and Transportation of Radioactive Material, 10 CFR 71 Subpart H, Dated January 31, 2012 and NRC Approved on March 21, 2012
2. U.S. Nuclear Regulatory Commission, 10 CFR Part 71--PACKAGING AND TRANSPORTATION OF RADIOACTIVE MATERIAL, dated March 7, 2012 and the following specific Sections:

71.31(a)(1)	71.31(a)(2)	71.33	71.35(a)
71.71	71.73	71.41(a)	71.45
71.85(b)	71.4	71.73(c)(1)	71.73(c)(3)
71.85	71.43	71.45(a)	71.45(b)
7.51	71.73(b)	71.71(c)	71.55(e)
71.59(a)(2)	71.85(b)	71.55	71.61
71.74	71.55(f)	71.75	

3. U.S. Nuclear Regulatory Commission, "Load Combinations for the Structural Analysis of Shipping Casks for Radioactive Material," Regulatory Guide 7.8.
4. U.S. Nuclear Regulatory Commission, "Design Criteria for the Structural Analysis of Shipping Cask Containment Vessels," Regulatory Guide 7.6.
5. U.S. Nuclear Regulatory Commission, "Fracture Toughness Criteria of Base Material for Ferritic Steel Shipping Cask Containment Vessels with a Maximum Wall Thickness of 4 Inches (0.1m)," Regulatory Guide 7.11.
6. U.S. Nuclear Regulatory Commission, "Fabrication Criteria for Shipping Containers," NUREG/CR-3854, March 1985.
7. ASME Boiler & Pressure Vessel Code 2007 Edition, Section III – Division 1 – Subsection ND, "Class 3 Components", The American Society of Mechanical Engineers, Three Park Avenue, New York, NY, www.asme.org.
8. ASME Boiler & Pressure Vessel Code 2007 Edition, Section III – Division 1 – Subsection NF, "Supports", The American Society of Mechanical Engineers, Three Park Avenue, New York, NY, www.asme.org.
9. U.S. Nuclear Regulatory Commission, "SCANS (Shipping Cask Analysis System): A Microcomputer Based Analysis System for Shipping Cask Design Review," NUREG/CR- 4554, Volumes 3, 6 and 7, February 1990.
10. U.S. Nuclear Regulatory Commission, "Stress Analysis of Closure Bolts for Shipping Casks," NUREG/CR-6007, January 1993.
11. NUREG/CR-0481, "An Assessment of Stress-Strain Data Suitable for Finite-Element Elastic-Plastic Analysis of Shipping Containers," Rack, H. & Knorovsky, G., Sandia Laboratories, Albuquerque, NM, September 1978, Retrieved on August 28, 2013, Retrieved from http://rampac.energy.gov/docs/nrcinfo/NUREG_0481.pdf.

12. U.S. Nuclear Regulatory Commission, Standard Review Plan for Transportation Packages for Radioactive Material, NUREG-1609, March 31, 1999
13. U.S. Government Code of Federal Regulations, Request for Withholding Information Contained in License Application, 10 CFR 2.790
14. U.S. Nuclear Regulatory Commission, "Dynamic Analysis to Establish Normal Shock and Vibration of Radioactive Material Shipping Packages, Volume 3: Final Summary Report," NUREG/CR-2146, Vol. 3, October 1983.
15. U.S. Nuclear Regulatory Commission, "Engineering Drawings for 10 CFR Part 71 Package Approvals," NUREG/CR-5502, May 1998.
16. U.S. Nuclear Regulatory Commission, "Fracture Toughness Criteria of Base Material for Ferritic Steel Shipping Cask Containment Vessels with a Wall Thickness Greater than 4 Inches (0.1m)," Regulatory Guide 7.12.
17. U.S. Nuclear Regulatory Commission, "Methods for Impact Analysis of Shipping Containers," NUREG/CR-3966, November 1987.
18. U.S. Nuclear Regulatory Commission, "Puncture Testing of Shipping Packages under 10 CFR Part 71," Bulletin 97-02, September 23, 1997.
19. U.S. Nuclear Regulatory Commission, "Recommended Welding Criteria for Use in the Fabrication of Shipping Containers for Radioactive Materials," NUREG/CR-3019, March 1985.
20. U.S. Nuclear Regulatory Commission Bulletin, 97-02.
21. U.S. Nuclear Regulatory Commission, "Shock and Vibration Environments for a Large Shipping Container During Truck Transport (Part II)," NUREG/CR-0128, August 1978.
22. U.S. Nuclear Regulatory Commission, Dynamic Analysis to Establish Normal Shock and Vibration of Radioactive Material Shipping Packages, NUREG-2146, Volumes 1, 2 and 3, dated January 1, 1981-March 31, 1981; April 1, 1981-June 30, 1981; and October 1993, respectively.
23. U.S. Nuclear Regulatory Commission, International Agreement Report, International Code Assessment and Applications Program: Summary of Code Assessment Studies Concerning RELAP5/MOD2, RELAP5/MOD3, and TRAC-B, December 1993.
24. Bickford, J. & Loomam, M., "Good Bolting Practices – A Reference Manual for Nuclear Power Plant Maintenance Personnel, Volume 1: Large Bolt Manual," Yalesville, CT: Electric Power Research Institute, 1987.
25. Blodgett, O. W., "Design of Welded Structures", The James F. Lincoln Arc Welding Foundation, Cleveland, Ohio.
26. AISC, "Guide to Design Criteria for Bolted and Riveted Joints", 2nd Edition, 2007.
27. Oberg, Erik, "Machinery's Handbook", 26th Edition.
28. ANSYS, Release 14.0, ANSYS, Inc., Canonsburg, PA, October, 2011
29. Young, Warren C., "Roark's Formulas for Stress and Strain", 6th Edition.

30. U.S. Nuclear Regulatory Commission, "Shock and Vibration Environments for a Large Shipping Container During Truck Transport" NUREG-0128.
31. ASME Boiler & Pressure Vessel Code 2010 Edition, Section II – Part D, "Materials", The American Society of Mechanical Engineers, Three Park Avenue, New York, NY, www.asme.org.
32. ASME Boiler & Pressure Vessel Code 2007 Edition, Section III – Division 1 – Subsection NB, "Class 1 Components", The American Society of Mechanical Engineers, Three Park Avenue, New York, NY, www.asme.org.
33. RTL-001-CALC-ST-0201, Rev. 5, "Lifting Structural Evaluation" (PROPRIETARY)
34. RTL-001-CALC-ST-0202, Rev. 4, "Tie-Down Evaluation" (PROPRIETARY)
35. RTL-001-CALC-ST-0402, Rev. 4, "Cask Body Structural Evaluation" (PROPRIETARY)
36. RTL-001-CALC-ST-0403, Rev. 4, "Pin Puncture Evaluation" (PROPRIETARY)
37. WM2001 Conference paper, "Benchmarking of LS-DYNA for Use with Impact Limiters," Joseph C. Nichols III, Michael E. Cohen, Robert A. Johnson, 2001.
38. RTL-001-CALC-TH-0102, Rev. 6, "RT-100 Cask Maximum Normal Operating Pressure Calculation" (PROPRIETARY)
39. Bickford, J. & Loram, M., "Good Bolting Practices – A Reference Manual for Nuclear Power Plant Maintenance Personnel, Volume 1: Large Bolt Manual," Yalesville, CT: Electric Power Research Institute, 1987.
40. RTL-001-CALC-ST-0401, Rev. 6, "RT-100 Cask Impact Limiter Drop Evaluation" (PROPRIETARY)
41. U.S. Nuclear Regulatory Commission, "Methods for Impact Analysis of Shipping Containers", NUREG/CR-3966.
42. RTL-001-CALC-TH-0102, Rev. 6, "RT-100 Cask Maximum Normal Operating Pressure Calculation" (PROPRIETARY)
43. RTL-001-CALC-TH-0202, Rev. 6, "RT-100 Cask Hypothetical Accident Condition Maximum Pressure Calculation" (PROPRIETARY)
44. ASME B1.13M-2005, METRIC SCREW THREADS: M PROFILE.
45. PAP 008, Specification D'approvisionnement - Mousse Polyurethane - Emballage de TRANSPORT RT-100 (Procurement Specification - Polyurethane Foam - Packaging of TRANSPORT RT-100), Rev. D, ROBATEL Industries (PROPRIETARY)
46. RES 001, Safety Analysis Robatel Package Model RT-100 Drop Test Report, Rev. E, ROBATEL Industries (PROPRIETARY)
47. Drawing 102885 MD 2021-06 Rev. D, "Robatel Transport Package RT100" (PROPRIETARY)
48. Certificate of Conformance for Purchase Order #117039 (Certificate for RT100 Scaled Foam Model) dated 09-07-2012 (PROPRIETARY)
49. U.S. Nuclear Regulatory Commission, "Standard Format and Content of Part 71 Applications for Approval of Packages for Radioactive Material," Regulatory Guide 7.9.

-
50. Parker O-Ring Handbook ORD 5700, Retrieved on August 28, 2013, Retrieved from http://www.parker.com/literature/ORD%205700%20Parker_O-Ring_Handbook.pdf.
 51. Baumeister T. and Marks, L.S. "Standard Handbook for Mechanical Engineers, 7th Edition". New York: McGraw-Hill Book Co., 1967.
 52. U.S. Nuclear Regulatory Commission Bulletin, 96-04.
 53. U.S. Nuclear Regulatory Commission Interim Staff Guidance, "Use of Computational Modeling Software", ISG-21.
 54. Glenn Lee, Radiation Resistance of Elastomers, IEEE Transactions on Nuclear Science, Vol. NS-32, No. 5, October 1985.
 55. Baumeister T. and Marks, L.S. "Standard Handbook for Mechanical Engineers, 9th Edition". New York : McGraw-Hill Book Co., 1987.
 56. ANSI N14.6-1978, "American National Standard for Special Lifting Devices for Shipping Containers Weighing 10000 pounds (4500 kg) or More for Nuclear Materials," American National Standards Institute, Inc., 11 West 42nd Street, New York, NY, www.ansi.org.
 57. KTA 3905, "Load Attaching Points on Loads in Nuclear Power Plants," Safety Standards of the (German) Nuclear Safety Standards Commission, June 1999 Edition including rectification of July 2000.
 58. TRELLEBORG Sealing Solutions O-Ring and Backup Rings Catalog, August 2011 Edition
 59. Shappert, L.B. "The Radioactive Materials Packaging Handbook". Oak Ridge, Tennessee: Oak Ridge National Laboratory, 1988. ORNL/M-5003.
 60. RTL-001-CALC-ST-0203, Rev. 6, "RT-100 Bolting Calculation" (PROPRIETARY)
 61. GENERAL PLASTICS Design Guide for LAST-A-FOAM FR-3700 Crash & Fire Protection of Radioactive Material Shipping Containers, Rev. 02.20.12

This page is intentionally left blank.

3. THERMAL EVALUATION

Robatel has performed a thermal evaluation of the RT-100 using the Nuclear Industry standards and under the RT Company Quality Assurance Program [Ref. 1]. This thermal evaluation shows that the RT-100 meets or exceeds all the 10 CFR 71 regulatory requirements [Ref. 2]. The thermal review is based in part on the descriptions and evaluations presented in the General Information Chapter 1 and Structural Evaluation Chapter 2 of the application. Similarly, results of the thermal review are considered in the review of several other sections of the application. An example of information flow for the thermal review is shown in Figure 3-1.

RT identified, described, discussed, and analyzed the principal thermal engineering design of the RT-100, components, and systems that are important to safety. Section 3 describes how the package complies with the performance requirements of 10 CFR 71 [Ref. 2]. Results of the thermal evaluation verified that the thermal performance of the RT-100 design (for both NCT and HAC) meets the thermal regulatory requirements as follows:

- The RT-100 design is evaluated to demonstrate that it satisfies the thermal requirements of 10 CFR 71.31(a)(1)]; 10 CFR 71.31(a)(2); 10 CFR 71.33, and 10 CFR 71.35(a) [*all* Ref. 2].
- The application identifies the established codes and standards used for the thermal design according to 10 CFR 71.31(c) [Ref. 2].
- The performance of the RT-100 is evaluated under the tests specified in 10 CFR Part 71.71 [Ref. 2] for NCT and 10 CFR Part 71.73 [Ref. 2] for HAC and also referenced 10 CFR 71.41(a) [Ref. 2].
- The RT-100 is designed, constructed, and prepared for transport so that there is no significant decrease in packaging effectiveness under the tests specified in 10 CFR 71.71 (NCT) and references in 10 CFR 71.43(f) and 71.51(a)(1) [*all* Ref. 2].
- The RT-100 is designed, constructed, and prepared for transport so that the accessible surface temperature does not exceed the regulatory limits specified in 10 CFR 71.43(g) [Ref. 2].
- The RT-100 design does not rely on mechanical cooling systems to meet containment requirements in reference to 10 CFR 71.51(c) [Ref. 2].
- The RT-100 has adequate thermal performance to meet the containment, shielding, sub-criticality, and temperature requirements of 10 CFR 71 [Ref. 2] for (NCT/HAC).

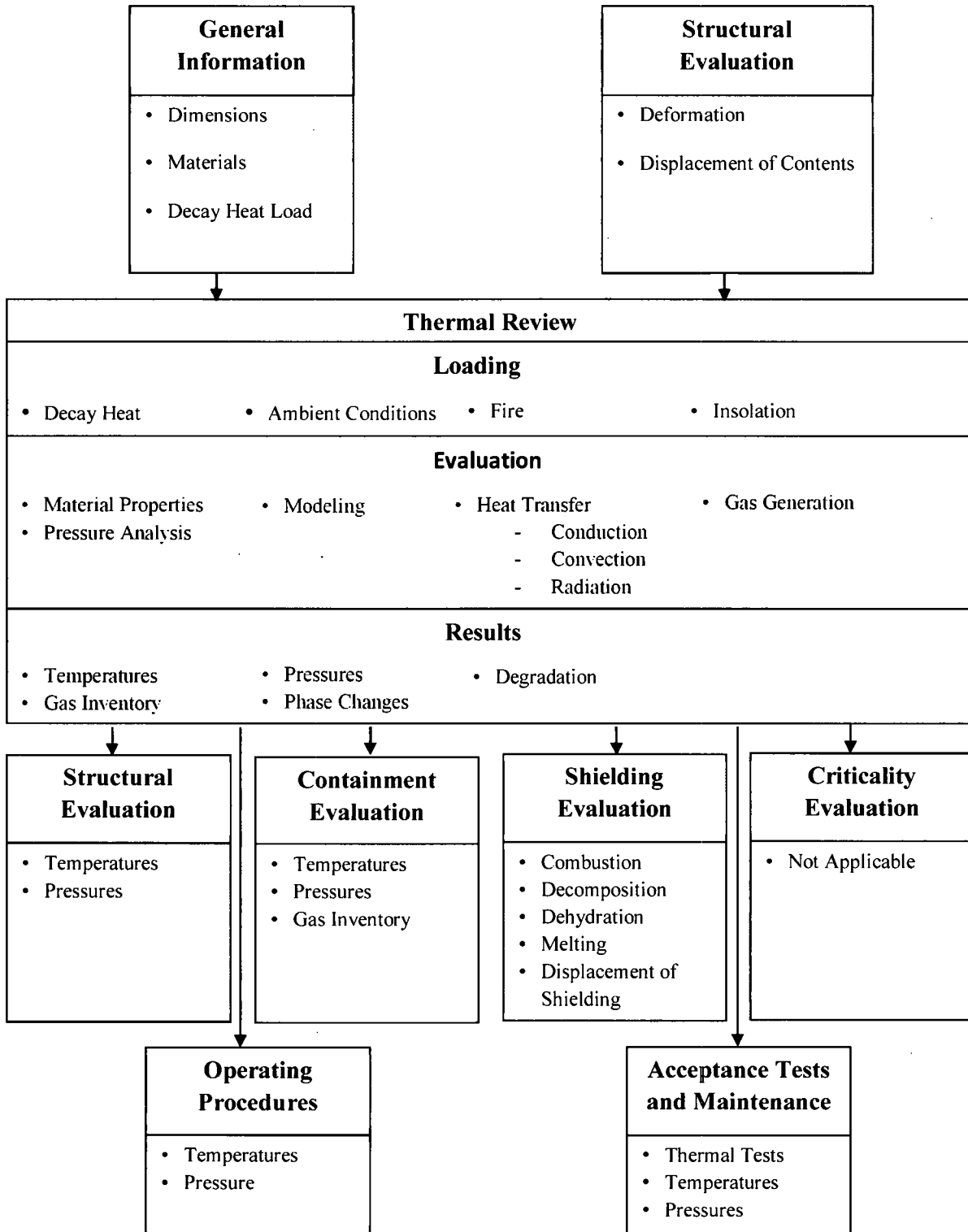


Figure 3-1 Information Flow for the Thermal Review

3.1 Description of Thermal Design

The thermal design aspects of the RT-100 are related primarily to protecting the sensitive components of the cask and the contents from the elevated temperatures produced by the hypothetical fire accident. The primary thermal criteria that are applied to the thermal evaluation are maintaining the lead shielding in the cask body and secondary lid below the melting temperature of lead, and the maximum temperature of the O-ring seals below their maximum operating temperature. The components primarily responsible for maintaining the temperatures of these components below their acceptance criteria are the impact limiters covering the top and bottom of the cask, and the thermal shield on the radial cask surface.

The impact limiters are made from a polyurethane foam material that has a low thermal conductivity. The impact limiters cover the top and bottom ends of the cask. They protect the lead in the bottom of the cask body and the O-rings in the primary lid, secondary lid, and the vent port cover plate. The impact limiters are designed to remain attached to the cask during normal operations and hypothetical accident conditions, and to insulate the lead and O-rings from the high temperatures of the hypothetical fire accident. The thermal shield covering the radial cask surface is made of a ceramic fiber material with a very low thermal conductivity. The ceramic fiber is covered by a thin, stainless steel cover that protects it from damage during normal handling. The ceramic fiber material is designed for use in insulating refractory furnaces, and providing an excellent thermal barrier for the fire accident, thus preventing the radial lead from exceeding its melting point.

The RT-100 is designed to accommodate contents with a maximum decay heat of 200 watts. This low decay heat value does not produce a significant temperature gradient through the cask body, and as a result, no specific design features are required to facilitate removing the heat from the cavity.

3.1.1 Design Features

As briefly described in Section 3.1, the RT-100 design has two primary thermal design features: the impact limiters and the radial thermal shield. These features are identified in Chapter 1, Figure 1.2.1-1 which highlights the primary components of the cask.

3.1.1.1 RT-100 Description

The RT-100 cask body consists of inner and outer shells constructed of 304/304L stainless steel. Lead shielding is provided between these radial shells, as well as between the 304/304L stainless steel bottom forging and bottom plate. The upper end of the cask comprises the upper 304/304L stainless steel forging that is attached to the inner and outer shells, and contains the mating surface for the primary lid. The primary and secondary lids are constructed of 304L stainless steel, as is the cover plate. The primary lid is attached using thirty-two (32) M48 hex head bolts and the secondary lid is secured using eighteen (18) M36 hex head bolts. The upper and lower impact limiter cover each end of the cask, and are constructed of 304L stainless steel shells containing polyurethane foam blocks. The impact limiters are secured to the body via twelve (12) M24 threaded studs. The RT-100 is described in greater detail in Chapter 1, Section 1.2.1.

Most of the outer shell of the cask is covered by a ceramic fiber thermal shield that is secured by a thin 304L stainless steel cover. Other portions of the radial cask surface are covered by the 318

stainless steel tie-down arms and tie-down arm baseplate, and by the 304L stainless steel lifting blocks. The exposed surfaces of the tie-down arm baseplate are covered by the ceramic fiber thermal shield and 304L stainless steel cover.

3.1.1.2 RT-100 Dimensions

The RT-100 thermal analysis is performed using the basic cask dimensions as presented in Appendix 1.4. The inner and outer shell thicknesses at the side of the cask are reduced to account for minimum thickness due to manufacturing tolerances. Specifically, the following material thicknesses are reduced by 2mm:

- Thicknesses of the cask body inner and outer stainless steel shells
- Bottom end of the cask body
- Stainless steel bottom forging welded to the inner shell
- Stainless steel bottom plate welded to the outer shell.

To represent the condition of undersized shells with a poured lead fill, lead thickness in both the sidewalls and the cask bottom end are simultaneously increased by 4 mm. This approach is conservative as it reduces the amount of stainless steel material protecting the lead from the HAC fire temperatures and thus, maximizes temperatures in the lead.

In order to maximize the amount of heat that can enter the cask body during the fire, no gaps are assumed between the lead and the outer shell. The lead and stainless steel outer shell are assumed to be in perfect contact. No other gaps are assumed in the thermal evaluation between the various components of the cask.

3.1.2 Content's Decay Heat

The RT-100 is designed for a maximum decay heat of 200 watts. This value is selected as the design basis, and is conservative for the contaminated resin and filter contents that are transported in the cask.

The analysis of the cask for normal condition of transport (NCT) and hypothetical accident conditions (HAC) is performed using the ANSYS finite element computer code [Ref. 3]. In this analysis, the decay heat of the contents is modeled as a uniform heat flux on the internal surfaces of the cask cavity.

To calculate this uniform heat flux over the inside surface of the cask, the inside diameter and the height of the cask cavity is used.

$$A_{in} = \pi dL + 2(\pi d^2/4)$$

where

$$\begin{aligned} A_{in} &= \text{inside surface area of the cask (m}^2\text{)} \\ d &= \text{inside diameter of the cask (m)} \end{aligned}$$

L = height of the cavity (m)

Based on the RT-100 drawing provided in Appendix 1.4, the cask inside diameter is 1.730 m and the height of the cavity is 1.956 m. The area is then

$$A_{in} = \pi \times 1.730 \times 1.956 + 2(\pi \times 1.730^2 / 4) = 15.332 \text{ m}^2$$

The uniform internal heat flux, q_{int} , is then

$$q_{int} = 200 \text{ W} / 15.332 \text{ m}^2 = 13.04 \text{ W/m}^2$$

3.1.3 Summary Tables of Temperatures

Section 3.1.3 presents summary tables of maximum temperatures occurring in the RT-100 as a result of the NCT and HAC evaluations described in detail in Sections 3.3 and 3.4. Limiting temperatures for consideration in the structural and containment evaluations are the maximum temperatures. Therefore, the following tables present maximum temperatures that occur in the various cask components under NCT and HAC. Table 3.1.3-1 presents the NCT maximum temperatures while Table 3.1.3-2 and Table 3.1.3-3 present the maximum temperatures HAC. For the fire accident evaluation, the time at which the component reaches its maximum temperature is listed along with the temperature. In some cases, temperatures are after cessation of the fire transient.

The tables also present the maximum averaged surface temperature of the inner shell at the cavity side. These averaged surface temperatures are used to predict the cavity pressure under normal and hypothetical conditions, respectively.

Table 3.1.3-1 RT-100 Maximum Normal Condition Temperature Summary

Component	Hot Case 1 (°C)	Hot Case 2 (°C)	Cold Case 1 (°C)	Cold Case 2 (°C)	Allowable Temperature (°C)	Reference
Primary Seal	68.7	42.1	-35.5	-24.5	150	Ref. 8
Secondary Seal	70.3	42.9	-34.7	-23.8	150	Ref. 8
Quick Disc. Valve Cover Seal	72.5 ^(a)	— ^(a)	— ^(a)	— ^(a)	150	Ref. 8
Lead Shield	73.2	43.1	-34.5	-23.6	328	Ref. 5 (p. 907)
Closure Bolts	70.0	42.8	-34.9	-23.9	—	—
Outer Surface	93.0	41.3	-36.3	-25.4	50/85 ^(b)	10 CFR 71.43(g)
Inner Shell Maximum	73.1	42.6	-35.1	-24.1	—	—
Inner Shell Average	71.0	41.7	-36.0	-25.0	—	—
Total Impact Limiter Average	67.4	39.5	-38.3	-27.3	—	—
Top Impact Limiter Average	72.5	39.5	-38.3	-27.4	—	—

- a. The NCT maximum temperature of the components surrounding the cover plate is the upper impact limiter average temperature (reported in Table 3.1.3-1) where the temperatures are higher on the external surfaces of the impact limiter. Thus the maximum temperature of the cover plate containment O-ring is considered to be 72.5°C with no further analysis. Since Hot Case 1 is the bounding upper temperature of this O-ring, the other NCT cases are not considered.
- b. 10 CFR 71.43(g)—A package must be designed, constructed, and prepared for transport so that in still air at 38°C (100°F) and in the shade, no accessible surface of a package would have a temperature exceeding 50°C (122°F) in a nonexclusive use shipment, or 85°C (185°F) in an exclusive use shipment.

Table 3.1.3-2 RT-100 Maximum Calculated Temperature of Cask under HAC with Pin Puncture Damage on Top Impact Limiter

Component	Temperature (°C)	Time After Start of Fire (Minutes)	Allowable Temperature (°C)	Reference
Primary Seal Maximum	110.8	291.6	150	Ref. 8
Secondary Seal Maximum	131.1	33.4	150	Ref. 8
Quick Disc. Valve Cover Seal	133.1 ^(c)	33.4 ^(c)	150	Ref. 8
Lead Shield Maximum	304.8	34.5	328	Ref. 5 (p. 907)
Closure Bolts Maximum	133.1	33.4	—	—
Cask Body Maximum	799.1	30.0	—	—
Inner Shell Average	136.3	—	—	—

- c. The port cover plate location is on the primary lid, close to the primary lid closure bolts. The cover plate is thermally insulated by the upper impact limiter. The highest temperature reported on the primary and secondary lid are the closure bolts (where the puncture bar penetrates the impact limiter) with a maximum temperature of 133.1°C (reported in Table 3.1.3-2). This temperature of 133.1°C being bonding to all the lids and cover plate recorded temperatures, the maximum temperature of the cover plate containment O-ring during HAC is considered to be 133.1°C with no further analysis.

Table 3.1.3-3 RT-100 Maximum Calculated Temperature of Cask under HAC with Pin Puncture Damage at the Side of the Cask Body

Component	Temperature (°C)	Time After Start of Fire (minutes)	Allowable Temperature (°C)	Reference
Primary Seal Maximum	110.3	285.1	150	Ref. 8
Secondary Seal Maximum	91.3	1624.4	150	Ref. 8
Quick Disc. Valve Cover Seal	— ^(d)	— ^(d)	150	Ref. 8
Lead Shield Maximum	304.7	34.5	328	Ref. 5 (p. 907)
Closure Bolts Maximum	91.9	1302.5	—	—
Cask Body Maximum	799.1	30.0	—	—
Inner Shell Average	137.0	—	—	—

d. The Quick-Disconnect Valve Cover Plate Seal maximum temperature is considered bounded by the result of the top impact limiter pin puncture HAC. Thus, the side puncture result is not reported.

3.1.4 Summary Tables of Maximum Pressures

The maximum internal pressures in the RT-100 are determined using the maximum temperatures presented in Table 3.1.3-1, Table 3.1.3-2, and Table 3.1.3-3 above. Details of these pressure calculations are presented in Section 3.3.2 for NCT and in Section 3.4.3 for HAC. Table 3.1.4-1 presents a summary of the maximum pressure calculations for normal and accident conditions. These pressures are utilized in the structural evaluation presented for the cask body in Sections 2.6 and 2.7.

Table 3.1.4-1 RT-100 Summary of Maximum Normal and Hypothetical Accident Condition Pressures

Condition	Maximum Pressure
Normal Conditions of Transport (MNOP)	342.7 kPa (49.7 psia)
Hypothetical Accident Conditions	689.4 kPa (100 psia)

3.2 Material Properties and Component Specifications

The material properties and specifications for the RT-100 materials of construction are presented in this section. The determination of material properties are carefully evaluated to ensure that for each thermal analysis:

- The appropriate thermal properties for the package materials are correctly incorporated into the thermal evaluations.
- Appropriate expressions are used for conductive, convective, and radiative heat transfer among package components, and from the surfaces of the package to the environment.

3.2.1 Material Properties

The thermal evaluation of the RT-100 is performed using material properties taken from standard industry references or manufacturer provided data in Tables 3.2.1-1 through 3.2.1-4. The thermal absorptivities and emissivities are appropriate for the package surface conditions and each thermal condition. When reporting a property as a single value, the evaluation shows that this value bounds the equivalent temperature-dependent property. This section includes references for the data provided.

Only room temperature values of conductivity, density, and specific heat are available for General Plastics FR-3700 series LAST-A-FOAM [Ref. 10, 11, and 12]. Quantitative temperature dependent material properties are not provided. However, most of the foam remains at temperatures close to ambient due to the dimensions of the RT-100 impact limiters which result in long heat conduction paths (see Figure 3.3.1-3). Thus, reduction in the foam thermal properties due to elevated temperatures will not be significant. Therefore, the use of temperature-independent thermal properties is justified.

Information on the EPDM O-ring material is provided in TRELLEBORG, Aug. 2011 Edition [Ref. 8] and PARKER O-RING Handbook [Ref. 16] for two different suppliers. The temperature range specified in Table 3.2.1-1 is conservative from the values specified in those two references. Additional information on the O-rings is presented in Appendices Attachment 3.5-1 and Attachment 3.5-2.

Table 3.2.1-1 Temperature-Independent Material Properties

Material	Properties	Reference Page Number	Value
Stainless Steel 304	Density	Ref.24: Page 744	8030 kg/m ³
	Emissivity (fire)	Ref. 2	0.9
	Emissivity (cool-down)	Ref. 2	0.8
	Emissivity (normal condition)	Ref. 5: Page 750 and 929	0.2
Lead	Density	Ref. 5: Page 907	11340 kg/m ³
	Melting Point	Ref. 5: Page 907	328°C (601 K)
Ceramic Paper	Density	Ref. 9	176.2 kg/m ³ (11 lb/ft ³)
	Specific Heat		1172.5 J/kg-K @1366.5K (0.28 BTU/lb-°F @ 2000°F)

Proprietary Information Content Withheld Under 10 CFR 2.390

Seal (EPDM)	Working Temperature	Ref. 8 & 16	-45°C to 150°C
-------------	---------------------	-------------	----------------

Table 3.2.1-2 Temperature-Dependent Material Properties—Stainless Steel 304

[Ref. 13, page 765]

Temperature (°C)	Specific Heat (J/kg-K)	Thermal Conductivity (W/m-K)
20	472.6	14.8
50	483.6	15.3
75	493.1	15.8
100	499.4	16.2
125	506.7	16.6
150	511.4	17.0
175	520.1	17.5
200	525.7	17.9
225	530.0	18.3
250	532.5	18.6
275	536.5	19.0
300	541.7	19.4
325	545.5	19.8
350	547.7	20.1
375	551.4	20.5
400	552.3	20.8
425	557.0	21.2
450	557.8	21.5
475	562.3	21.9
500	563.1	22.2
525	566.3	22.6
550	568.1	22.9
575	571.2	23.3
600	572.9	23.6
625	575.9	24.0
650	577.5	24.3
675	580.4	24.7
700	581.9	25.0
725	585.8	25.4
750	587.2	25.7

Table 3.2.1-3 Temperature-dependent Material Properties—Lead

[Ref. 5, page 907]

Temperature (°C)	Specific Heat (J/kg- K)	Thermal Conductivity (W/m- K)
-173.15	118	3.97E+01
-73.15	125	3.67E+01
26.85	129	3.53E+01
126.8	132	3.40E+01
326.8	142	3.14E+01

Table 3.2.1-4 Temperature-dependent Material Properties—Ceramic Paper

[Ref. 9]

Temperature (°C)	Thermal Conductivity (W/m-K)
93.3	4.759E-02
204.4	5.206E-02
315.6	5.912E-02
426.7	6.907E-02
537.8	8.219E-02
648.9	9.834E-02
760.0	1.174E-01
871.1	1.396E-01

3.2.2 Component Specifications

This section includes the technical specifications of RT-100 components that are important to the thermal performance, as illustrated by the following examples:

- In the case of seals, the operation temperature limits
- Maximum allowable service temperatures for package components
- Minimum allowable service temperature of all components, which are less than or equal to -40 °C (-40 °F).

Table 3.2.2-1 lists the maximum and/or minimum allowable temperatures for the critical cask components.

Table 3.2.2-1 Component Specifications – Minimum and Maximum Temperatures

Material	Min. Temp.	Max. Temp.	Reference
304/ 304L SS	-	>1400°C (Melting Temp.)	Ref. 14
Lead	-	328°C (Melting Temp.)	Ref. 5
Polyurethane Foam	-	1093°C (2000°F of Foam Char Temp.)	Ref. 15
Seal (EPDM)	-45°C	150°C	Ref. 8 & 16

3.2.3 Content Properties

As described in Chapter 1, Section 1.2.2.3 (Physical and Chemical Form – Density, Moisture Content and Moderators), the RT-100 is designed to transport contents that include contaminated resins and filters. The contents include secondary containers and may also include shoring. Resins are made of thermoplastics such as polystyrene, or material such as inorganic carbon or zeolite. Filters may be constructed from thermoplastics such as nylon, polyester, or polypropylene, or paper. Secondary containers are constructed of either coated/painted carbon steel or stainless steel, or a thermoplastic such as polyethylene or polypropylene. The filter media may be held within a stainless steel cartridge. Shoring can be made of wood or one or several of the materials comprising the secondary containers.

Based on the ASME code, Section II-D [Ref. 13], the acceptable temperature of the carbon steel and stainless steel material is approximately 525°C (977°F) for the range of loads and stresses occurring under NCT and HAC.

The melting temperatures of thermoplastics range from 100°C (212°F) up to 250°C (482°F) SFPE Handbook of Fire Protection Engineering, [Ref. 21], which typically soften at these temperatures and do not produce volatiles that could react with any of the contents. The auto-ignition temperature of thermoplastics is above 300°C (572°F) [Ref. 21].

The auto-ignition temperatures of paper and wood vary widely and are a function of their specific composition and moisture content. A commonly accepted value for the auto-ignition point for paper is 232°C (450°F) “Fundamentals of Combustion Processes,” [Ref. 22]. The auto-ignition point for wood has been shown to be at least 300°C (572°F) An Experimental Study of Autoignition of Wood, T. Poespowati, World Academy of Science, Engineering and Technology 23, 2008. [Ref. 23].

A summary of the maximum temperature specifications for the RT-100 contents is provided in Table 3.2.3-1.

Table 3.2.3-1 Maximum Temperature Limits for RT-100 Content Materials

Material	Maximum Temperature	Reference
Carbon/Stainless Steel	525°C	Ref. 13
Thermoplastics	300°C	Ref. 21
Paper	232°C	Ref. 22
Wood	300°C	Ref. 23

3.3 Thermal Evaluation under Normal Conditions of Transport

This section describes the thermal evaluations performed for the RT-100 for the NCT specified in 10 CFR 71.71 [Ref. 2]. The evaluation considers the response of the RT-100 to a range of temperature and environmental conditions as described in Section 3.3.1. The results are compared with allowable limits of temperature, pressure, etc., for the package components. The information is presented in summary tables, along with statements and appropriate comments. Information that is to be used in other sections of the review is identified. The margins of safety for package temperatures, pressures, and thermal stresses, including the effects of uncertainties in thermal properties, test conditions and diagnostics, and analytical methods are addressed.

The analyses are shown to be reliable and repeatable.

The following general information is considered and included in addressing the sections below, as appropriate:

- Assumptions that are used in the analysis are clearly described and justified.
- For computer analyses, including finite element analyses, the computer program is described and shown to be well benchmarked, widely used for thermal analyses, and applicable to the evaluation.
- Models and modeling details are clearly described.
- The methods used are properly referenced or developed in the application.
- These methods are correctly applied.
- The evaluation considers changes in package geometry and material properties resulting from structural and thermal tests under NCT and HAC.
- The required temperature and thermal boundary conditions for normal conditions of transport and hypothetical accident conditions are correctly applied.
- The time interval after the fire test is adequate to assure that maximum component temperatures and post-fire steady-state temperatures are achieved.

- The maximum temperatures and pressures of the components do not exceed their allowable values.
- Combustion of package components are considered, including the heat produced.
- Temperature data is reported at gaskets, valves, and other containment boundaries, particularly for temperature-sensitive materials as well as, for the overall package.
- Appropriate corrections and evaluations that account for differences in the thermal test are included for conditions like ambient temperature, decay heat of the contents, or package emissivity or absorptivity.
- Both interior and exterior temperatures are included.
- The damage caused by the tests and the results of any measurements made is reported in detail, including photographs of the testing and the test specimen.

3.3.1 Heat and Cold

Section 3.3.1 demonstrates that the tests for NCT do not result in a significant reduction in the RT-100 effectiveness. The following items are considered and addressed:

- Degradation of the heat-transfer capability of the packaging (such as creation of new gaps between components)
- Changes in material conditions or properties (e.g., expansion, contraction, gas generation, and thermal stresses) affecting structural performance
- Changes in the packaging affecting containment, shielding, or criticality (such as thermal decomposition or melting of materials)
- Ability of the packaging to withstand the tests under HAC

The component temperatures and pressures are compared to their allowable values and do not exceed them. This section explicitly shows that the package meets the maximum temperature of the accessible package surface is less than 50 °C (122 °F) for non-exclusive-use shipment or 85 °C (185 °F) for exclusive use shipment when the package is subjected to the heat conditions of 10 CFR 71.43(g) [Ref. 2].

3.3.1.1 Load Cases

Four load cases are analyzed in order to evaluate the RT-100 for the range of temperature and solar insolation conditions specified in 10 CFR 71.71 [Ref. 2] for normal conditions:

- Hot Case 1
- Hot Case 2
- Cold Case 1

- Cold Case 2

Hot case 1 is based on the requirements of 10 CFR 71.71(c)(1) [Ref. 2], which is one of the extreme initial conditions for normal conditions and a precursor for the hypothetical fire accident evaluation. It has the following conditions:

- Ambient temperature, 38°C (100°F)
- Initial temperature, 38°C (100°F)
- Heat transfer to ambient by natural convection, still air
- Heat transfer to ambient by radiation
- Steady-state solar insolation, 776 W/m² for flat surface and 388 W/m² for curved surface
- Internal heat load as a uniform heat flux, 13.04 W/m²

Hot case 2 is based on the requirements of 10 CFR 71.43(g) [Ref. 2] and has the following conditions:

- Ambient temperature, 38°C (100°F)
- Initial temperature, 38°C (100°F)
- Heat transfer to ambient by natural convection, still air
- Heat transfer to ambient by radiation
- No solar insolation, in shade
- Internal heat load as a uniform heat flux, 13.04 W/m²

Cold case 1 is based on the requirements of 10 CFR 71.71(c)(2) [Ref. 2], which is another extreme initial condition for the NCT test evaluation. It has the following conditions:

- Ambient temperature, -40°C (-40°F)
- Initial temperature, -40°C (-40°F)
- Heat transfer to ambient by natural convection, still air
- Heat transfer to ambient by radiation
- No solar insolation, in shade
- Internal heat load as a uniform heat flux, 13.04 W/m²

Cold case 2 is based on requirements of 10 CFR 71.71(b) [Ref. 2] and has the following conditions:

- Ambient temperature, -29°C (-20°F)
- Initial temperature, -29°C (-20°F)
- Heat transfer to ambient by natural convection, still air
- Heat transfer to ambient by radiation
- No solar insolation
- Internal heat load as a uniform heat flux, 13.04 W/m²

Among them, Hot case 1 and Cold case 1 are two extreme conditions for the analyses. Hot case 1

is also referred to as the “normal hot” condition on which conservative boundary conditions are applied. This case provides the highest temperature distributions within the cask, and is used as initial conditions for evaluation of the hypothetical fire accident event as described in Section 3.4.

3.3.1.2 Analytical Model

The thermal evaluation of the RT-100 is performed using the ANSYS finite element computer software [Ref. 3]. The cask model is made of 3D thermal solid elements (SOLID90) that represent the major components of the cask. Contact between the lead and the inner and outer shells are modeled as bonded surfaces for thermal analyses in order to maximize heat input to the lead. The contact between the upper flange and the primary lid is modeled by a pair of 3D thermal contact elements (CONTA174) and 3D target elements (TARGE170), as are the other contacts between the primary lid and the secondary lid, the bolts with the primary lid, and the bolts with the secondary lid.

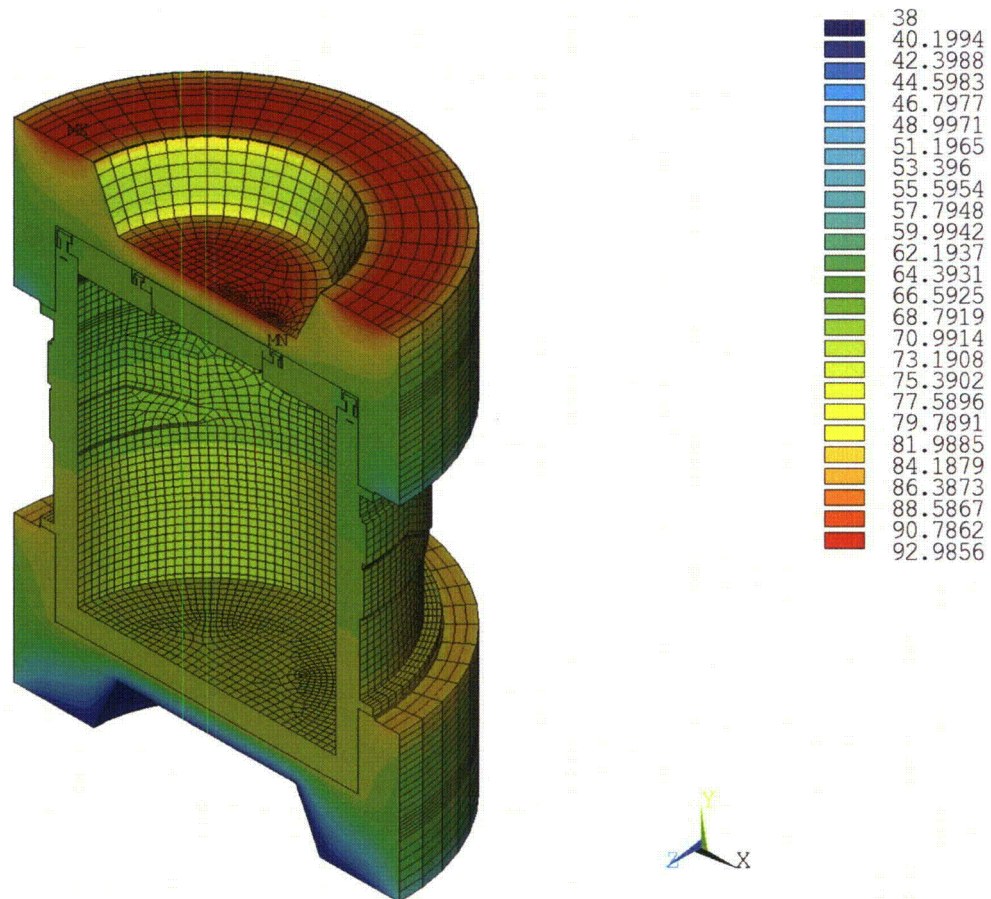
For conservatism, the top impact limiter is modeled as without the stainless steel plate covering the central hollow portion of the limiter. Thus, the concave area on the top impact limiter is exposed to solar insolation and/or fire. This approach leads to a conservatively high temperature over the top impact limiter. The contacts between the impact limiters and the cask body are also modeled by pairs of 3D thermal contact elements (CONTA174) and 3D target elements (TARGE170) between the relative surfaces.

A depiction of the ANSYS thermal model of the RT-100 is provided in Figure 3.3.1-1 and Figure 3.3.1-2. Additional details regarding the modeling and analysis of the RT-100 are presented in Calculation Package RTL-001-CALC-TH-0201, Rev. 6 [Ref. 4].

**WITHHELD PER
10 CFR 2.390**

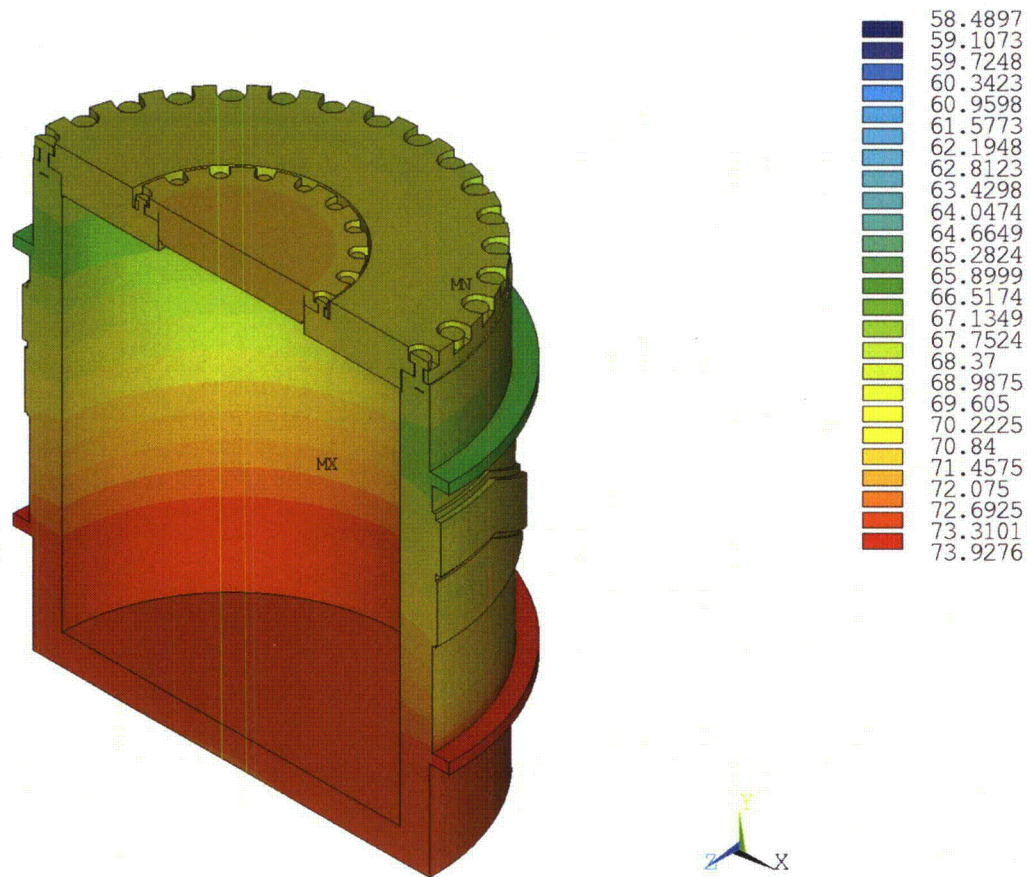
3.3.1.3 Analysis Results

The results of the steady state analyses of the cask model with impact limiters are presented in the form of temperature contour plots. Figure 3.3.1-3 through Figure 3.3.1-6 show the temperature contour plots for Hot case 1. Hot case 1 predicts the maximum temperatures experienced during NCT. The figures show the package, cask body, inner shell surface and lead shielding material, respectively. Figure 3.3.1-7 and Figure 3.3.1-8 provide the results for Hot case 2. Figure 3.3.1-9 and Figure 3.3.1-10 provide the results for Cold case 1. Cold case 1 represents the temperatures experienced by the package during extreme cold conditions. Figure 3.3.1-11 and Figure 3.3.1-12 provide the results for Cold case 2. Maximum temperature results are obtained by selecting the FE model component or material of interest and sorting the nodal results. Table 3.1.3-1 shows the maximum temperatures of the cask under NCT based on the steady state solution.



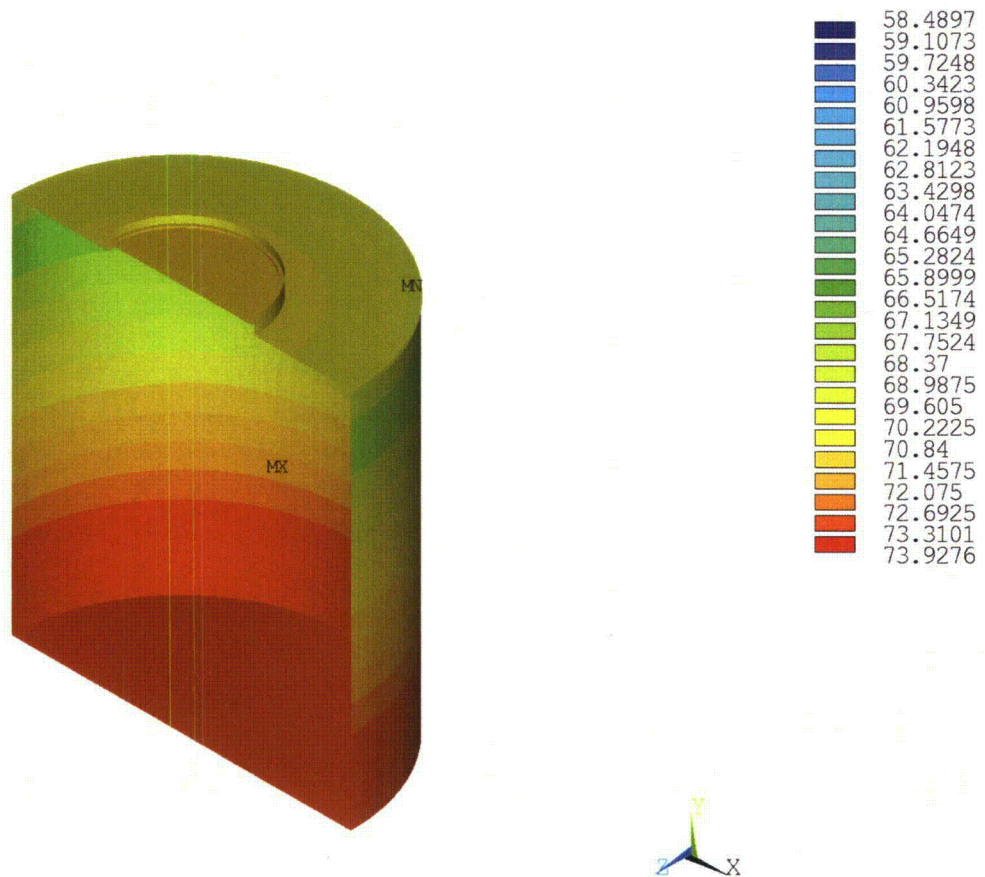
NCT—Case 1, Steady-State Boundary Conditions (Degrees Celsius)

Figure 3.3.1-3 Temperature Contour Plot of Package—Hot Case 1



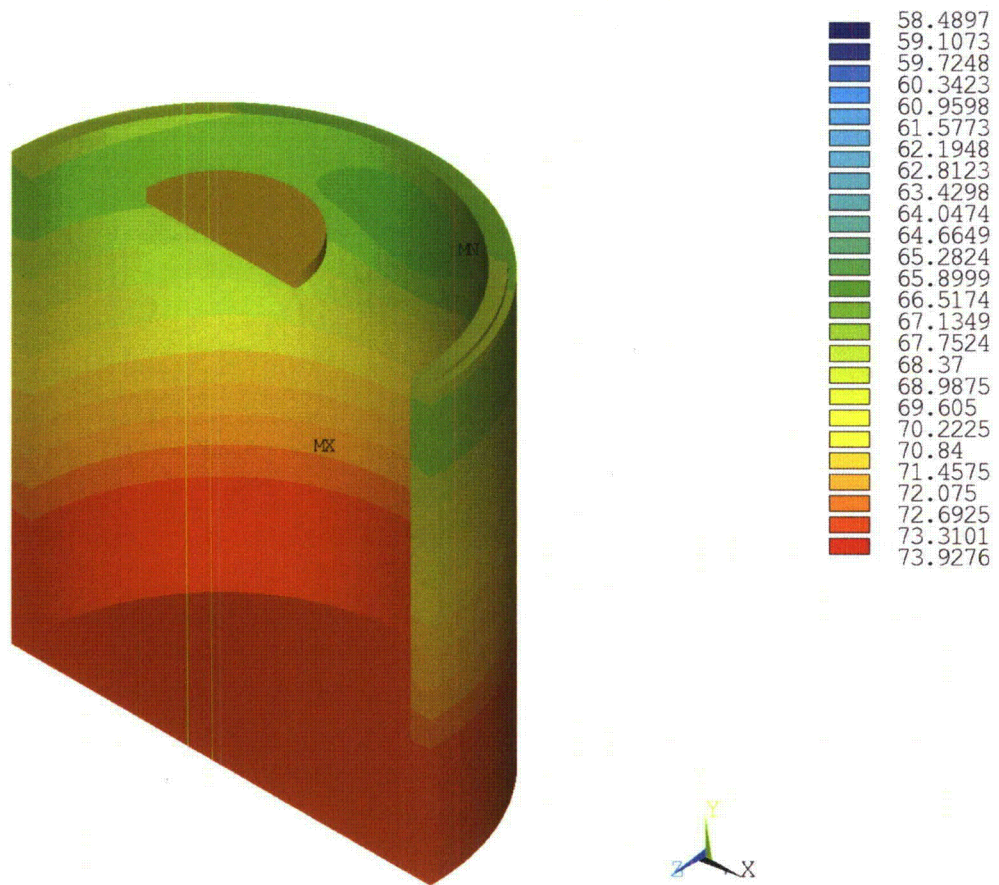
NCT--Case 1, Steady-State Boundary Conditions (Degrees Celsius)

Figure 3.3.1-4 Temperature Contour Plot of Cask Body—Hot Case 1



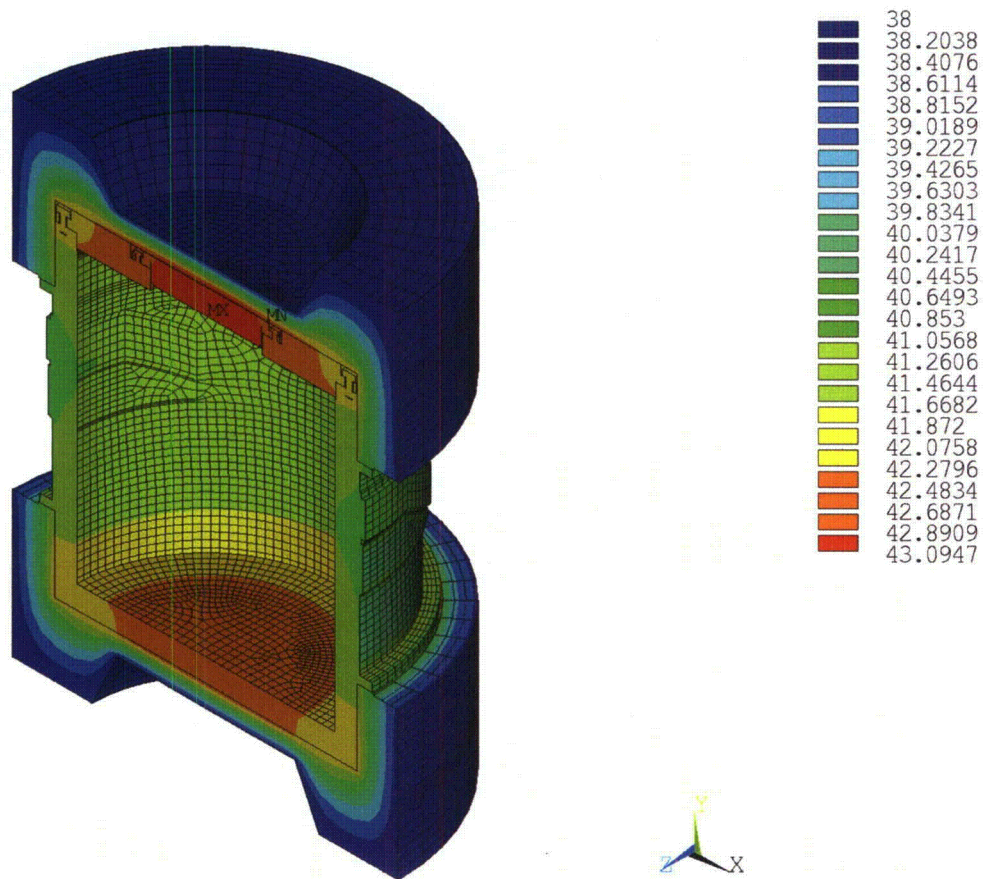
NCT—Case 1, Steady-State Boundary Conditions (Degrees Celsius)

Figure 3.3.1-5 Temperature Contour Plot of Inner Shell Surface—Hot Case 1



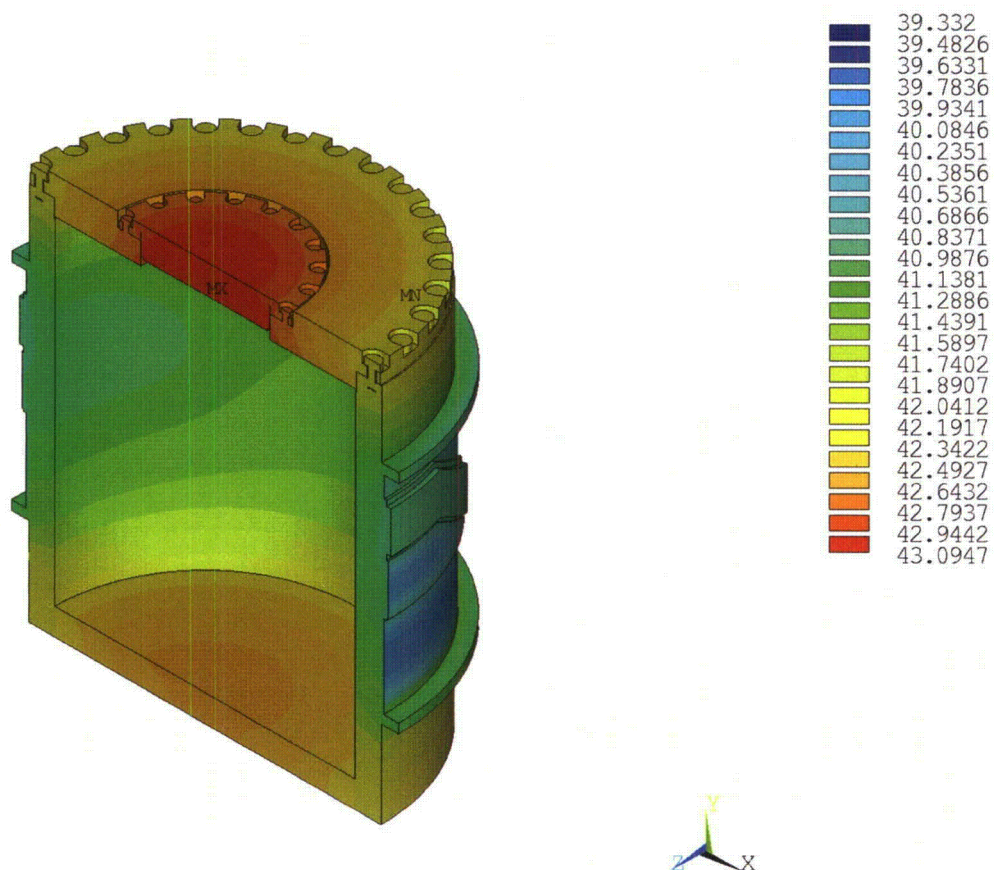
NCT—Case 1, Steady-State Boundary Conditions (Degrees Celsius)

Figure 3.3.1-6 Temperature Contour Plot of Lead Shielding—Hot Case 1



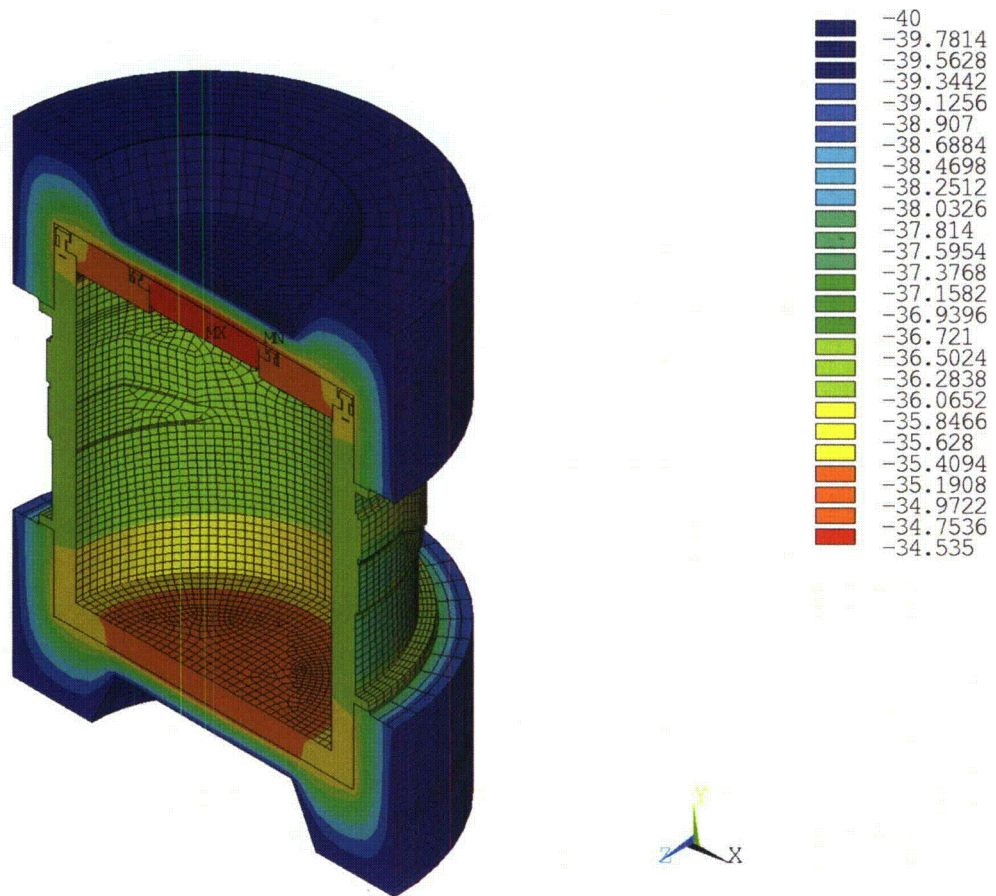
NCT—Case 2, Steady-State Boundary Conditions (Degrees Celsius)

Figure 3.3.1-7 Temperature Contour Plot of Package—Hot Case 2



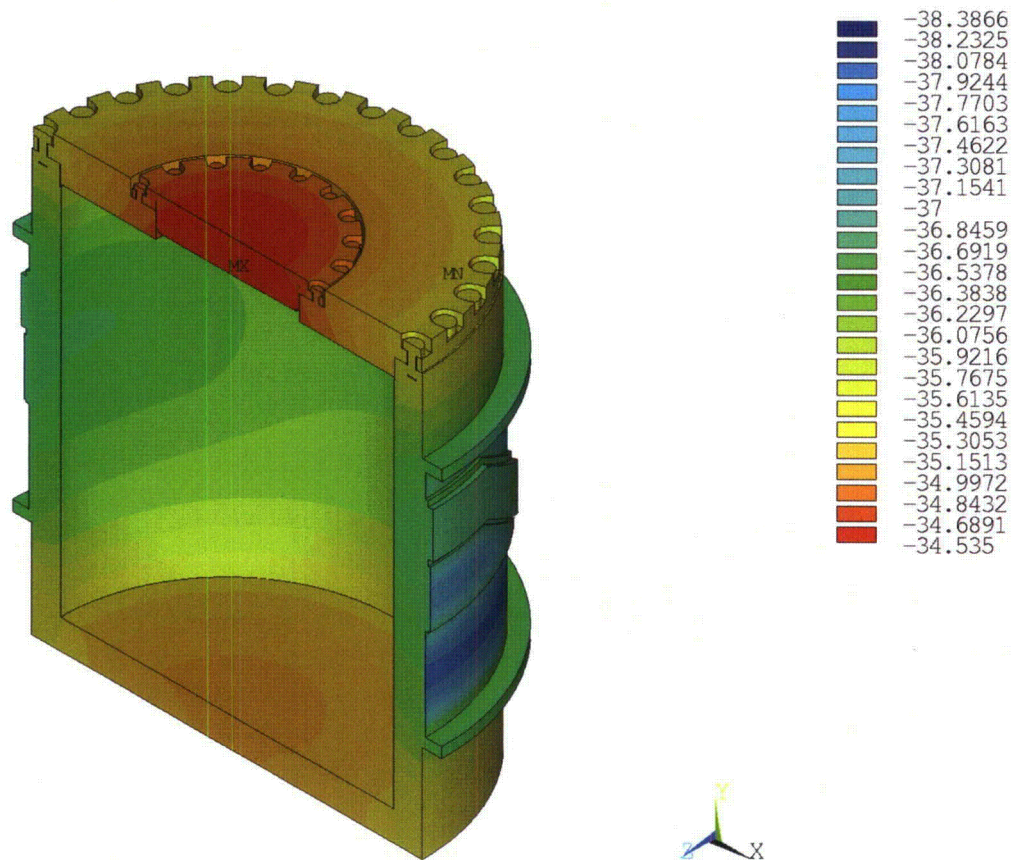
NCT—Case 2, Steady-State Boundary Conditions (Degrees Celsius)

Figure 3.3.1-8 Temperature Contour Plot of Cask Body—Hot Case 2



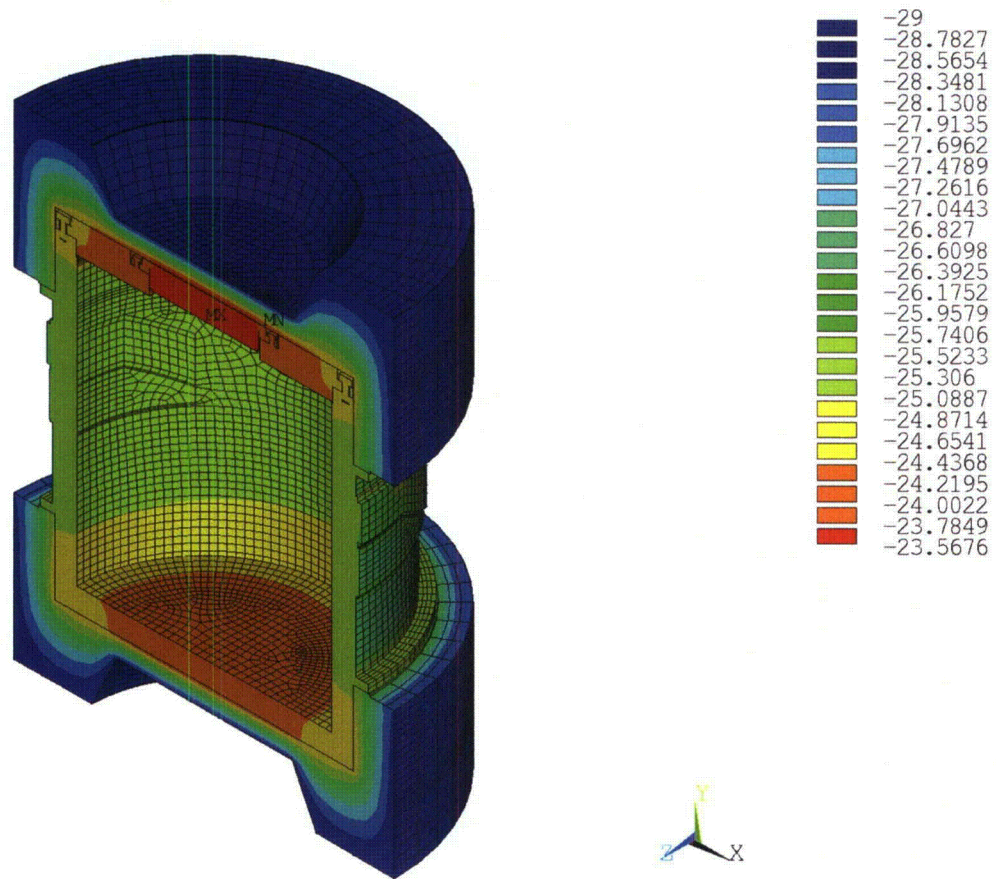
NCT—Case 3, Steady-State Boundary Conditions (Degrees Celsius)

Figure 3.3.1-9 Temperature Contour Plot of Package—Cold Case 1



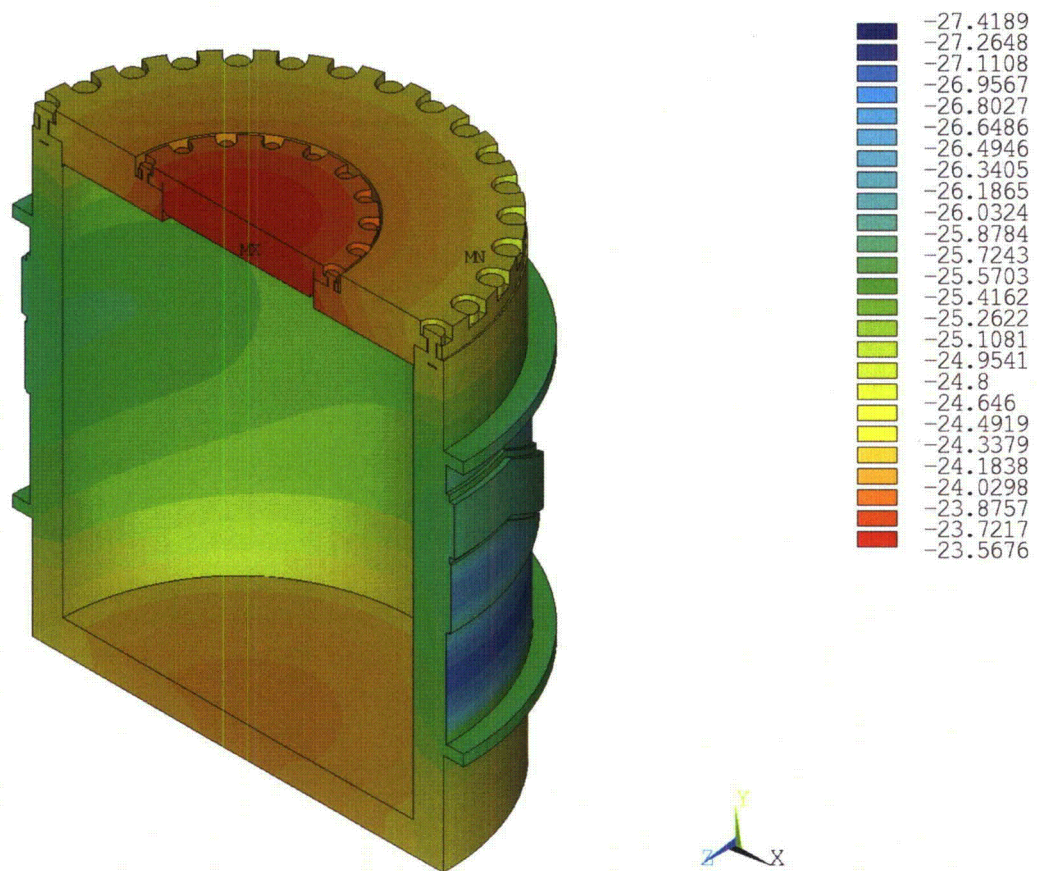
NCT—Case 3, Steady-State Boundary Conditions (Degrees Celsius)

Figure 3.3.1-10 Temperature Contour Plot of Cask Body—Cold Case 1



NCT—Case 4, Steady-State Boundary Conditions (Degrees Celsius)

Figure 3.3.1-11 Temperature Contour Plot of Package—Cold Case 2



NCT—Case 4, Steady-State Boundary Conditions (Degrees Celsius)

Figure 3.3.1-12 Temperature Contour Plot of Cask Body Cold Case 2

3.3.2 Maximum Normal Operating Pressure

The maximum pressure in the RT-100 for NCT is calculated using the maximum temperatures determined for the range of normal condition load cases. The calculation considers possible sources of gases including the following:

- Gases initially present in the package
- Saturated vapor, including water vapor from the contents or packaging
- Hydrogen or other gases resulting from thermal- or radiation-induced decomposition of materials such as water or plastics

Summary of the pressure calculation is provided in the following sections. Additional details are provided in Calculation Package RTL-001-CALC-TH-0102, Rev. 6 [Ref. 6].

3.3.2.1 Calculation Method

To determine the maximum normal operating pressure, the temperature of gas mixture within the cask is evaluated. Maximum temperature of the cask cavity under normal condition is bounded by the upper and lower temperature range of 80 °C (176°F) to -29 °C (-20°F). The total pressure in the cavity is represented by the sum of the primary contributors to the pressure. These are the pressure due to the increased temperature of the cavity gas (ideal gas law), the pressure due to the presence of water vapor, and the pressure due to the generation of gas via radiolysis.

The restriction of the contents to inorganic materials eliminates the potential for gas generation due to thermal degradation or biological activity. Thus, these gas sources are not considered in the evaluation. However, water vapor is present in trace quantities. Therefore, the analysis considers the contribution from the radiolytic decomposition of residual water in the cask cavity.

Per the ideal gas law, air pressure and water vapor pressure are directly proportional to the temperature, and with increase in temperature the pressure also increases. The upper bound temperature results in a higher maximum normal operating pressure for the cask compared to the lower bound. The gas mixture in the cavity is conservatively assumed to be at 80 °C (176°F).

3.3.2.2 Pressure Due to the Initially Sealed Air in the Cavity

Per the ideal gas law, the partial pressure of the air (P_{air}) initially sealed in the fixed volume of the cask at the ambient temperature as it is heated to 80 °C (176 °F) is:

$$P_1 \times T_2 = P_2 \times T_1$$

$$P_{\text{air}} = 101.35 \text{ kPa}[(353.15 \text{ K}) / (294.25 \text{ K})] = 121.64 \text{ kPa (17.64 psia)}$$

3.3.2.3 Pressure Due to the Water Vapor in the Cask

The cask cavity is assumed to contain a small amount of water. By conservatively assuming a condensing surface temperature of 80 °C (176 °F), the water vapor pressure, P_{wv} , at this temperature is:

47.34 kPa [6.87 psia], Fundamentals of Fluid Mechanics, Table B.2, pg. 831 [Ref. 17], Attachment 3.5-3.

Adding the water vapor pressure at 80 °C (176 °F) to the partial pressure of the air in the sealed cask at this temperature gives:

$$\begin{aligned} P_2 &= P_{\text{air}} + P_{\text{wv}} = 121.64 + 47.34 = 169.0 \text{ kPa} \\ &= 169.0 \text{ kPa} \times 0.145 \text{ psi/kPa} = [24.51 \text{ psia}] \end{aligned}$$

3.3.2.4 Pressure Due to Generation of Gas

Solidified or dewatered material may contain some water. Therefore, radiolytic generation of gases from this water could occur. Hydrogen and oxygen may be produced in the cask by radiolytic decomposition of residual water in the cask contents. As described in Chapter 1, Section 1.2.2.6, the maximum quantity of hydrogen must be limited to less than 5% to ensure that an explosive quantity does not accumulate.

The cask atmosphere can be assumed to contain 5% of hydrogen (H₂) gas due to radiolysis of the water. By stoichiometry of the water molecule (H₂O), the cask atmosphere will also contain 2.5% oxygen (O₂) gas generated by radiolysis. Partial pressures in an ideal gas mixture are additive and behave the same as ideal gas volume fraction or mole fractions. Therefore, the partial pressure of hydrogen is described by the following equation:

$$\begin{aligned} P_{\text{H}_2} &= 0.05 P_{\text{pt}} \\ \text{Where, } P_{\text{pt}} &= P_{\text{air}} + P_{\text{wv}} + P_{\text{H}_2} + P_{\text{O}_2} \\ \text{Combining } P_{\text{air}} + P_{\text{wv}} &= P_2 \text{ and noting that } P_{\text{O}_2} = 0.5 \times P_{\text{H}_2}. \\ P_{\text{H}_2} &= 0.05 \times (P_2 + 1.5 P_{\text{H}_2}) \\ \text{Solving the equation explicitly for } P_{\text{H}_2} &\text{ give:} \\ P_{\text{H}_2} &= [0.05 P_2] / [1 - 0.05 (1.5)] \\ &= [0.05 * 169.0 \text{ kPa}] / [1 - 0.05 (1.5)] \\ &= 9.14 \text{ kPa [1.32 psia]} \end{aligned}$$

3.3.2.5 Total Pressure

Based on the stoichiometric relationship between hydrogen and oxygen liberated by radiolysis of water, and again combining the pressure of the initially sealed air and water vapor as P₂, the total pressure in the cask at 80°C (176°F) is:

$$\begin{aligned} P_{\text{Total}} &= P_2 + 1.5 P_{\text{H}_2} \\ &= 169.0 \text{ kPa} + 1.5 * 9.14 \text{ kPa} \\ &= 182.71 \text{ kPa [26.5 psia]} \text{ (actual calculated MNOP)} \end{aligned}$$

The design basis maximum normal operating pressure (MNOP) value is conservatively set at 342.7 kPa (49.7 psia or 35 psig) for use in the cask structural analyses for NCT.

3.4 Thermal Evaluation under Hypothetical Accident Conditions

This section describes the thermal evaluation of the RT-100 under hypothetical accident conditions. The RT-100 is evaluated by finite element computer analysis rather than physical testing to demonstrate the performance of the cask in response to the fire test conditions specified in 10 CFR 71.73(c) [Ref. 2]. The HAC defined in 10 CFR 71.73(c) [Ref. 2] are applied sequentially, considering the damaged condition of the packaging following the 30-foot free drop and pin puncture accident events prior to the fire transient. For the accident condition thermal evaluation, the general comments in Section 3.3 are considered and addressed, as appropriate.

As described in Chapter 2, Section 2.7.3 (Puncture), different pin puncture configurations are considered in order to determine the worst case for the accident event. For the structural evaluation, the orientations considered are directly in the middle of the secondary lid to maximize the bending loads in the primary and secondary lids and prying forces in the bolts. The second configuration considers the pin impact directly into the side of the RT-100 to ensure that the outer shell is not punctured by the pin. For the thermal analysis, these two events are also considered to be limiting. The differences are in the location of the pin at impact.

3.4.1 HAC Fire Analysis—Pin Puncture Damage to Top Impact Limiter

The analytical model described in Section 3.3.1.2 is used to evaluate the RT-100 package with damage on the top impact limiter. For this case, the limiting configuration for the thermal analysis considers a pin puncture through the top impact limiter directly into the secondary lid at the location of the O-rings. The model placed a 150 mm (6 in) diameter hole through the upper impact limiter, directly exposing the secondary lid to the thermal environment of the hypothetical accident fire. The following section evaluates both pin puncture orientations to determine the effect to critical components such as the seal locations and lead shielding.

3.4.1.1 Initial Conditions—Pin Puncture Damage to Top Impact Limiter

Per Regulatory Position 1.1 in Regulatory Guide 7.8 [Ref. 20], the initial cask temperature distribution is considered to be at steady state with an ambient temperature of 38°C (100°F) and solar insolation prior to the HAC fire accident. To meet this requirement, the steady-state solution for NCT hot case 1 is used, obtained to the initial temperatures of the cask prior to the fire. The steady-state temperatures are applied as the first load step of the transient solutions. To account for damage to the package that results during the sequential drop accidents, damage due to pin puncture is considered during the top and side puncture. For the top impact limiter 150 mm diameter volume of material including the steel shell and FR3740 foam is removed at the point closest to the elastomer O-ring. This is a conservative approach since the puncture probe will not penetrate through the top skin of the impact limiter and compressed foam will remain beneath the point of impact. Figure 3.4.1-1 shows the temperature contour of the package prior to the fire accident and localized higher temperatures in the region of the damaged impact limiter. Figure 3.4.1-2 and Figure 3.4.1-3 show the cask body and inner shell cavity temperature distribution prior to the fire accident.

3.4.1.2 HAC Fire and Cool-down Analysis—Pin Puncture Damage to Top Impact Limiter

The thermal analysis for HAC includes a 30 minute transient fire followed by the prescribed post-fire cool-down period. The FE model described in Section 3.3.1.2 is analyzed by applying

the following boundary conditions. Following the initial load step in which the steady-state temperatures are applied, the analysis proceeds with the HAC fire transient for 30 minutes (1,800 seconds) followed by a cool-down period with the boundary conditions associated with NCT Hot case 1. The NCT Hot case 1 boundary conditions are applied as constants ignoring the day/night cool-down cycle. The following is a summary of the fire transient boundary conditions:

- Environment temperature, 800°C (1472°F)
- No solar insolation, 0 W/m²
- Forced convection, heat transfer coefficient = 10 W/m²·°C
- Radiation from the environment to package surface, flame emissivity = 0.9
- Internal heat load as a uniform heat flux, 13.04 W/m²

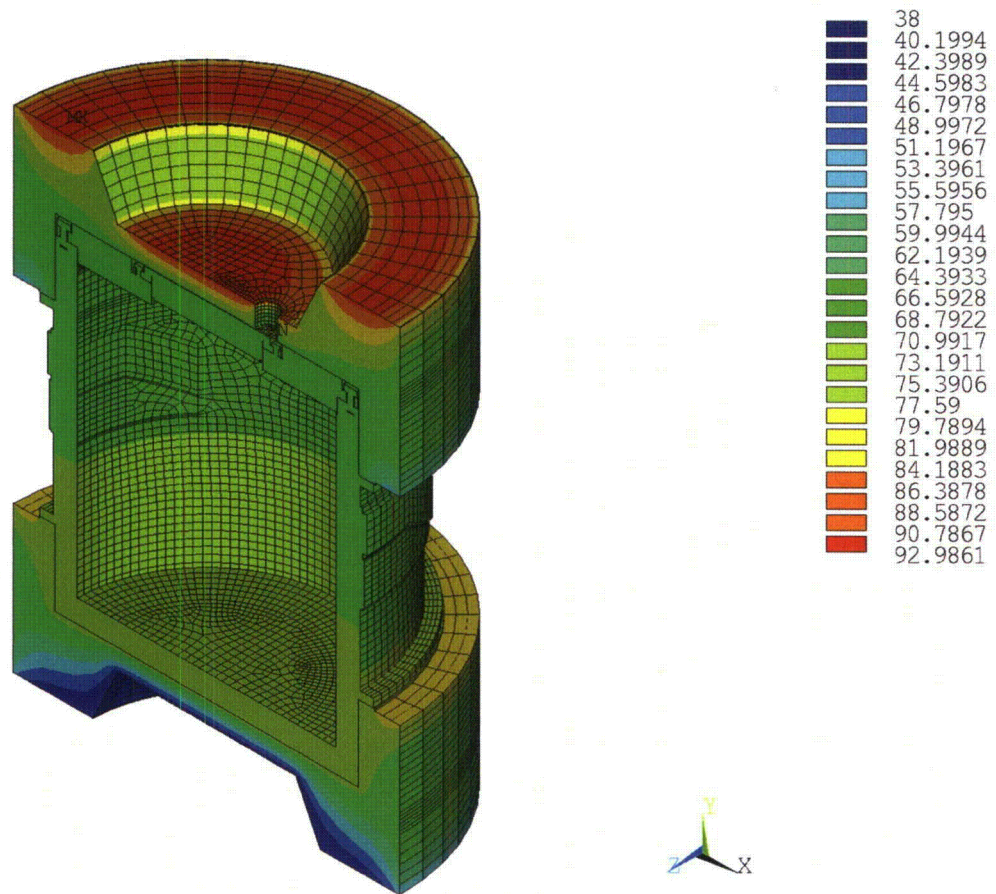
The cool-down analysis is performed for 216,000 seconds (2.5 days) with the following boundary conditions:

- Environment temperature, 38°C (100°F)
- Solar insolation applied as constant, 776 W/m² for flat surfaces and 388 W/m² for curved surfaces.
- Natural convection, heat transfer coefficient = 5 W/m²·°C
- Radiation from package surface to the environment, package emissivity = 0.8
- Internal heat load as a uniform heat flux, 13.04 W/m²

3.4.1.3 HAC Fire Analysis Results—Pin Puncture Damage to Top Impact Limiter

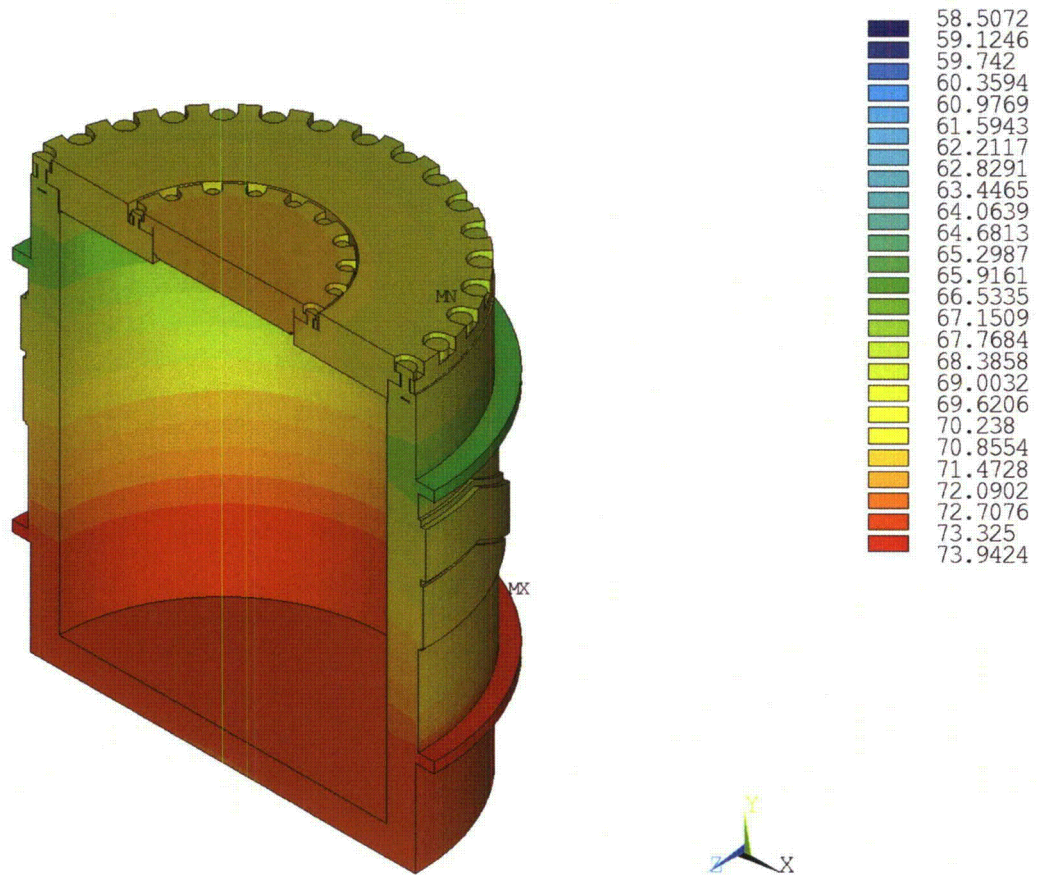
The temperature contour plots of the RT-100 package and cask body at the end of fire are shown in Figure 3.4.1-4 and Figure 3.4.1-5, respectively. Figure 3.4.1-6 and Figure 3.4.1-7 show the package and cask body temperature contours after the cool-down period. Figure 3.4.1-8 shows the temperature time-history from the start of the fire through the cool-down. As Figure 3.3.1-8 shows, the average inner shell temperature is 136.3°C (277.3°F) and is representative of the contents during the fire/cool-down transient. Figure 3.4.1-9 provides an enhanced view of the time-history data through the 30 minute fire and 2.5 hours of the cool down process. Figure 3.4.1-10 identifies the highest inner shell temperature at the point that it occurs, 48 minutes from the start of the fire. Figure 3.4.1-11 identifies the maximum lead shield temperature occurring 35 minutes after the start of the fire, at a point underneath the tie-down arms. This figure indicates that no melting of the lead shield occurs during the HAC fire.

Table 3.1.3-2 summarizes the maximum temperatures of the cask under HAC fire with pin puncture damage at the side of the cask body.



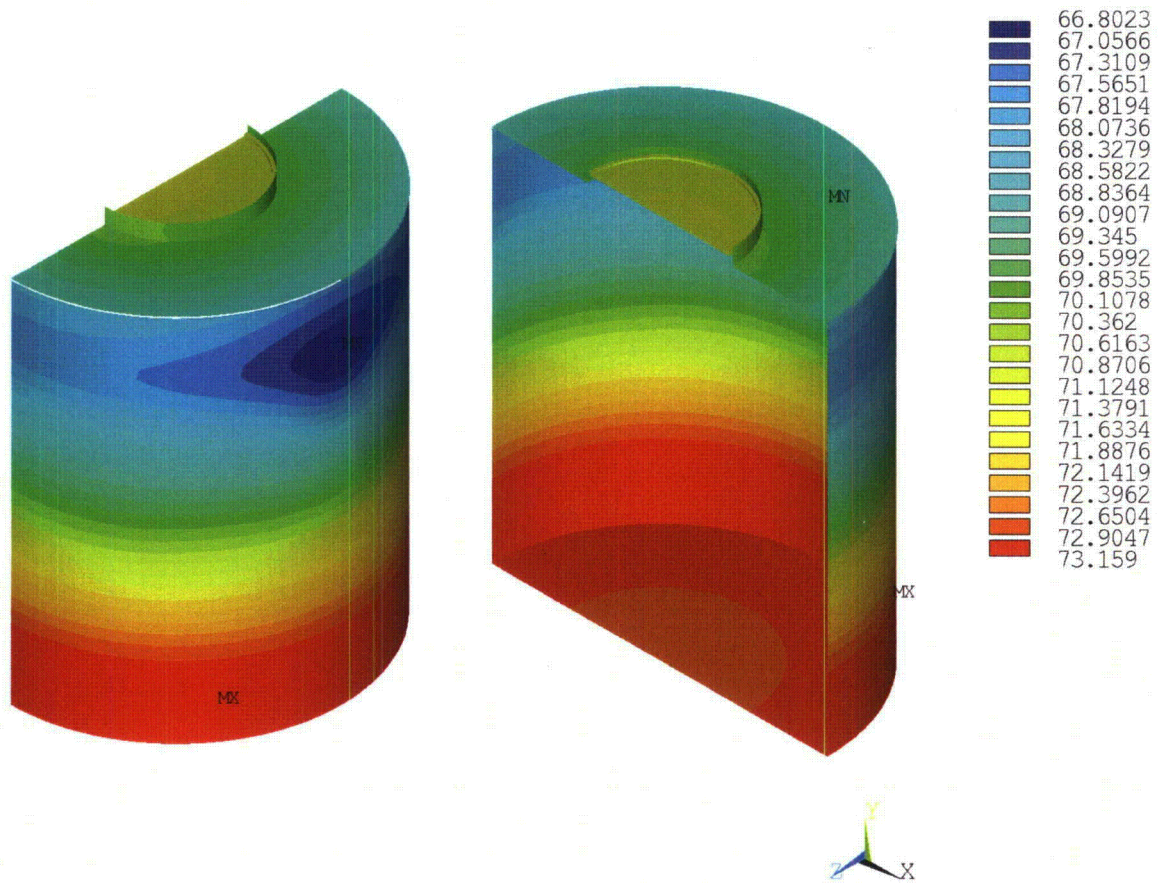
HAC—Fire Top Puncture, Steady-State Initial Conditions (Degrees Celsius)

**Figure 3.4.1-1 Temperature Contour Plot of Package Pre-Fire Fire Condition—
HAC Pin Damage on Top Impact Limiter**



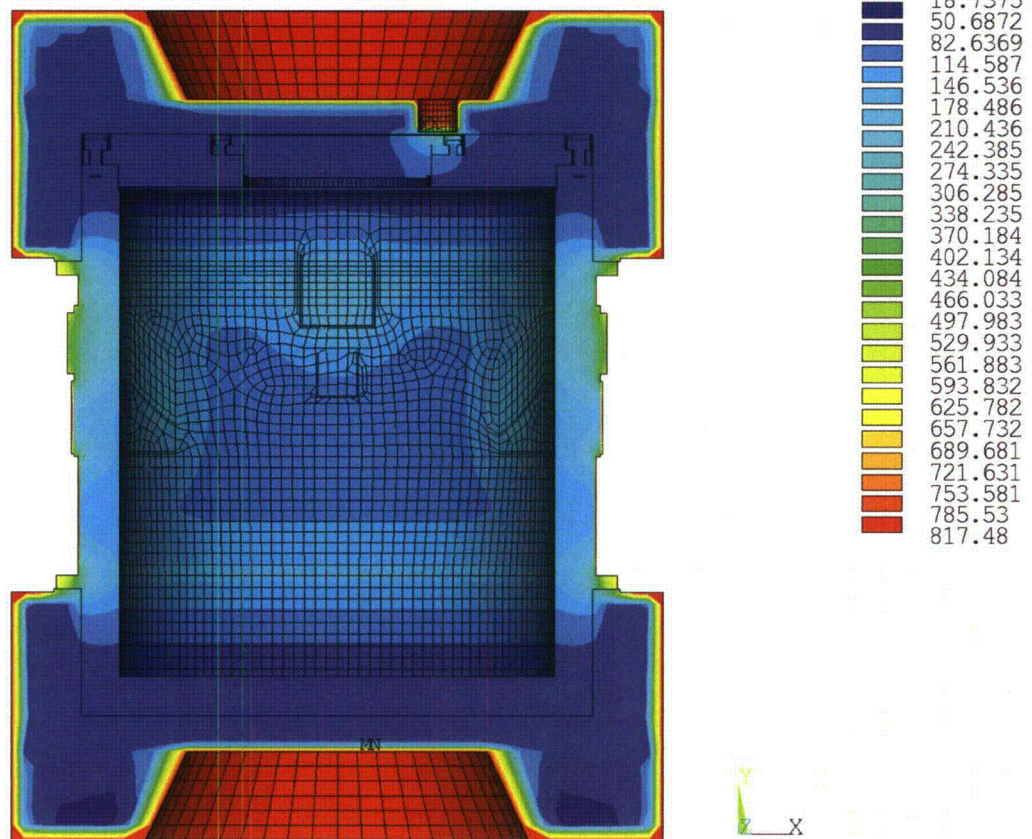
HAC—Fire Top Puncture, Steady-State Initial Conditions (Degrees Celsius)

Figure 3.4.1-2 Temperature Contour Plot of Cask Body Pre-Fire Condition—HAC Pin Damage on Top Impact Limiter



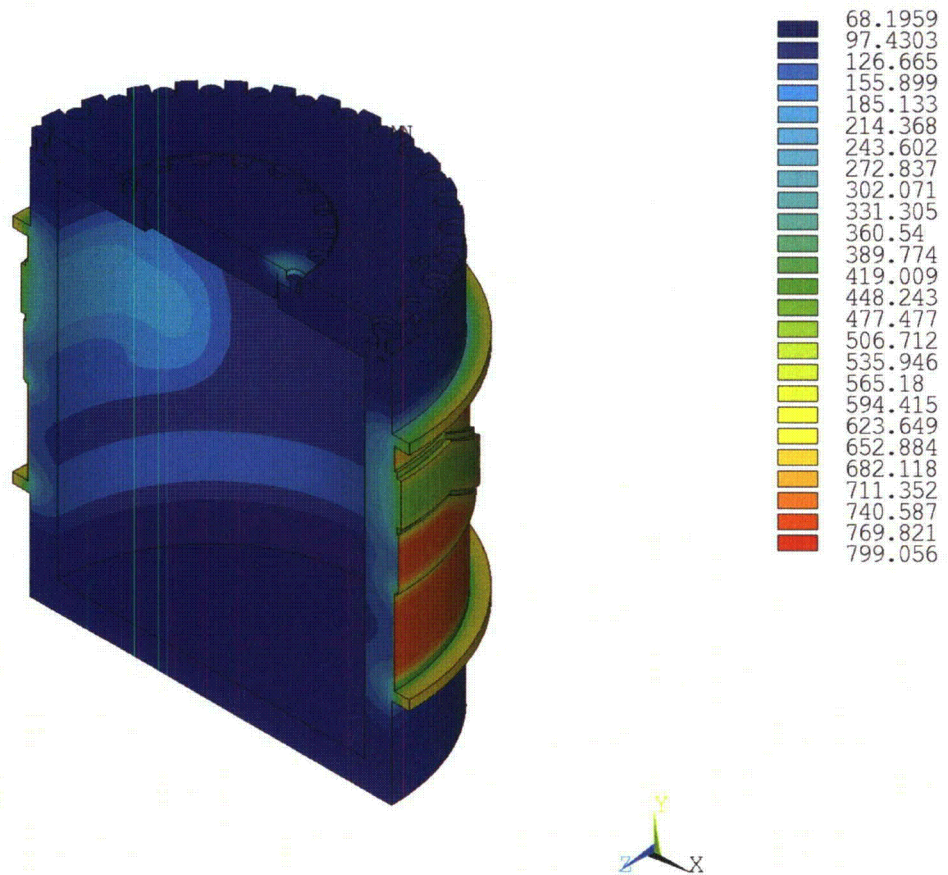
HAC—Fire Top Puncture, Steady-State Initial Conditions (Degrees Celsius)

**Figure 3.4.1-3 Temperature Contour Plot of Inner Shell Pre-Fire Condition—HAC
Pin Damage on Top Impact Limiter**



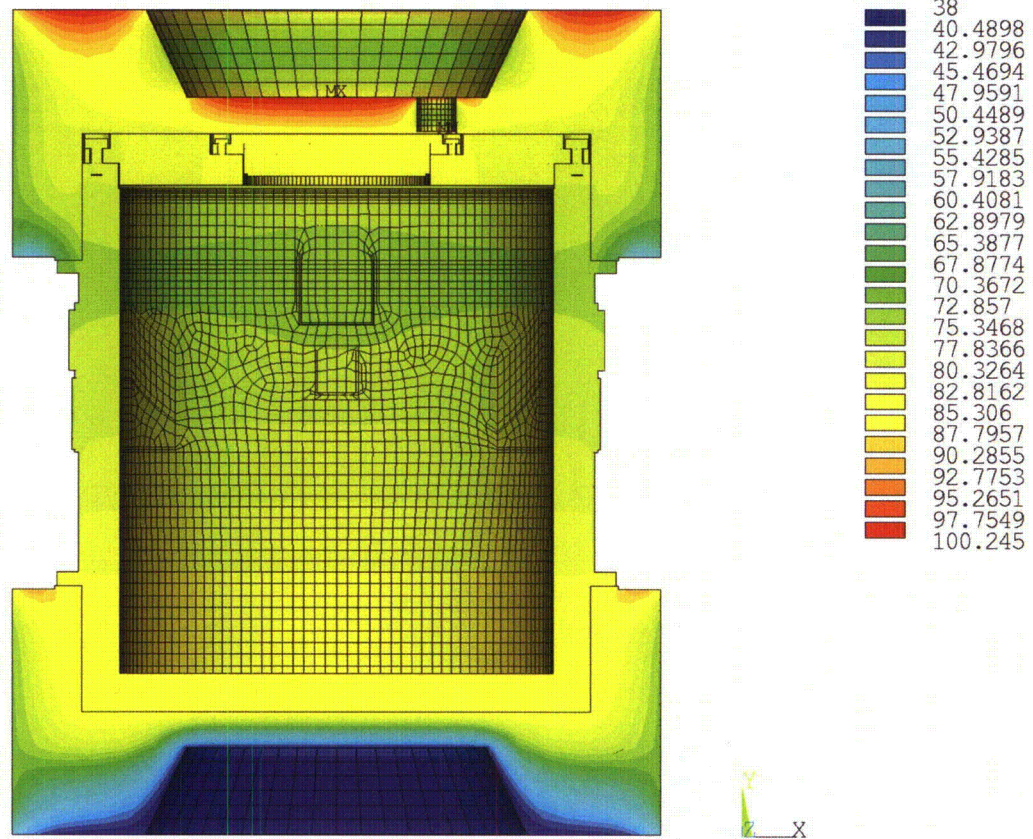
HAC—Fire Top Puncture, Steady-State Initial Conditions (Degrees Celsius)

Figure 3.4.1-4 Temperature Contour Plot of Package at the End of Fire—HAC Pin Damage on Top Impact Limiter



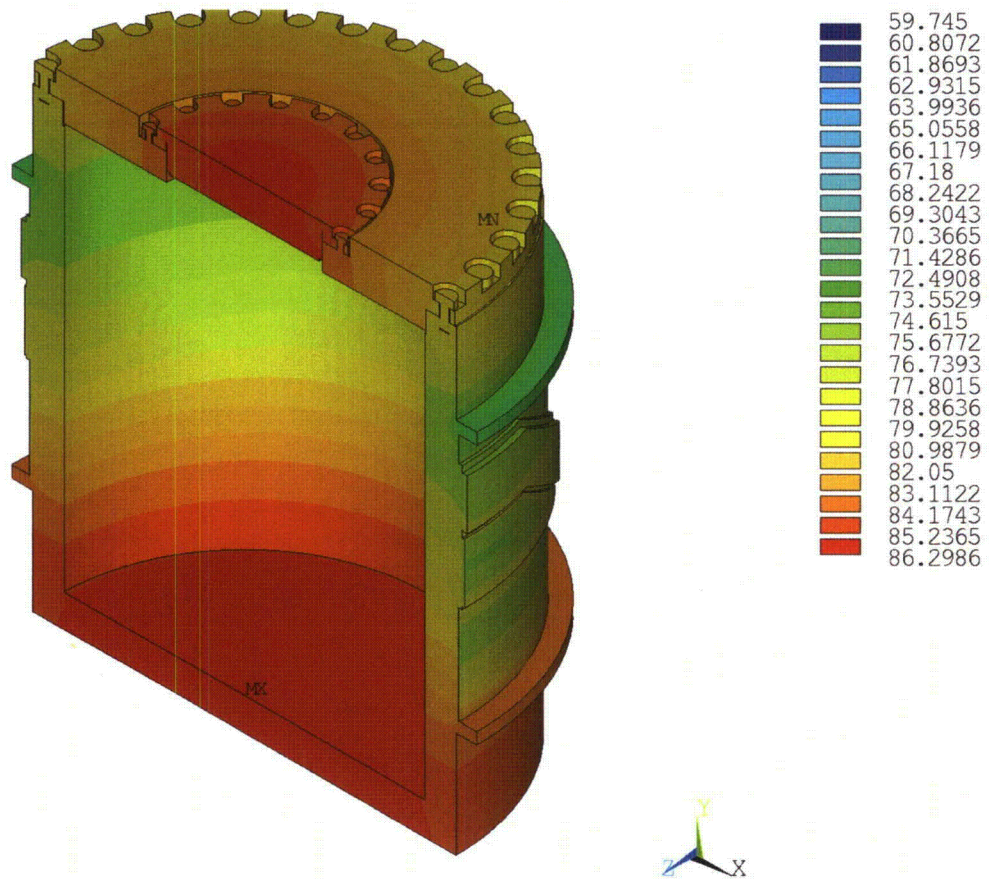
HAC—Fire Top Puncture, Steady-State Initial Conditions (Degrees Celsius)

**Figure 3.4.1-5 Temperature Contour Plot of Cask Body at the End of Fire—HAC
Pin Damage on Top Impact Limiter**



HAC—Fire Top Puncture, Steady-State Initial Conditions (Degrees Celsius)

Figure 3.4.1-6 Temperature Contour Plot of Package after Cool-Down—HAC Pin Damage on Top Impact Limiter



HAC—Fire Top Puncture, Steady-State Initial Conditions (Degrees Celsius)

Figure 3.4.1-7 Temperature Contour Plot of Cask Body after Cool-Down—HAC Pin Damage on Top Impact Limiter

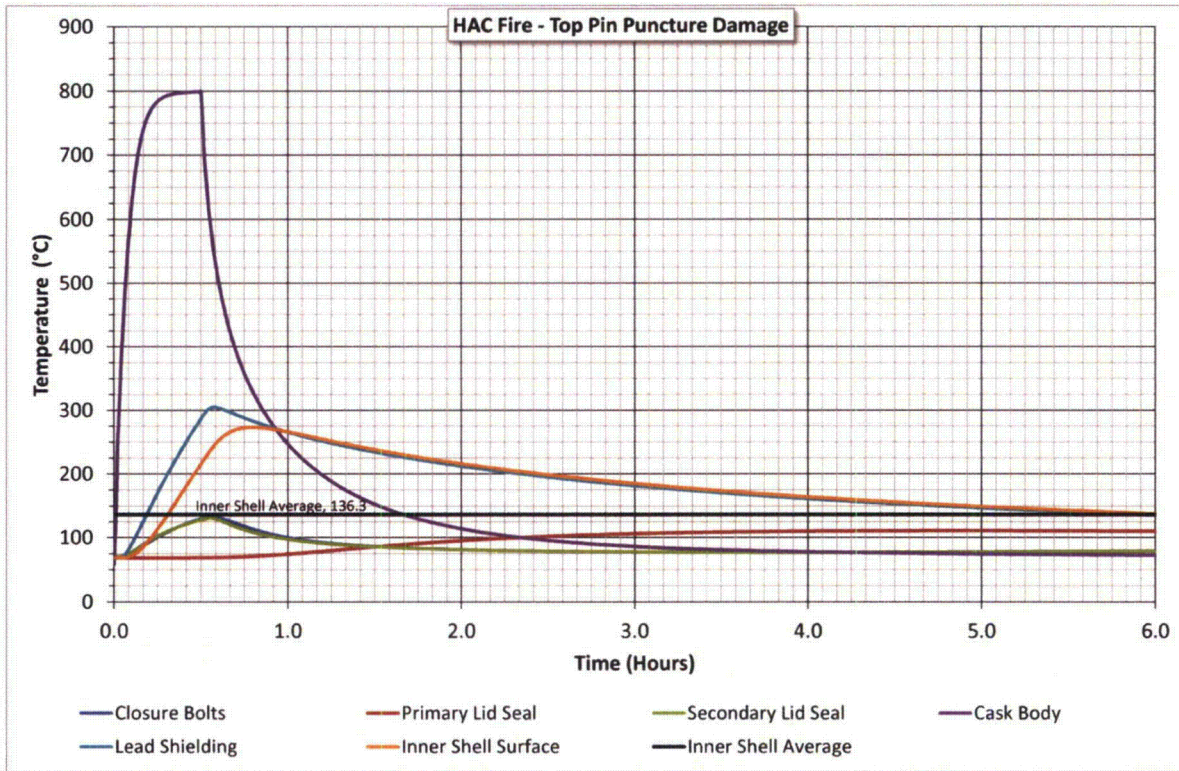
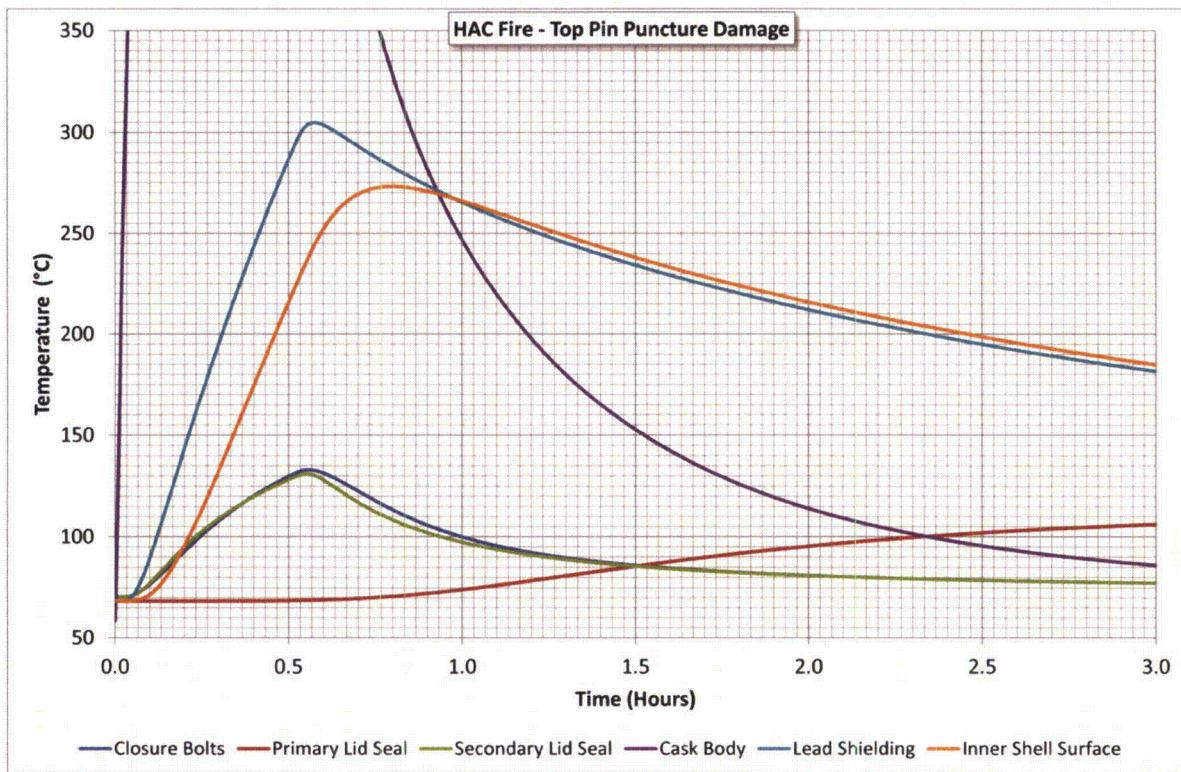
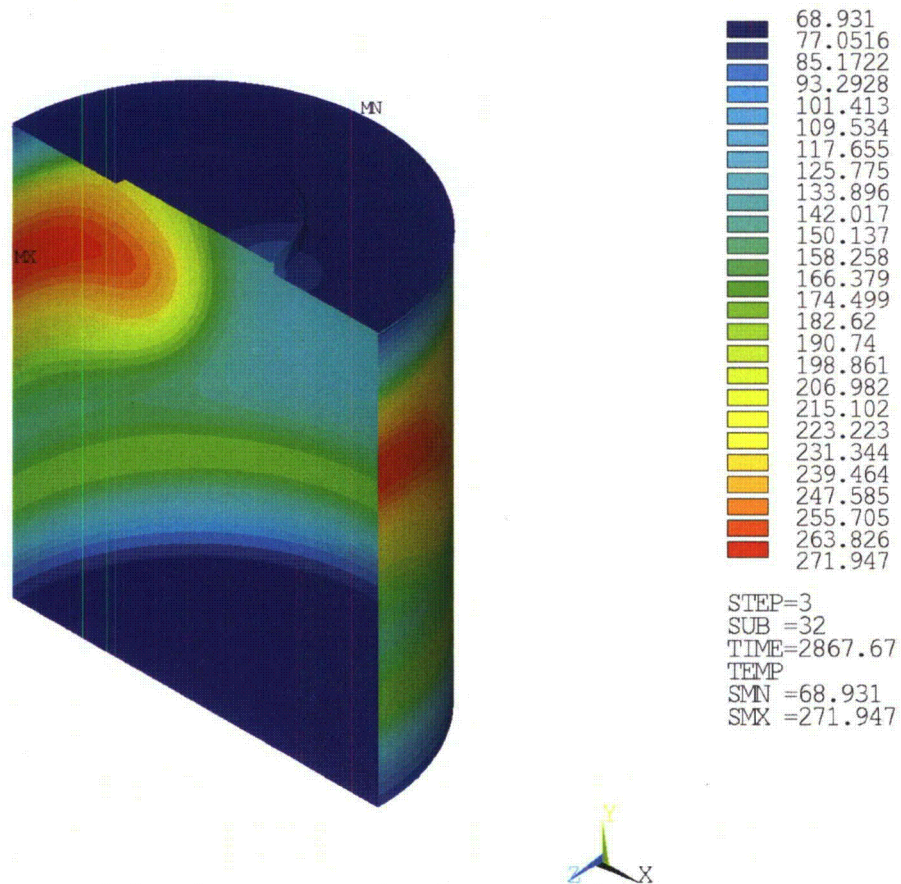


Figure 3.4.1-8 Time-History Plot of Critical Package Components—HAC Pin Damage on Top Impact Limiter

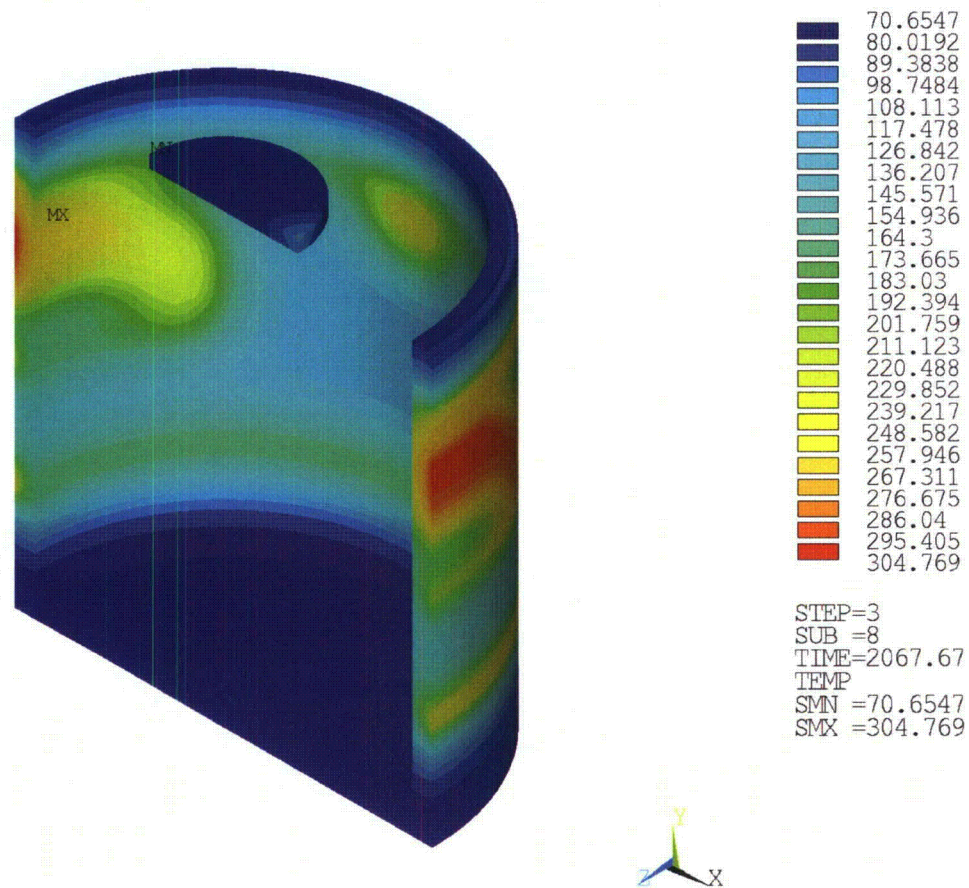


**Figure 3.4.1-9 Time-History Enhanced View Plot of Critical Package Components—
HAC Pin Damage on Top Impact Limiter**



HAC—Fire Top Puncture, Steady-State Initial Conditions (Degrees Celsius)

Figure 3.4.1-10 Maximum Temperature of the Inner Shell—HAC Pin Damage on Top Impact Limiter



HAC—Fire Top Puncture, Steady-State Initial Conditions (Degrees Celsius)

Figure 3.4.1-11 Maximum Temperature of Lead Shielding—HAC Pin Damage on Top Impact Limiter

3.4.2 HAC Fire Evaluation—Pin Puncture Damage to the Side of the Cask Body

The analytical model described in Section 3.3.1.2 is used to evaluate the RT-100 with damage on the cask side wall. For this case, the limiting configuration considers the pin puncturing the thermal shield directly below the lifting block. This configuration increases the area of the outer shell of the cask that is not protected by the thermal shield and maximizes the heat input into the lead. The following section evaluates both pin puncture orientations to determine the effect to critical components such as the seal locations and lead shielding.

3.4.2.1 Initial Condition—Pin Puncture Damage to the Side of the Cask Body

Figure 3.4.2-1 shows the FE model of the cask body due to pin puncture damage on the side. The location of the damage is chosen below the lifting pocket in a region where no thermal insulation exists. Therefore, the heat flow is maximized into the package. The removed elements at this area cover a surface area greater than the area of the pin. As with the pin puncture on the top impact limiter case, NCT Hot case 1 steady state solution is used as the initial condition for the fire cases. The steady-state temperatures are applied as a boundary condition during the first

load step of the transient solution, prior to initiating the HAC fire transient. Figure 3.4.2-2 shows the package temperature distribution prior to the fire. The cask body and inner shell pre-fire temperatures are shown in Figure 3.4.2-3 and Figure 3.4.2-4.

3.4.2.2 HAC Fire Analysis—Pin Puncture Damage to the Side of the Cask Body

The thermal analysis for HAC includes a 30 minute transient fire followed by the prescribed post-fire cool-down period. The FE model described in Section 3.3.1.2 is analyzed by applying the following boundary conditions. Following the initial load step in which the steady-state temperatures are applied, the analysis proceeds with the HAC fire transient for 30 minutes (1,800 seconds) followed by a cool-down period with the boundary conditions associated with NCT hot case 1. The NCT hot case 1 boundary conditions are applied as constants, ignoring the day/night cool-down cycle. The following is a summary of the fire transient boundary conditions:

- Environment temperature, 800°C (1472°F)
- No solar insolation, 0 W/m²
- Forced convection, heat transfer coefficient = 10 W/m²·°C
- Radiation from the environment to package surface, flame emissivity = 0.9
- Internal heat load as a uniform heat flux, 13.04 W/m²

The cool-down analysis is performed for 216,000 seconds (2.5 days) with the following boundary conditions:

- Environment temperature, 38°C (100°F)
- Solar insolation applied as constant, 776 W/m² for flat surfaces and 388 W/m² for curved surfaces.
- Natural convection, heat transfer coefficient = 5 W/m²·°C
- Radiation from package surface to the environment, package emissivity = 0.8
- Internal heat load as a uniform heat flux, 13.04 W/m²

3.4.2.3 HAC Fire and Cool-down Analysis—Pin Puncture Damage to the Side of the Cask Body

The boundary conditions for the top and side pin puncture cases are the same as the case with pin puncture damage at the top impact limiter described in Section 3.4.2.1. The temperature contour plots of the package and the cask body at the end of fire are shown in Figure 3.4.2-5 and Figure 3.4.2-6. Figure 3.4.2-6 shows the maximum temperature at the lifting pockets and puncture location. Figure 3.4.2-7 and Figure 3.4.2-8 shows the package and cask body after the cool-down period.

Time-history temperature data is obtained in the transient analysis for critical components of the package including the outer shell, inner shell, closure bolts, lead shield, and O-rings. Maximum temperature results are obtained during post-processing by selecting the FE model component or material of interest and sorting the nodal results. Figure 3.4.2-9 shows the temperature time-history from the start of the fire through the cool-down. As Figure 3.4.2-9 shows, the average inner shell temperature is 137°C and is representative of the contents during the fire/cool-down

transient. Figure 3.4.2-10 provides an enhanced view of the time-history data through the 30 minute fire and 2.5 hours of the cool down process. Figure 3.4.2-11 identifies the highest inner shell temperature at the instant it occurs, 48 minutes from the start of the fire. Figure 3.4.2-12 identifies the maximum lead shield temperature occurring 35 minutes after the start of the fire, at a point underneath the tie-down arms. This figure indicates that no melting of the lead shield occurs during the HAC fire.

Table 3.1.3-3 summarizes the maximum temperatures of the cask under HAC fire with pin puncture damage at the side of the cask body.

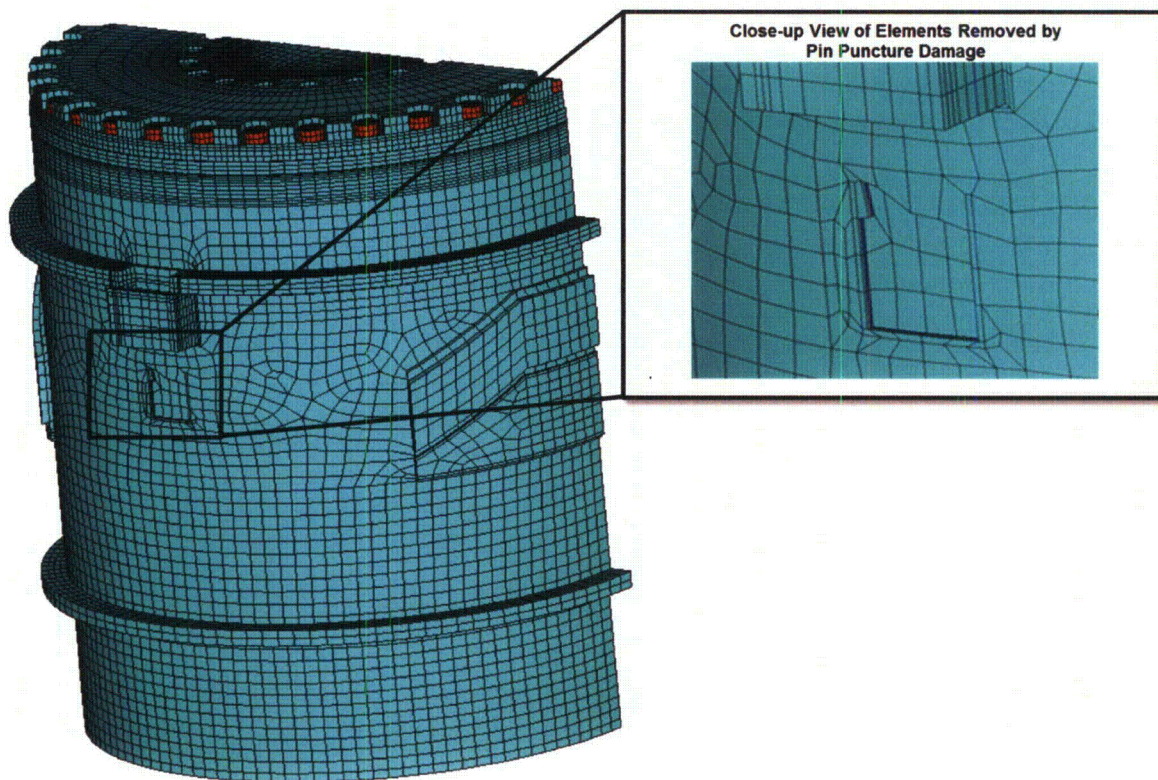
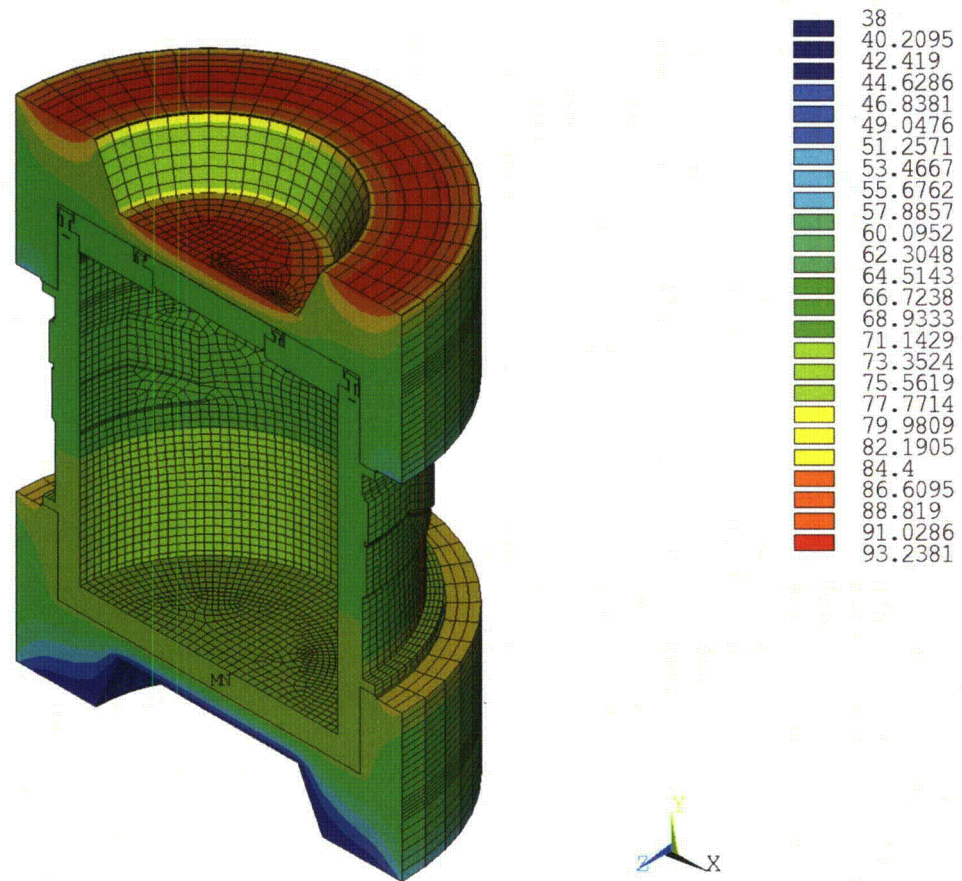
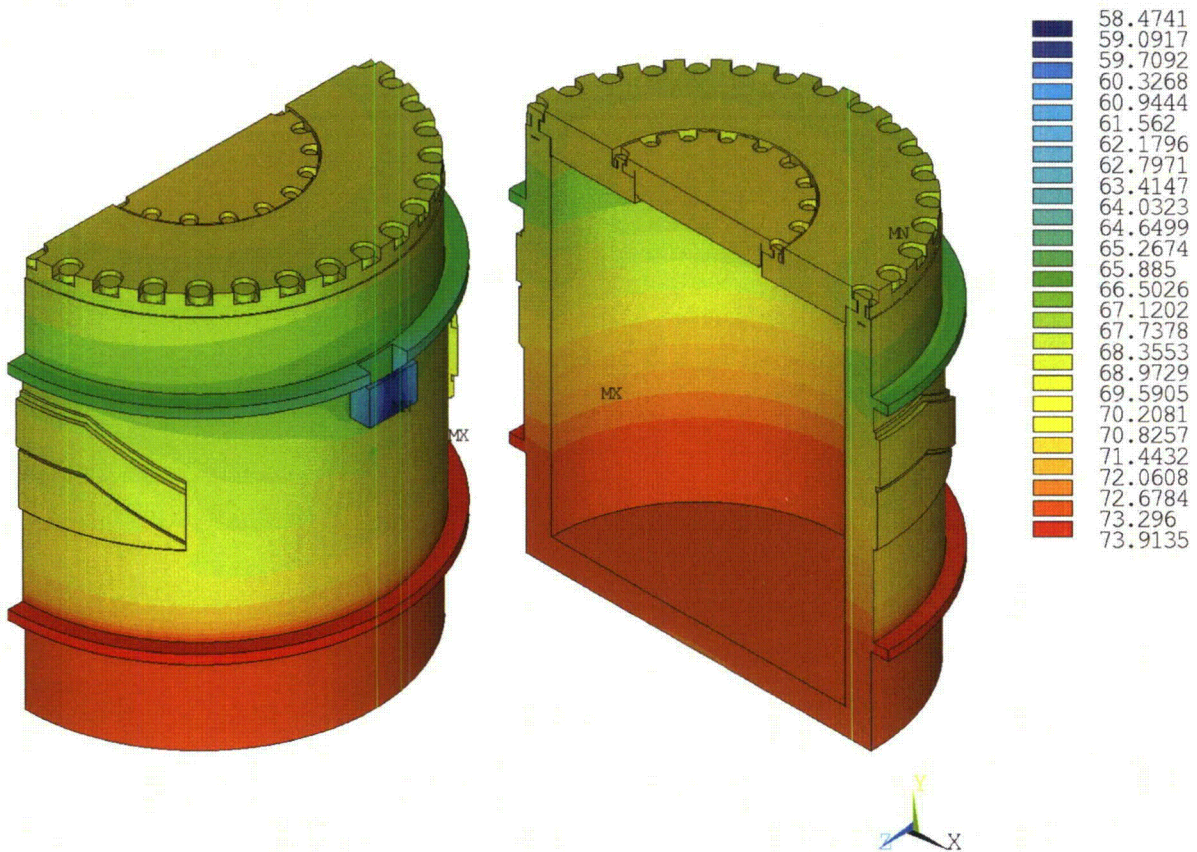


Figure 3.4.2-1 Cask Model-HAC Pin Damage on Cask Body Side

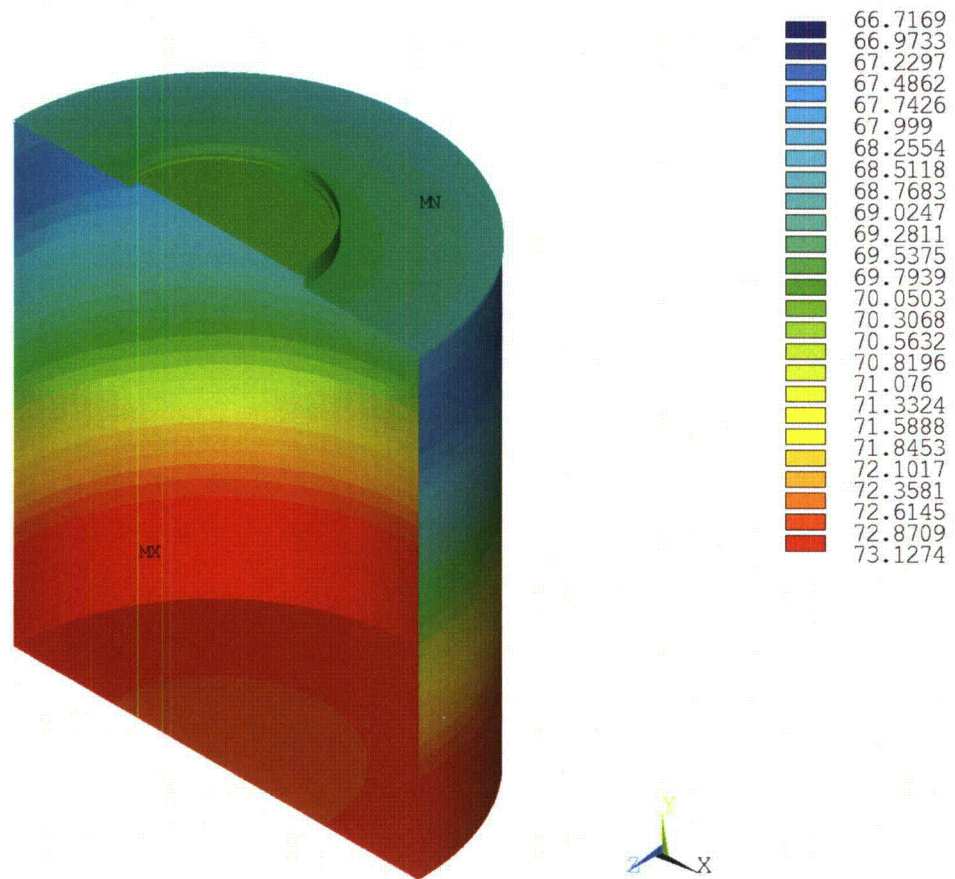


HAC—Fire Side Puncture, Steady-State Initial Conditions (Degrees Celsius)

Figure 3.4.2-2 Temperature Contour Plot of Package Pre-Fire Condition—HAC Pin Damage on Cask Body Side

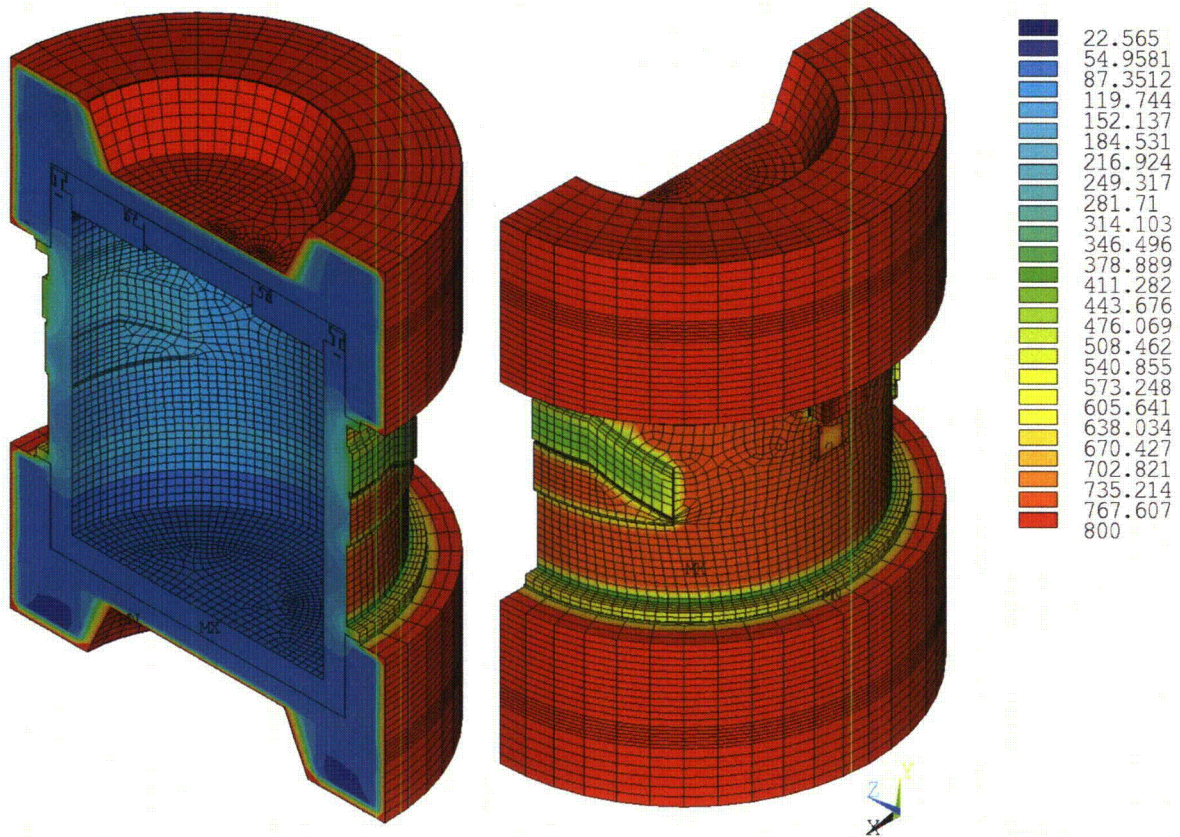


HAC—Fire Side Puncture, Steady-State Initial Conditions (Degrees Celsius)
**Figure 3.4.2-3 Temperature Contour Plot of Cask Body Pre-Fire Condition—HAC
Pin Damage on Cask Body Side**

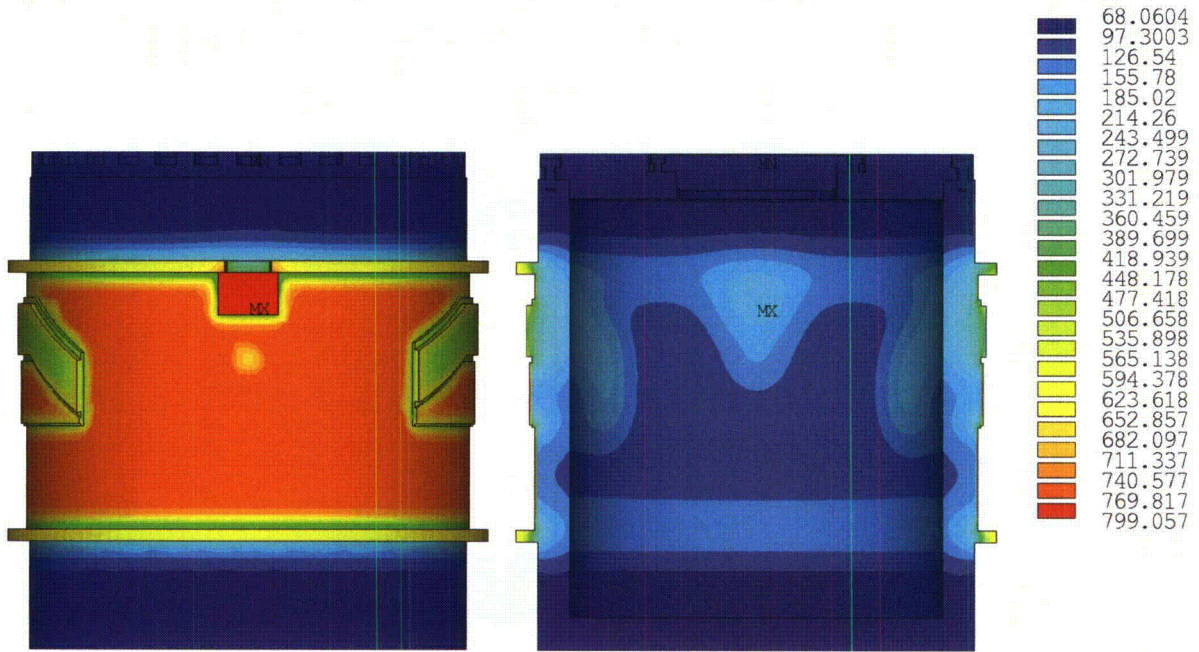


HAC—Fire Side Puncture, Steady-State Initial Conditions (Degrees Celsius)

Figure 3.4.2-4 Temperature Contour Plot of Inner Shell Pre-Fire Condition—HAC
Pin Damage on Cask Body Side

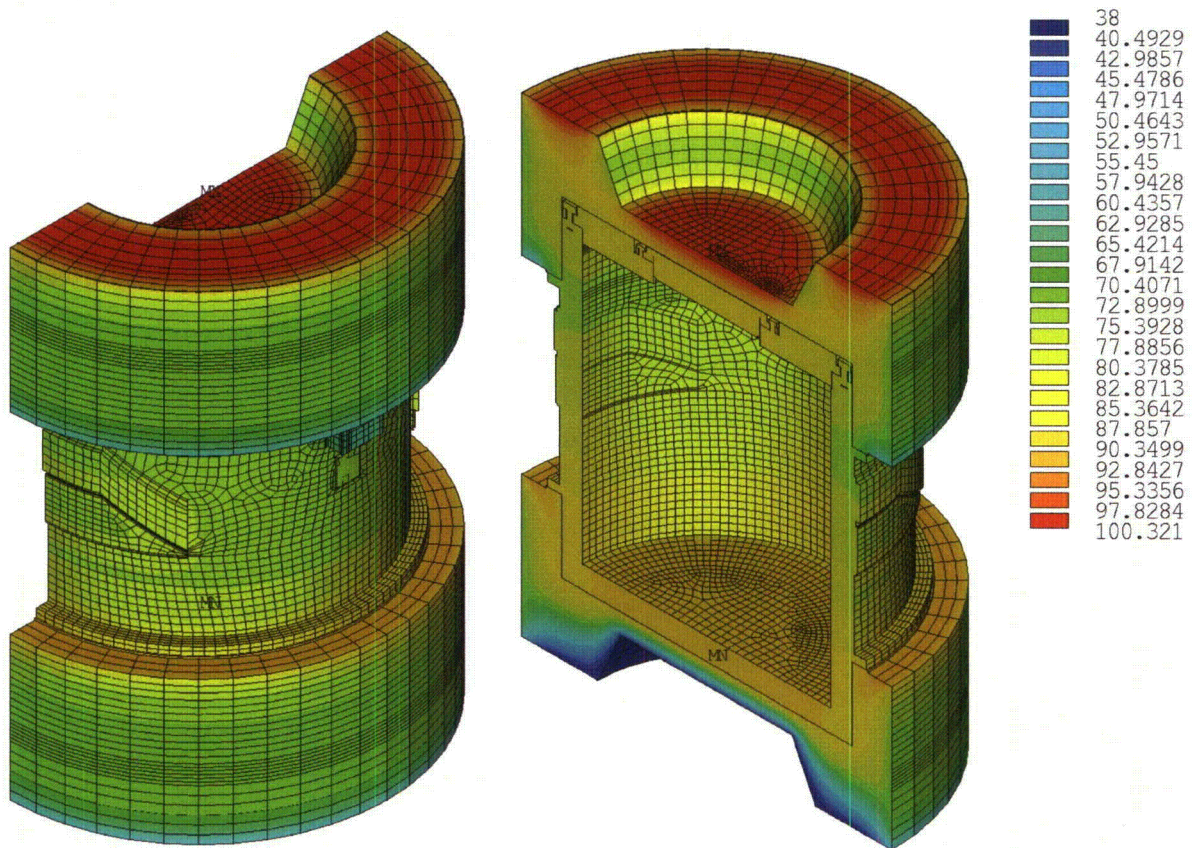


HAC—Fire Side Puncture, Steady-State Initial Conditions (Degrees Celsius)
**Figure 3.4.2-5 Temperature Contour Plot of Package at the End of Fire—HAC Pin
Damage on Cask Body Side**

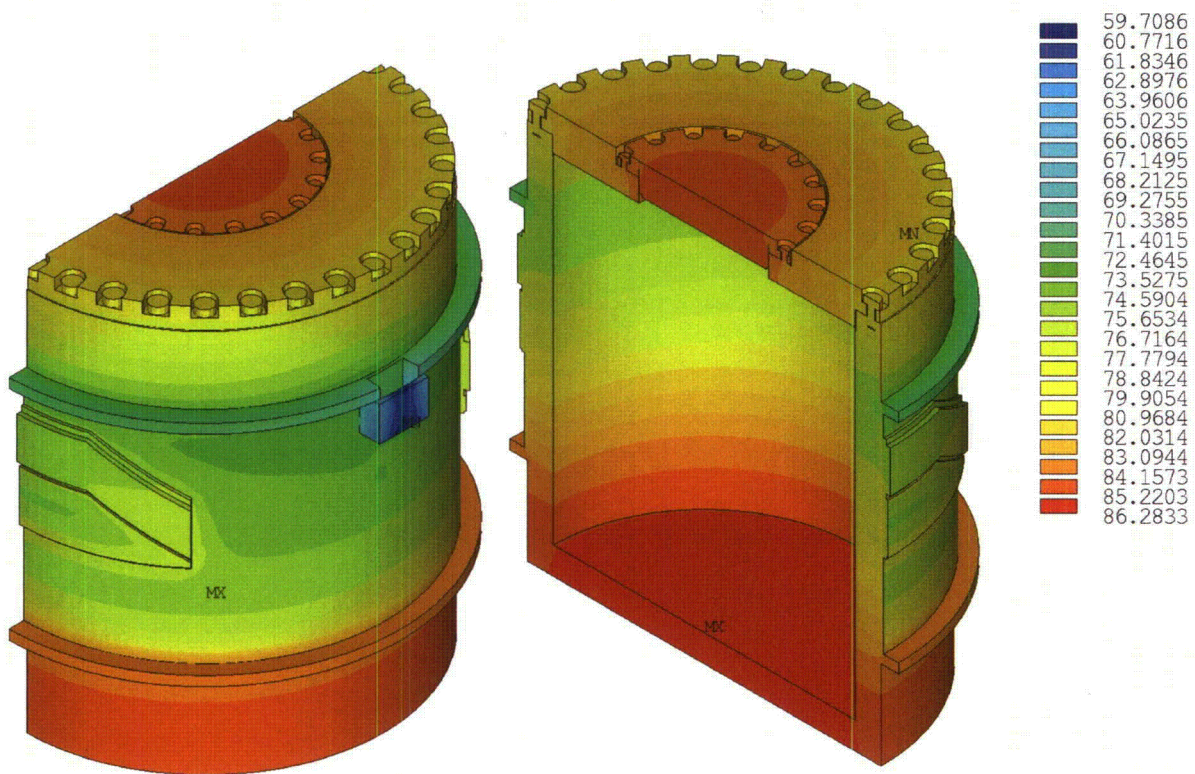


HAC—Fire Side Puncture, Steady-State Initial Conditions (Degrees Celsius)

**Figure 3.4.2-6 Temperature Contour Plot of Cask Body at the End of Fire—HAC
Pin Damage on Cask Body Side**



HAC—Fire Side Puncture, Steady-State Initial Conditions (Degrees Celsius)
Figure 3.4.2-7 Temperature Contour Plot of Package after Cool-Down—HAC Pin Damage on Cask Body Side



HAC—Fire Side Puncture, Steady-State Initial Conditions (Degrees Celsius)
Figure 3.4.2-8 Temperature Contour Plot of Cask Body After Cool-Down—HAC Pin Damage on Cask Body Side

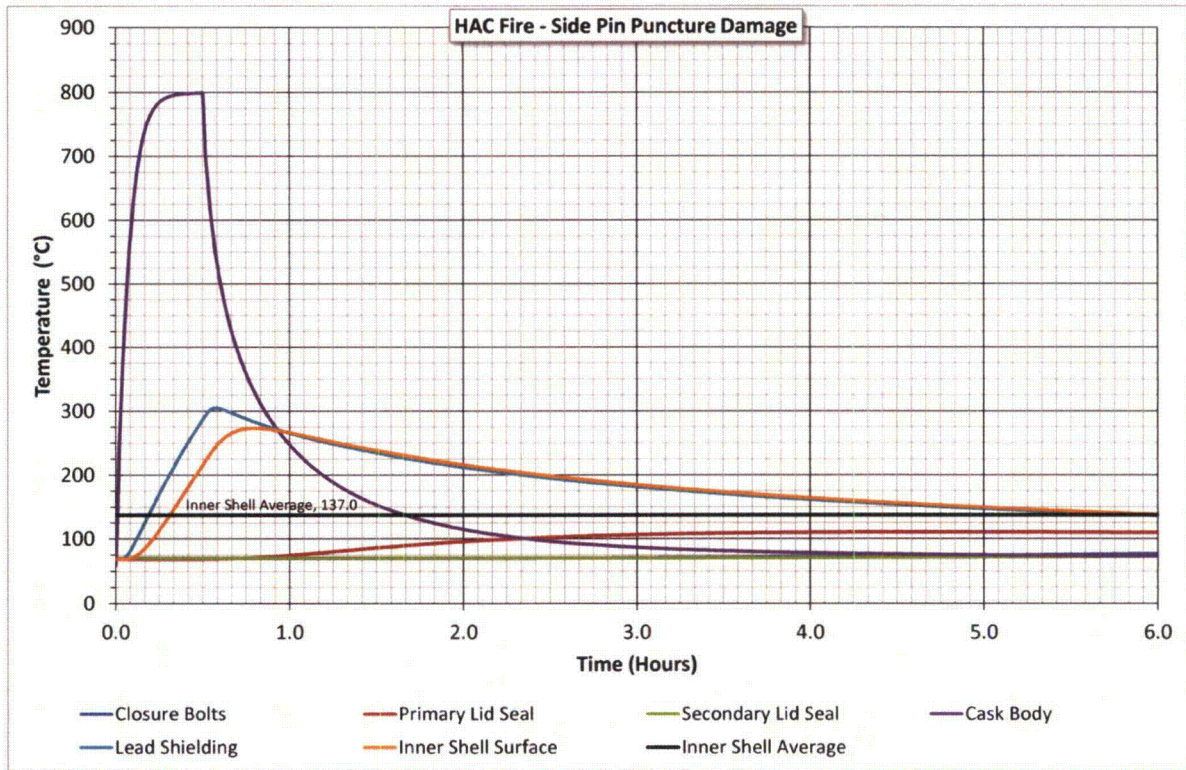
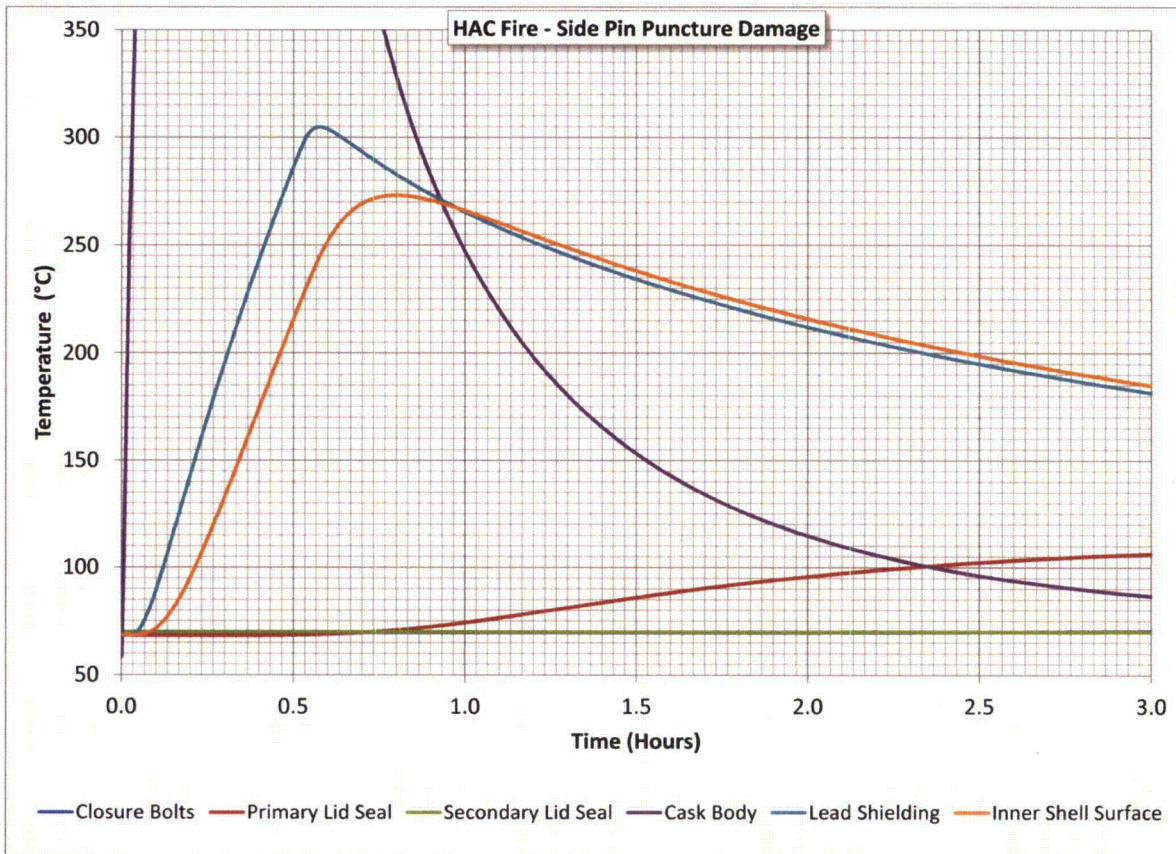
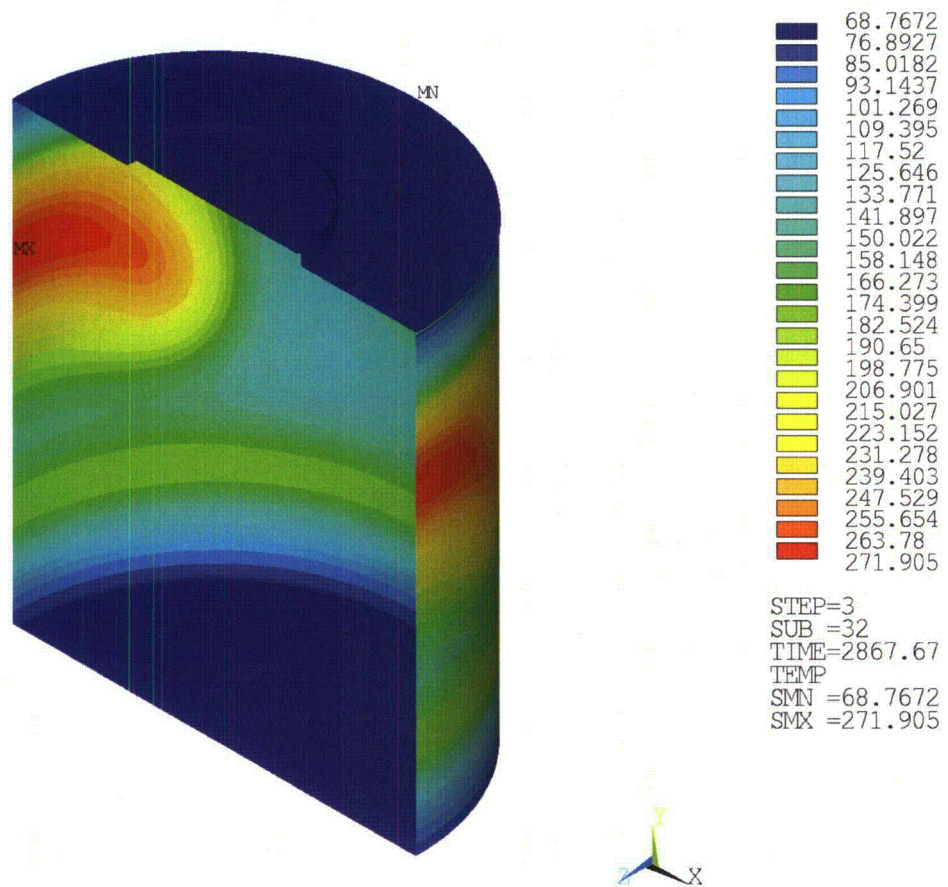


Figure 3.4.2-9 Time-History Plot of Critical Package Components—HAC Pin Damage on Cask Body Side

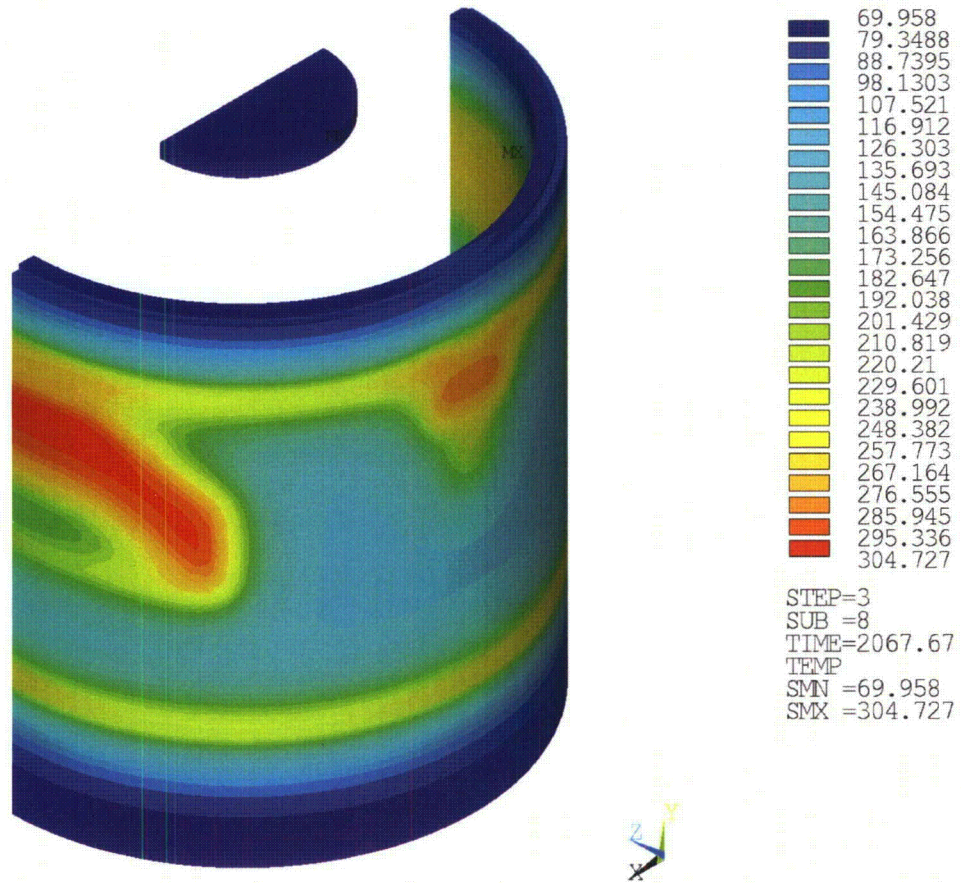


**Figure 3.4.2-10 Time-History Enhanced View Plot of Critical Package Components—
HAC Pin Damage on Cask Body Side**



HAC—Fire Side Puncture, Steady-State Initial Conditions (Degrees Celsius)

Figure 3.4.2-11 Maximum Temperature of the Inner Shell—HAC Pin Damage on Cask Body Side



HAC—Fire Side Puncture, Steady-State Initial Conditions (Degrees Celsius)

Figure 3.4.2-12 Maximum Temperature of Lead Shielding—HAC Pin Damage on Cask Body Side

3.4.3 Maximum Temperatures and Pressure

This section summarizes the peak accident condition temperatures of RT-100 components as a function of time both during and after the fire, as well as the maximum temperatures from the post-fire, steady-state condition. This section includes those temperatures at locations in the package that are significant to the safety analysis and review. The calculations of transient temperatures trace the temperature-time history up to and past the time at which maximum temperatures are achieved and begin to fall. The calculations confirm that these temperatures do not exceed their maximum allowable values. It also confirms that lead shielding does not reach melting temperature.

The RT-100 is evaluated structurally for the maximum HAC temperatures and pressures in Chapter 2, Section 2.7.4 (Thermal).

3.4.3.1 Maximum Temperatures

Section 3.4.1 and 3.4.2 present a summary of the evaluation of the RT-100 for the hypothetical accident condition fire transient. Provided in the summary are figures depicting temperature distributions and time histories as a function of time during and after the fire transient. Maximum temperatures for various cask components as a result of the HAC are presented in Table 3.1.3-2 and Table 3.1.3-3.

Of interest in this section is the determination of the maximum internal pressure in the cask cavity as a result of the fire test. As shown in Table 3.1.3-3, the maximum average inner shell temperature during the fire transient is 137°C. The temperature of the cask body components is increased due to the fire transient, with a maximum normal condition inner shell temperature of 73.1°C as reported in Table 3.1.3-1. Because the temperature of the inner shell of the cask is raised by 64°C as a result of the fire transient and because the maximum internal decay heat of the contents is only 200 watts, it is conservative to assume that the cavity temperatures are bounded by the average inner shell temperatures. For conservatism, the inner shell can be assumed to be at 150°C for the pressure calculations presented in Section 3.4.3.2.

As previously discussed, the primary components of interest during the fire transient from a temperature standpoint are the lead gamma shielding and the O-ring seals in the primary and secondary lids. As described in detail in Section 3.4.2, the lead and O-ring materials do not exceed their allowable, and in fact have safety margins of more than 23°C below their maximum allowable temperatures. The temperature distributions within the cask, as a result of the hypothetical accident condition fire transient, are fully considered in the structural evaluation of the cask presented in Chapter 2, Section 2.7.4 (Thermal).

3.4.3.2 Maximum Accident Condition Pressure

The evaluation of the maximum pressure in the RT-100 is based on the maximum normal operating pressure, and considers fire-induced increases in package temperatures, thermal combustion or decomposition processes, phase changes, etc. (Fuel rod failure is not applicable). The value of this maximum pressure is consistent with the values used in the Structural Evaluation and Containment sections.

Similar to the calculation of the maximum normal operating pressure in Section 3.3.2, the maximum accident condition pressure is calculated using bounding assumptions for the temperatures in the cask as a result of the hypothetical accident condition fire transient. The maximum pressure is the sum of four components:

1. The pressure due to the initially sealed air in the cavity
2. The pressure due to water vapor in the cask
3. The pressure due to the hydrogen and oxygen gases generated by radiolysis
4. The pressure due to the thermal decomposition of the contents

The following sections present a summary of the maximum accident condition pressure calculation. Details of the calculation are provided in Calculation Package RTL-001-CALC- TH-0202, Rev. 6 [Ref. 7], and RTL-001-CALC-TH-0301, Rev. 1 [Ref. 25].

3.4.3.2.1 Calculation Method

The internal cavity pressure due to accident condition temperatures is determined using the same method used to calculate the maximum normal condition pressure in Section 3.3.2. The method presented below is equal to that used previously, with the maximum normal operating pressure and internal temperatures used along with the maximum internal temperature determined in Section 3.4.3.1 to calculate the maximum accident condition pressure.

3.4.3.2.2 Pressure Due to the Initially Sealed Air in the Cavity

Per the ideal gas law, the partial pressure of the air (P_{air}) initially sealed in the fixed volume of the cask at the ambient temperature as it is heated to 150 °C is:

$$P_1 \times T_2 = P_2 \times T_1$$

$$P_{\text{air}} = 101.35 \text{ kPa}[(423.15 \text{ K}) / (294.25 \text{ K})] = 145.8 \text{ kPa} (21.15 \text{ psia})$$

3.4.3.2.3 Pressure Due to the Water Vapor in the Cask

The RT-100 cavity is assumed to contain a small amount of water. By conservatively assuming a condensing surface temperature of 150 °C, the water vapor pressure, P_{wv} , at this temperature is 475.8 kPa [69 psia] Fundamentals of Engineering Thermodynamics, 5th Edition, Table A-2 on pg. 761 [Ref. 18], also see Attachment 3.5-4. Adding the water vapor pressure at 150 °C to the partial pressure of the air in the sealed cask at this temperature gives:

$$P_2 = P_{\text{air}} + P_{\text{wv}} = 145.8 + 475.8 = 621.6 \text{ kPa} [90.16 \text{ psia}]$$

3.4.3.2.4 Pressure Due to Generation of Gas

Solidified or dewatered material may contain some water. Therefore, radiolytic generation of gases from this water could occur. Hydrogen and oxygen may be produced in the cask by radiolytic decomposition of residual water in the cask contents. As described in Section 1.2.2.6, the maximum quantity of hydrogen must be limited to less than 5% to ensure that an explosive quantity does not accumulate.

The cask atmosphere can be assumed to contain 5% of hydrogen (H₂) gas due to radiolysis of the water. By stoichiometry of the water molecule (H₂O), the cask atmosphere will also contain 2.5% oxygen (O₂) gas generated by radiolysis. Partial pressures in an ideal gas mixture are additive and behave the same as ideal gas volume fraction or mole fractions. Therefore, the partial pressure of hydrogen is described by the following equation:

$$P_{H_2} = 0.05 P_{pt}$$

$$\text{Where, } P_{pt} = P_{air} + P_{wv} + P_{H_2} + P_{O_2}$$

Combining $P_{air} + P_{wv} = P_2$ and noting that $P_{O_2} = 0.5 \times P_{H_2}$.

$$P_{H_2} = 0.05 \times (P_2 + 1.5 P_{H_2})$$

Solving the equation explicitly for P_{H_2} gives:

$$\begin{aligned} P_{H_2} &= [0.05 P_2] / [1 - 0.05 (1.5)] \\ &= [0.05 * 621.6\text{kPa}] / [1 - 0.05 (1.5)] \\ &= 33.6 \text{ kPa [4.87 psia]} \end{aligned}$$

3.4.3.2.5 Total Pressure

Based on the stoichiometric relationship between hydrogen and oxygen liberated by radiolysis of water, and again combining the pressure of the initially sealed air and water vapor as P_2 , the total pressure in the cask at 150 °C is:

$$\begin{aligned} P_{Total} &= P_2 + 1.5 P_{H_2} \\ &= 621.6 \text{ kPa} + 1.5 * 33.6 \text{ kPa} \\ &= 672 \text{ kPa [97.47 psia]} \end{aligned}$$

The maximum pressure is 672 kPa [97.47 psia] under HAC. For conservatism, the maximum accident pressure is assumed to be 689.4 kPa [100 psia] for the structural analyses presented in Chapter 2, Section 2.7.4 (Thermal).

3.4.3.2.6 Total Pressure Accounting for Combustion of Contents

In addition to the natural effect of temperature increases on pressure buildup in the package, other thermally driven phenomena can contribute to the pressure buildup within the containment boundary of a package. As discussed previously, these include phase transformation of materials in the package and radiolysis of the contents by radioactive decay. Additionally, the pressure increases due to the contribution of the partial pressure that results from the thermal decomposition of the package contents [Ref 25].

Solid polymeric materials, including cellulose such as wood and paper, undergo both physical and chemical changes when heat is applied. Thermal decomposition is a process of extensive

chemical species change caused by heat, generating gaseous fuel vapors which can burn above the solid material. The process is self-sustaining when the burning gases feed back sufficient heat to the material to continue the production of gaseous fuel vapors or volatiles. These volatiles react with the oxygen in the air to generate heat, and part of this heat is transferred back to the polymer to continue the process.

The Robatel RT-100 contents include filters that may be constructed from thermoplastics (nylon, polyester, polypropylene) or paper and shoring made of wood may be contained in the package. Although it is unlikely that temperatures under HAC will approach the auto-ignition temperatures of the contents, the following analysis is performed to evaluate the effect of combustion on the package pressure.

Combustion in a sealed container is limited by the amount of air present to support the chemical reaction for the thermal decomposition of the fuel. Heats from the exothermic combustion reaction will increase the temperature of the contents and packaging. The maximum temperature in a sealed container will determine the maximum pressure, along with some additional pressure from emitted gases. The sealed inner containment of the RT-100 cask contains only enough air (5.75 kg) for complete combustion of approximately 1.127 kg of cellulosic material, paper or wood; or 0.390 kg of polyethylene.

Gibbs-Dalton Law defines total pressure, P_T , equal to the sum of the partial pressures of the individual gases present. The total pressure P_T , in the package containment is the sum of pressures due to phase transformation of materials in the package P_v (Ref. 25, p. 25, where $P_v = P_{sat}$), radiolysis of the contents by radioactive decay P_r ($1.5 P_{H_2}$ from Section 3.4.3.2.5), and thermal decomposition of the package contents P_f (Ref. 25, p. 25, where $P_f = P_{fwood}$). The vapor pressure from the phase transformation of water and the partial pressures of hydrogen and oxygen gases generated from the radiolysis of water in the contents are considered in the total pressure calculation.

$$P_T = P_v + P_r + P_f$$

$$P_T = 463.2 \text{ kPa} + 50.4 \text{ kPa} + 171.0 \text{ kPa} = 684.6 \text{ kPa} [99.3 \text{ psia}]$$

where the total pressure of the inner cavity is based on the complete combustion of wood, which has the highest heat of combustion. Since the temperature required to ignite wood are not sustainable, complete combustion is not considered a credible event, therefore, the maximum pressure is taken as 97.47 psia as demonstrated in Section 3.4.3.2.5.

3.4.4 Maximum Thermal Stress

The RT-100 cask is evaluated for the stresses produced by the temperature gradients in the cask body that result from exposure of the cask to the HAC fire transient. This evaluation, which utilizes the temperature distributions resulting from the fire accident as described in Section 3.4.3, is presented in detail in Chapter 2, Section 2.7.4 (Thermal).

3.4.5 Accident Conditions for Fissile Material Packages for Air Transport

This Section is NOT APPLICABLE. The RT-100 is not be used for fissile material air transport.

3.5 Appendix

Attachment 3.5-1 EPDM Temperature Specifications [Ref. 16]

Not compatible with:

- Fuels of high aromatic content (for flex fuels a special compound must be used).
- Aromatic hydrocarbons (benzene).
- Chlorinated hydrocarbons (trichloroethylene).
- Polar solvents (ketone, acetone, acetic acid, ethylene-ester).
- Strong acids.
- Brake fluid with glycol base.
- Ozone, weather and atmospheric aging.

2.2.2 Carboxylated Nitrile (XNBR)

Carboxylated Nitrile (XNBR) is a special type of nitrile polymer that exhibits enhanced tear and abrasion resistance. For this reason, XNBR based materials are often specified for dynamic applications such as rod seals and rod wipers.

Heat resistance

- Up to 100°C (212°F) with shorter life @ 121°C (250°F).

Cold flexibility

- Depending on individual compound, between -18°C and -48°C (0°F and -55°F).

Chemical resistance

- Aliphatic hydrocarbons (propane, butane, petroleum oil, mineral oil and grease, diesel fuel, fuel oils) vegetable and mineral oils and greases.
- HFA, HFB and HFC hydraulic fluids.
- Many diluted acids, alkali and salt solutions at low temperatures.

Not compatible with:

- Fuels of high aromatic content (for flex fuels a special compound must be used).
- Aromatic hydrocarbons (benzene).
- Chlorinated hydrocarbons (trichloroethylene).
- Polar solvents (ketone, acetone, acetic acid, ethylene-ester).
- Strong acids.
- Brake fluid with glycol base.
- Ozone, weather and atmospheric aging.

2.2.3 Ethylene Acrylate (AEM, Vamac)

Ethylene acrylate is a terpolymer of ethylene and methyl acrylate with the addition of a small amount of carboxylated curing monomer. Ethylene acrylate rubber is not to be confused with polyacrylate rubber (ACM).

Heat resistance

- Up to 149°C (300°F) with shorter life up to 163°C (325°F).

Cold flexibility

- Between -29°C and -40°C (-20°F and -40°F).

Chemical resistance

- Ozone.
- Oxidizing media.
- Moderate resistance to mineral oils.

Not compatible with:

- Ketones.
- Fuels.
- Brake fluids.

2.2.4 Ethylene Propylene Rubber (EPR, EPDM)

EPR copolymer ethylene propylene and ethylene-propylene-diene rubber (EPDM) terpolymer are particularly useful when sealing phosphate-ester hydraulic fluids and in brake systems that use fluids having a glycol base.

Heat resistance

- Up to 150°C (302°F) (max. 204°C (400°F)) in water and/or steam).

Cold flexibility

- Down to approximately -57°C (-70°F).

Chemical resistance

- Hot water and steam up to 149°C (300°F) with special compounds up to 260°C (500°F).
- Glycol based brake fluids (Dot 3 & 4) and silicone-based brake fluids (Dot 5) up to 149°C (300°F).
- Many organic and inorganic acids.
- Cleaning agents, sodium and potassium alkalis.
- Phosphate-ester based hydraulic fluids (HFD-R).
- Silicone oil and grease.
- Many polar solvents (alcohols, ketones, esters).
- Ozone, aging and weather resistant.

Not compatible with:

- Mineral oil products (oils, greases and fuels).

2.2.5 Butyl Rubber (IIR)

Butyl (isobutylene, isoprene rubber, IIR) has a very low permeability rate and good electrical properties.

Heat resistance

- Up to approximately 121°C (250°F).

Cold flexibility

- Down to approximately -59°C (-75°F).

Chemical resistance

- Hot water and steam up to 121°C (250°F).
- Brake fluids with glycol base (Dot 3 & 4).
- Many acids (see Fluid Compatibility Tables in Section VII).
- Salt solutions.
- Polar solvents, (e.g. alcohols, ketones and esters).
- Poly-glycol based hydraulic fluids (HFC fluids) and phosphate-ester bases (HFD-R fluids).
- Silicone oil and grease.
- Ozone, aging and weather resistant.

Not compatible with:

- Mineral oil and grease.
- Fuels.
- Chlorinated hydrocarbons.

Attachment 3.5-2 Seal Material EPDM Working Temperature
 [Ref. 8]

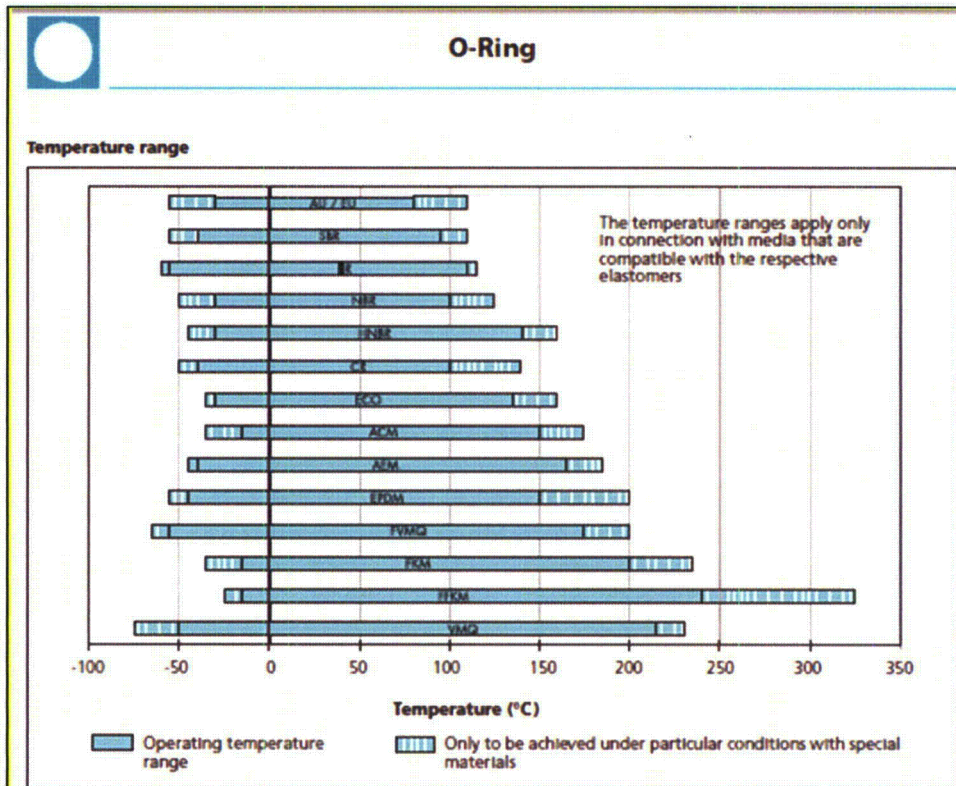


Figure 4 Temperature range of various elastomers

General field of application

Elastomer materials are used to cover a large number of fields of application. The various elastomers can be characterised as follows:

ACM (Polyacrylate Rubber)

ACM shows excellent resistance to ozone, weathering and hot air, although it shows only a medium physical strength, low elasticity and a relatively limited low temperature capability. The operating temperatures range from -20 °C and +150 °C (for a short period of time up to +175 °C). Special types can be used down to -35 °C. ACM-materials are mainly used in automotive applications which require special resistance to lubricants containing many additives (incl. sulphur) at high temperatures.

CR (Chloroprene Rubber)

In general the CR materials show relatively good resistances to ozone, weathering, chemicals and aging. Also they show good non-flammability, good mechanical properties and cold flexibility. The operating temperatures range between -35 °C and +90 °C (for a short period of time up to +120 °C). Special types can be used down to

-55 °C. CR materials are found in sealing applications such as refrigerants, for outdoor applications and in the glue industry.

EPDM (Ethylene Propylene Diene Rubber)

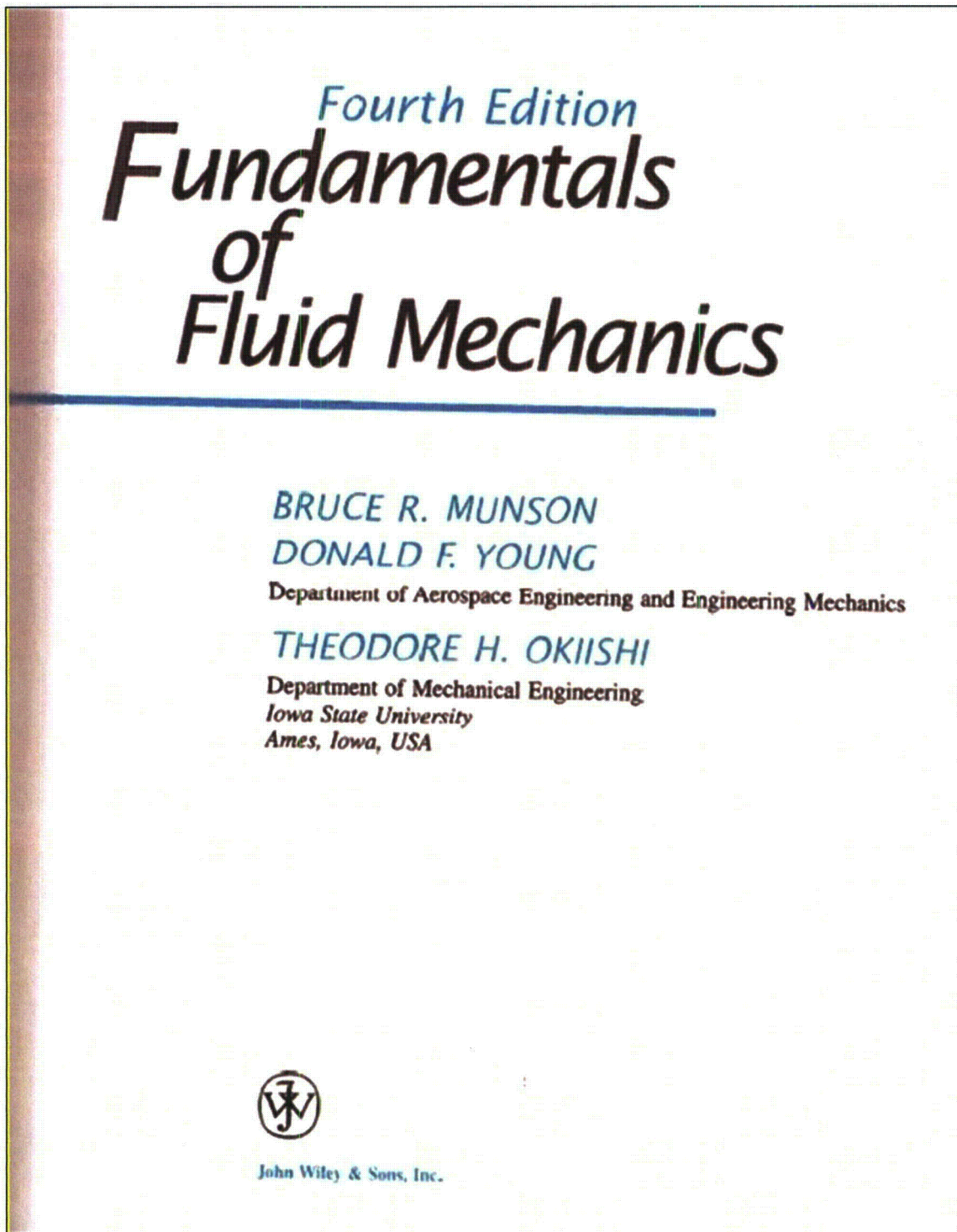
EPDM shows good heat, ozone and aging resistance. In addition they also exhibit high levels of elasticity, good low temperature behaviour as well as good insulating properties. The operating temperatures of applications for EPDM range between -45 °C and +150 °C (for a short period of time up to +175 °C). With sulphur cured types the range is reduced to -45 °C and +130 °C (for short period of time up to +150 °C). EPDM can often be found in applications with brake fluids (based on glycol) and hot water.

FFKM (Perfluoro Rubber)

Perfluoroelastomers show broad chemical resistance similar to PTFE as well as good heat resistance. They show low swelling with almost all media. Depending on the material the operating temperatures range between -25 °C and +240 °C. Special types can be used up to +325 °C. Applications for FFKM can be mostly found in the chemical and process industries and in all applications with either aggressive environments or high temperatures.



Attachment 3.5-3 Water Vapor Pressure Reference (80°C)
[Ref. 17]



Attachment 3.5-3 Water Vapor Pressure Reference (80°C) (Continued)
[Ref. 17]

ACQUISITIONS EDITOR: Wayne Anderson
ASSITANT EDITOR: Jennifer Welter
MARKETING MANAGER: Katherine Hepburn
SENIOR PRODUCTION EDITOR: Valerie A. Vargas
PRODUCTION SERVICES MANAGER: Jeanine Furino
COVER DESIGNER: Madelyn Lesure
ELECTRONIC ILLUSTRATIONS: Radiant Illustration and Design
PRODUCTION MANAGEMENT SERVICES: Ingrao Associates

This book was set in 10/12 by TechBooks and printed and bound by R. R. Donnelley & Sons.
The cover was printed by Phoenix Color.

This book is printed on acid-free paper. ☹

Copyright 2002© John Wiley & Sons, Inc. All rights reserved.

No part of this publication may be reproduced, stored in a retrieval system or transmitted in any form by any means, electronic, mechanical, photocopying, recording, scanning or otherwise, except as permitted by Sections 107 or 108 of the 1976 United States Copyright Act, without either the prior written permission of Publisher, or authorization through payment of the appropriate per-copy fee to the Copyright Clearance Cent 222 Rosewood Drive, Danvers, MA 01923, (978) 750-8400, fax (978) 750-4470. Requests to the Publisher for permission should be addressed to the Permissions Department, John Wiley & Sons, Inc., 111 River Street, Hoboken, NJ 07030, (201) 748-6011, fax (201) 748-6008, E-Mail: PERMREQ @ WILEY.COM.
To order books please call 1(800)-225-5945.

ISBN: 0-471-44250-X

Printed in the United States of America

1098765

Attachment 3.5-3 Water Vapor Pressure Reference (80°C) (Continued)
 [Ref. 17]

Appendix B / Physical Properties of Fluids ■ 831

■ TABLE B.1
 Physical Properties of Water (BG Units)*

Temperature (°F)	Density, ρ (slugs/ft ³)	Specific Weight ^b , γ (lb/ft ³)	Dynamic Viscosity, μ (lb·s/ft ²)	Kinematic Viscosity, ν (ft ² /s)	Surface Tension ^c , σ (lb/ft)	Vapor Pressure, P_v [lb/in ² (abs)]	Speed of Sound ^d , c (ft/s)
32	1.940	62.42	3.732 E - 5	1.924 E - 5	5.18 E - 3	8.854 E - 2	4603
40	1.940	62.43	3.228 E - 5	1.664 E - 5	5.13 E - 3	1.217 E - 1	4672
50	1.940	62.41	2.730 E - 5	1.407 E - 5	5.09 E - 3	1.781 E - 1	4748
60	1.938	62.37	2.344 E - 5	1.210 E - 5	5.03 E - 3	2.563 E - 1	4814
70	1.936	62.30	2.037 E - 5	1.052 E - 5	4.97 E - 3	3.631 E - 1	4871
80	1.934	62.22	1.791 E - 5	9.262 E - 6	4.91 E - 3	5.069 E - 1	4819
90	1.931	62.11	1.500 E - 5	8.233 E - 6	4.86 E - 3	6.979 E - 1	4960
100	1.927	62.00	1.423 E - 5	7.383 E - 6	4.79 E - 3	9.493 E - 1	4995
120	1.918	61.71	1.164 E - 5	6.067 E - 6	4.67 E - 3	1.692 E + 0	5049
140	1.908	61.38	9.743 E - 6	5.106 E - 6	4.53 E - 3	2.888 E + 0	5091
160	1.896	61.00	8.315 E - 6	4.385 E - 6	4.40 E - 3	4.736 E + 0	5101
180	1.883	60.58	7.207 E - 6	3.827 E - 6	4.26 E - 3	7.507 E + 0	5195
200	1.869	60.12	6.342 E - 6	3.393 E - 6	4.12 E - 3	1.152 E + 1	5089
212	1.860	59.83	5.886 E - 6	3.165 E - 6	4.04 E - 3	1.469 E + 1	5062

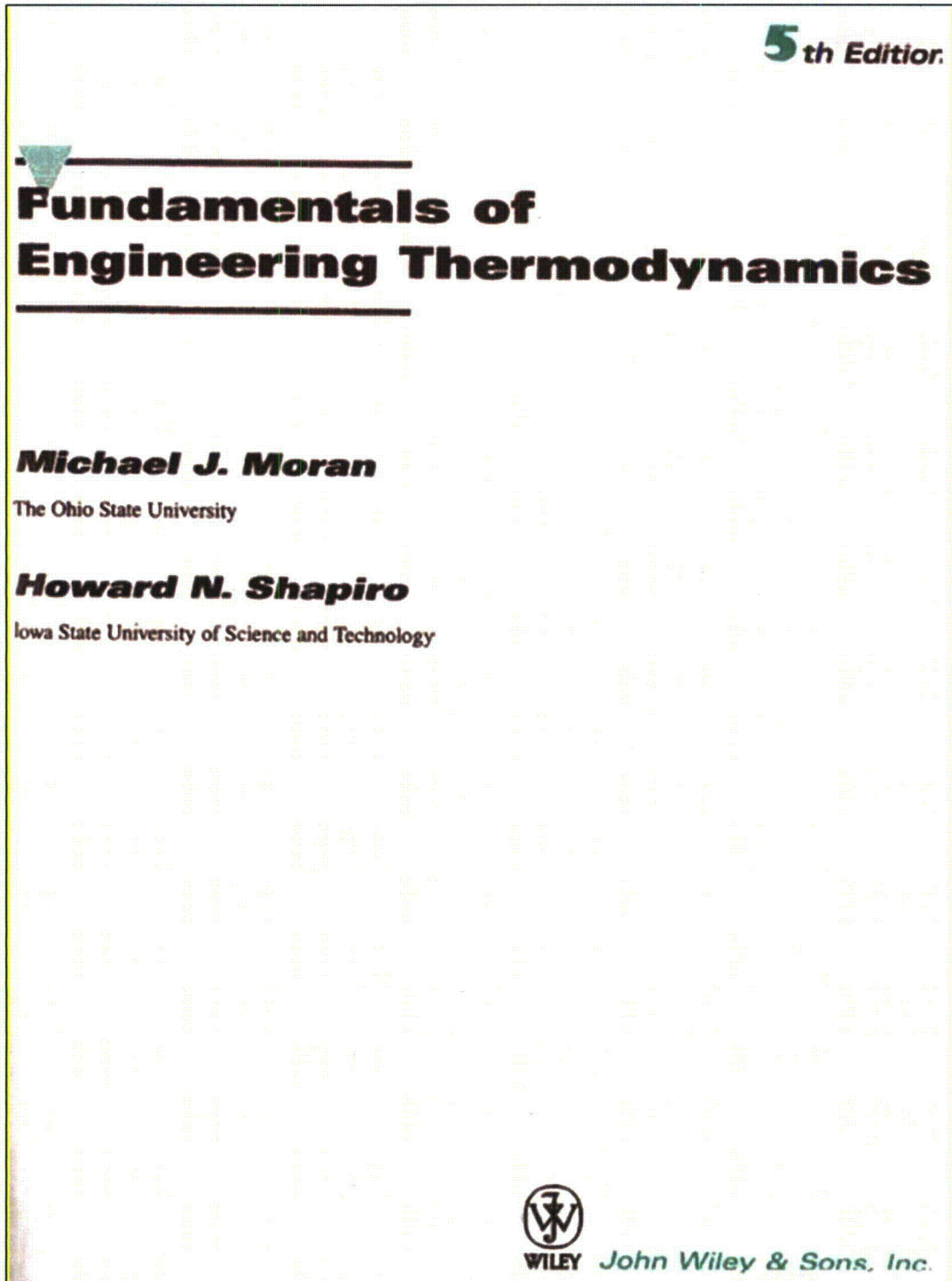
*Based on data from *Handbook of Chemistry and Physics*, 69th Ed., CRC Press, 1988. Where necessary, values obtained by interpolation.
^bDensity and specific weight are related through the equation $\gamma = \rho g$. For this table, $g = 32.174 \text{ ft/s}^2$.
^cIn contact with air.
^dFrom R. D. Blevins, *Applied Fluid Dynamics Handbook*, Van Nostrand Reinhold Co., Inc., New York, 1984.

■ TABLE B.2
 Physical Properties of Water (SI Units)*

Temperature (°C)	Density, ρ (kg/m ³)	Specific Weight ^b , γ (kN/m ³)	Dynamic Viscosity, μ (N·s/m ²)	Kinematic Viscosity, ν (m ² /s)	Surface Tension ^c , σ (N/m)	Vapor Pressure, P_v [N/m ² (abs)]	Speed of Sound ^d , c (m/s)
0	999.9	9.806	1.787 E - 3	1.787 E - 6	7.56 E - 2	6.105 E + 2	1403
5	1000.0	9.807	1.519 E - 3	1.519 E - 6	7.49 E - 2	8.722 E + 2	1427
10	999.7	9.804	1.307 E - 3	1.307 E - 6	7.42 E - 2	1.228 E + 3	1447
20	998.2	9.789	1.002 E - 3	1.004 E - 6	7.28 E - 2	2.338 E + 3	1481
30	995.7	9.765	7.975 E - 4	8.009 E - 7	7.12 E - 2	4.243 E + 3	1507
40	992.2	9.731	6.529 E - 4	6.580 E - 7	6.96 E - 2	7.376 E + 3	1526
50	988.1	9.690	5.468 E - 4	5.534 E - 7	6.79 E - 2	1.233 E + 4	1541
60	983.2	9.642	4.665 E - 4	4.745 E - 7	6.62 E - 2	1.992 E + 4	1552
70	977.8	9.589	4.042 E - 4	4.134 E - 7	6.44 E - 2	3.116 E + 4	1555
80	971.8	9.530	3.547 E - 4	3.650 E - 7	6.26 E - 2	4.734 E + 4	1555
90	965.3	9.467	3.147 E - 4	3.260 E - 7	6.08 E - 2	7.010 E + 4	1550
100	958.4	9.399	2.818 E - 4	2.940 E - 7	5.89 E - 2	1.013 E + 5	1543

*Based on data from *Handbook of Chemistry and Physics*, 69th Ed., CRC Press, 1988.
^bDensity and specific weight are related through the equation $\gamma = \rho g$. For this table, $g = 9.807 \text{ m/s}^2$.
^cIn contact with air.
^dFrom R. D. Blevins, *Applied Fluid Dynamics Handbook*, Van Nostrand Reinhold Co., Inc., New York, 1984.

Attachment 3.5-4 Water Vapor Pressure Reference (150°C)
[Ref. 18]



Attachment 3.5-4 Water Vapor Pressure Reference (150°C) (Continued)
[Ref. 18]

Acquisitions Editor	<i>Joseph Hayton</i>
Senior Marketing Manager	<i>Katherine E. Hepburn</i>
Production Editor	<i>Sandra Dumas</i>
Text and Cover Designer	<i>Madelyn Lesure</i>
Cover Illustration	<i>Roy Wiemann</i>
Production Management Services	<i>Ingram Associates</i>
Illustrations	<i>Precision Graphics</i>

This book was typeset in 10/12 Times by TechBooks and printed and bound by Von Hoffmann Corporation. The cover was printed by Von Hoffmann Corporation.

The paper in this book was manufactured by a mill whose forest management programs include sustained yield harvesting of its timberlands. Sustained yield harvesting principles ensure that the number of trees cut each year does not exceed the amount of new growth.

This book is printed on acid-free paper. ©

Copyright © 2004 by John Wiley & Sons, Inc. All rights reserved.

No part of this publication may be reproduced, stored in a retrieval system or transmitted in any form or by any means, electronic, mechanical, photocopying, recording, scanning or otherwise, except as permitted under Sections 107 or 108 of the 1976 United States Copyright Act, without either the prior written permission of the Publisher or authorization through payment of the appropriate per-copy fee to the Copyright Clearance Center, 222 Rosewood Drive, Danvers, MA 01923, (978) 750-8400, fax (978) 750-4470. Requests to the Publisher for permission should be addressed to the Permissions Department, John Wiley & Sons, Inc., 111 River Street, Hoboken, NJ 07030, (201) 748-6011, fax (201) 748-6008, E-mail: PERMREQ@WILEY.COM. To order books or for customer service call 1-800-CALL-WILEY (225.5945).

Moran, Michael J.
Fundamentals of engineering thermodynamics/Michael J. Moran, Howard N. Shapiro.—5th ed.

ISBN 0-471-27471-2
WH: ISBN 0-471-45241-6

Printed in the United States of America.

10 9 8 7 6 5 4 3 2

Attachment 3.5-4 Water Vapor Pressure Reference (150°C) (Continued)
 [Ref. 18]

760 Tables in SI Units *Divide by 1000*

TABLE A-2 Properties of Saturated Water (Liquid-Vapor): Temperature Table

Temp. °C	Sat. Press. bar	Specific Volume m ³ /kg		Internal Energy kJ/kg		Enthalpy kJ/kg			Entropy kJ/kg · K		Temp. °C
		Sat. Liquid $v_f \times 10^3$	Sat. Vapor v_g	Sat. Liquid u_f	Sat. Vapor u_g	Sat. Liquid h_f	Evap. h_{fg}	Sat. Vapor h_g	Sat. Liquid s_f	Sat. Vapor s_g	
01	0.00611	1.0002	206.136	0.00	2375.3	0.01	2501.3	2501.4	0.0000	9.1562	01
4	0.00813	1.0001	157.232	16.77	2380.9	16.78	2491.9	2508.7	0.0610	9.0514	4
5	0.00872	1.0001	147.120	20.97	2382.3	20.98	2489.6	2510.6	0.0761	9.0257	5
6	0.00935	1.0001	137.734	25.19	2383.6	25.20	2487.2	2512.4	0.0912	9.0003	6
8	0.01072	1.0002	120.917	33.59	2386.4	33.60	2482.5	2516.1	0.1212	8.9501	8
10	0.01228	1.0004	106.379	42.00	2389.2	42.01	2477.7	2519.8	0.1510	8.9008	10
11	0.01312	1.0004	99.857	46.20	2390.5	46.20	2475.4	2521.6	0.1658	8.8765	11
12	0.01402	1.0005	93.784	50.41	2391.9	50.41	2473.0	2523.4	0.1806	8.8524	12
13	0.01497	1.0007	88.124	54.60	2393.3	54.60	2470.7	2525.3	0.1953	8.8285	13
14	0.01598	1.0008	82.848	58.79	2394.7	58.80	2468.3	2527.1	0.2099	8.8048	14
15	0.01705	1.0009	77.926	62.99	2396.1	62.99	2465.9	2528.9	0.2245	8.7814	15
16	0.01818	1.0011	73.333	67.18	2397.4	67.19	2463.6	2530.8	0.2390	8.7582	16
17	0.01938	1.0012	69.044	71.38	2398.8	71.38	2461.2	2532.6	0.2535	8.7351	17
18	0.02064	1.0014	65.038	75.57	2400.2	75.58	2458.8	2534.4	0.2679	8.7123	18
19	0.02198	1.0016	61.293	79.76	2401.6	79.77	2456.5	2536.2	0.2823	8.6897	19
20	0.02339	1.0018	57.791	83.95	2402.9	83.96	2454.1	2538.1	0.2966	8.6672	20
21	0.02487	1.0020	54.514	88.14	2404.3	88.14	2451.8	2539.9	0.3109	8.6450	21
22	0.02645	1.0022	51.447	92.32	2405.7	92.33	2449.4	2541.7	0.3251	8.6229	22
23	0.02810	1.0024	48.574	96.51	2407.0	96.52	2447.0	2543.5	0.3393	8.6011	23
24	0.02985	1.0027	45.883	100.70	2408.4	100.70	2444.7	2545.4	0.3534	8.5794	24
25	0.03160	1.0029	43.360	104.88	2409.8	104.89	2442.3	2547.2	0.3674	8.5580	25
26	0.03363	1.0032	40.994	109.06	2411.1	109.07	2439.9	2549.0	0.3814	8.5367	26
27	0.03567	1.0035	38.774	113.25	2412.5	113.25	2437.6	2550.8	0.3954	8.5156	27
28	0.03782	1.0037	36.690	117.43	2413.9	117.43	2435.2	2552.6	0.4093	8.4946	28
29	0.04008	1.0040	34.733	121.60	2415.2	121.61	2432.8	2554.5	0.4231	8.4739	29
30	0.04246	1.0043	32.894	125.78	2416.6	125.79	2430.5	2556.3	0.4369	8.4533	30
31	0.04496	1.0046	31.165	129.96	2418.0	129.97	2428.1	2558.1	0.4507	8.4329	31
32	0.04759	1.0050	29.540	134.14	2419.3	134.15	2425.7	2559.9	0.4644	8.4127	32
33	0.05034	1.0053	28.011	138.32	2420.7	138.33	2423.4	2561.7	0.4781	8.3927	33
34	0.05324	1.0056	26.571	142.50	2422.0	142.50	2421.0	2563.5	0.4917	8.3728	34
35	0.05628	1.0060	25.216	146.67	2423.4	146.68	2418.6	2565.3	0.5053	8.3531	35
36	0.05947	1.0063	23.940	150.85	2424.7	150.86	2416.2	2567.1	0.5188	8.3336	36
38	0.06632	1.0071	21.602	159.20	2427.4	159.21	2411.5	2570.7	0.5458	8.2950	38
40	0.07384	1.0078	19.523	167.56	2430.1	167.57	2406.7	2574.3	0.5725	8.2570	40
45	0.09593	1.0099	15.258	188.44	2436.8	188.45	2394.8	2583.2	0.6387	8.1648	45

Attachment 3.5-4 Water Vapor Pressure Reference (150°C) (Continued)
 [Ref. 18]

Tables in SI Units 761

TABLE A-2 (Continued)

Temp. °C	Press. bar	Specific Volume m ³ /kg		Internal Energy kJ/kg		Enthalpy kJ/kg			Entropy kJ/kg · K		Temp. °C
		Sat. Liquid $v_f \times 10^3$	Sat. Vapor v_g	Sat. Liquid u_f	Sat. Vapor u_g	Sat. Liquid h_f	Evap. h_{fg}	Sat. Vapor h_g	Sat. Liquid s_f	Sat. Vapor s_g	
50	1.235	1.0121	12.032	209.32	2443.5	209.33	2382.7	2592.1	.7038	8.0763	50
55	1.576	1.0146	9.568	230.21	2450.1	230.23	2370.7	2600.9	.7679	7.9913	55
60	1.994	1.0172	7.671	251.11	2456.6	251.13	2358.5	2609.6	.8312	7.9076	60
65	2.503	1.0199	6.197	272.02	2463.1	272.06	2346.2	2618.3	.8955	7.8310	65
70	3.119	1.0228	5.042	292.95	2469.6	292.98	2333.8	2626.8	.9549	7.7553	70
75	3.858	1.0259	4.131	313.90	2475.9	313.93	2321.4	2635.3	1.0155	7.6824	75
80	4.739	1.0291	3.407	334.86	2482.2	334.91	2308.8	2643.7	1.0753	7.6122	80
85	5.783	1.0325	2.828	355.84	2488.4	355.90	2296.0	2651.9	1.1343	7.5445	85
90	7.014	1.0360	2.361	376.85	2494.5	376.92	2283.2	2660.1	1.1925	7.4791	90
95	8.455	1.0397	1.982	397.88	2500.6	397.96	2270.2	2668.1	1.2500	7.4159	95
100	1.014	1.0435	1.673	418.94	2506.5	419.04	2257.0	2676.1	1.3069	7.3549	100
110	1.433	1.0516	1.210	461.14	2518.1	461.30	2230.2	2691.5	1.4185	7.2387	110
120	1.985	1.0603	0.8919	503.50	2529.3	503.71	2202.6	2706.3	1.5276	7.1296	120
130	2.701	1.0697	0.6685	546.02	2539.9	546.31	2174.2	2720.5	1.6344	7.0269	130
140	3.613	1.0797	0.5089	588.74	2550.0	589.13	2144.7	2733.9	1.7391	6.9299	140
150	4.758	1.0905	0.3928	631.68	2559.5	632.20	2114.3	2746.5	1.8418	6.8379	150
160	6.178	1.1020	0.3071	674.86	2568.4	675.55	2082.6	2758.1	1.9427	6.7502	160
170	7.917	1.1143	0.2428	718.33	2576.5	719.21	2049.5	2768.7	2.0419	6.6663	170
180	10.02	1.1274	0.1941	762.09	2583.7	763.22	2015.0	2778.2	2.1396	6.5857	180
190	12.54	1.1414	0.1565	806.19	2590.0	807.62	1978.8	2786.4	2.2359	6.5079	190
200	15.54	1.1565	0.1274	850.65	2595.3	852.45	1940.7	2793.2	2.3309	6.4323	200
210	19.06	1.1726	0.1044	895.53	2599.5	897.76	1900.7	2798.5	2.4248	6.3585	210
220	23.18	1.1900	0.08619	940.87	2602.4	943.62	1858.5	2802.1	2.5178	6.2861	220
230	27.95	1.2088	0.07158	986.74	2603.9	990.12	1813.8	2804.0	2.6099	6.2146	230
240	33.44	1.2291	0.05976	1033.2	2604.0	1037.3	1766.5	2803.8	2.7015	6.1437	240
250	39.73	1.2512	0.05013	1080.4	2602.4	1085.4	1716.2	2801.5	2.7927	6.0730	250
260	46.88	1.2755	0.04221	1128.4	2599.0	1134.4	1662.5	2796.6	2.8838	6.0019	260
270	54.99	1.3023	0.03564	1177.4	2593.7	1184.5	1605.2	2789.7	2.9751	5.9301	270
280	64.12	1.3321	0.03017	1227.5	2586.1	1236.0	1543.6	2779.6	3.0668	5.8571	280
290	74.36	1.3656	0.02557	1278.9	2576.0	1289.1	1477.1	2766.2	3.1594	5.7821	290
300	85.81	1.4036	0.02167	1332.0	2563.0	1344.0	1404.9	2749.0	3.2534	5.7045	300
320	112.7	1.4988	0.01549	1444.6	2525.5	1461.5	1238.6	2700.1	3.4480	5.5362	320
340	145.9	1.6379	0.01080	1570.3	2464.6	1594.2	1027.9	2622.0	3.6594	5.3357	340
360	186.5	1.8925	0.006945	1725.2	2351.5	1760.5	720.5	2481.0	3.9147	5.0526	360
374.14	220.9	3.155	0.003155	2029.6	2029.6	2099.3	0	2099.3	4.4298	4.4298	374.14

Source: Tables A-2 through A-5 are extracted from J. H. Keenan, F. G. Keyes, P. G. Hill, and J. G. Moore, *Steam Tables*, Wiley, New York, 1969.

3.6 References

1. Robatel Technologies, LLC, Quality Assurance Program for Packaging and Transportation of Radioactive Material, 10 CFR 71 Subpart H, Dated January 31, 2012 and NRC Approved on March 21, 2012
2. U.S. Nuclear Regulatory Commission, 10 CFR Part 71--PACKAGING AND TRANSPORTATION OF RADIOACTIVE MATERIAL, dated March 7, 2012
3. ANSYS, Release 14.0, ANSYS, Inc., Canonsburg, PA, October, 2011
4. RTL-001-CALC-TH-0201, Rev. 6, "RT-100 Cask Thermal Analyses" (PROPRIETARY)
5. Fundamentals of Heat and Mass Transfer, Frank P. Incropera, David P. DeWitt, 2002, 5th ed., John Wiley & Sons, Inc.
6. RTL-001-CALC-TH-0102, Rev. 6, "RT-100 Cask Maximum Normal Operating Pressure Calculation" (PROPRIETARY)
7. RTL-001-CALC-TH-0202, Rev. 6, "RT-100 Cask Hypothetical Accident Condition Maximum Pressure Calculation" (PROPRIETARY)
8. TRELLEBORG Sealing Solutions O-Ring and Backup Rings Catalog, August 2011 Edition
9. UNIFRAX Fiberfrax 970 Ceramic Paper Data Sheet
Proprietary Information Content Withheld Under 10 CFR 2.390

13. ASME Boiler & Pressure Vessel Code 2007 Edition, Section II – Part D, "Materials", The American Society of Mechanical Engineers, Three Park Avenue, New York, NY, www.asme.org.
14. Sanghavi Bothra Engineering Co. Pvt. Ltd.(SBE) 304/304L Stainless Steel Product Mechanical and Physical Properties
15. GENERAL PLASTICS Design Guide for LAST-A-FOAM FR-3700 Crash & Fire Protection of Radioactive Material Shipping Containers, Rev. 02.20.12
16. Parker O-Ring Handbook ORD 5700, Retrieved on August 28, 2013, Retrieved from http://www.parker.com/literature/ORD%205700%20Parker_O-Ring_Handbook.pdf.
17. Fundamentals of Fluid Mechanics, B. Munson, D. Young and T. Okiishi, 4th ed., John Wiley & Sons, Inc.
18. Fundamentals of Engineering Thermodynamics, M. Moran and H. Shapiro, 5th ed., John Wiley & Sons, Inc.
19. Glenn Lee, Radiation Resistance of Elastomers, IEEE Transactions on Nuclear Science, Vol. NS-32, No. 5, October 1985
20. U.S. Nuclear Regulatory Commission, "Load Combinations for the Structural Analysis of

- Shipping Casks for Radioactive Material," Regulatory Guide 7.8.
21. SFPE Handbook of Fire Protection Engineering, "Thermal Decomposition of Polymers," C.L. Hirschler, M. Marvelo, Chapter 7 of 3rd Edition, NFPA, 1 Batterymarch Park, Quincy, MA, 2001, www.nfpa.org.
 22. "Fundamentals of Combustion Processes," A. McAllister, J. Chen, A. Fernandez-Pello, Springer, 2011.
 23. An Experimental Study of Autoignition of Wood, T. Poespowati, World Academy of Science, Engineering and Technology, Vol. 23, 2008., Retrieved on August 28, 2013, Retrieved from <http://www.waset.org/journals/waset/v23/v23-13.pdf>.
 24. ASME Boiler & Pressure Vessel Code, 2010, Section II, Part D, Materials, The American Society of Mechanical Engineers, New York, NY 2010
 25. RTL-001-CALC-TH-0301, Rev. 1, "RT-100 Cask Hypothetical Accident Condition Combustion Analysis" (PROPRIETARY)

This page is intentionally left blank.